FINITE ELEMENT ANALYSIS OF A CRACK AND DETERMINATION OF CRACK OPENING AND CLOSING STRESSES IN FATIGUE LOADING FOR MATERIALS HAVING DIFFERENT WORK HARDENING EXPONENTS

A Thesis Submitted to
Babu Banarasi Das University
for the Degree Of

Doctor of Philosophy

in
Mechanical Engineering

BY
Nirpesh Vikram

Under the Supervision of
Prof. (Dr.) Raghuvir Kumar

Department of Mechanical Engineering
School of Engineering
Babu Banarasi Das University
Lucknow-226028, (U.P.), India
June, 2015

……..dedicated to Late Prof. (Dr.) S.B.L Garg Sir

CERTIFICATE

This is to certify that the thesis entitled "**Finite Element Analysis of a crack and determination of crack opening and closing stresses in Fatigue loading for materials having different work hardening exponents**" submitted by **Mr. Nirpesh Vikram** for the award of Degree of Doctor of Philosophy in Mechanical Engineering from Babu Banarasi Das University, Lucknow (UP), is a record of authenticate work carried out by him under my supervision.

To the best of my knowledge, the matter embodied in this thesis is the original work of the candidate and has not been submitted elsewhere for the award of any other Degree or Diploma.

Prof. (Dr.) Raghuvir Kumar
Director
BBDNIIT
Lucknow

DECLARATION

I, hereby, declare that the work presented in this thesis entitled **"Finite Element Analysis of a crack and determination of crack opening and closing stresses in Fatigue loading for materials having different work hardening exponents"** in fulfillment of the requirement for the Degree of Doctor of Philosophy, Department of Mechanical Engineering, Babu Banarasi Das University, Lucknow is an authentic record of my own research work carried out under the supervision of Prof. (Dr.) Raghuvir Kumar.

I also declare the work embodied in the present thesis is my original work and has not been submitted by me for any other degree or diploma of any university or institution.

(Nirpesh Vikram)

AKNOWLEDGEMENTS

I express my deep sense of gratitude and profound regards to Prof. (Dr.) Raghuvir Kumar, Director Engineering, BBDNIIT, Lucknow who as my supervisor has given me invaluable guidance, help.

Encouragement and criticism in bringing up the present work. I am grateful to Dr. A.K. Mittal, Vice Chancellor, Babu Banarasi Das University and Dr. Seethalaksmi K, Dean, School of Engineering, Babu Banarasi Das University, Dr. S. Ahamad Ali, Dean, Applied Sciences, Babu Banarasi Das University and Mr. Sunil Kumar, Head, Department of Mechanical Engineering, Babu Banarasi Das University for their constant support, encouragement under this aura of academic Excalibur, their enormous experience, their sincerity towards their duty which have truly inspired me leaps and bounds.

I must not forget to appreciate the extreme support of Prof. (Dr.) Manuj Darbari, Department of Information and Technology, BBDNITM. patience and support of my wife Shira and son Rudransh. I am really thankful to her. I also owe this research work to my grandfather, parents, my in-laws, brother who were extremely affectionate and supportive throughout.

I appreciate the extreme patience and support of my wife Shira and son Rudransh. I am really thankful to them for giving me environment and time to study at home also. I also owe this research work to my grandfather, my parents who were extremely affectionate and supportive throughout.

I thank my friends for their constant encouragement without which this assignment would not be possible.

Last but not the least I would like to thank the almighty for showering on me his choicest blessing and helping me to achieve my goal.

NIRPESH VIKRAM

ABSTRACT

Fracture and failure due to fatigue is a challenging issue in design engineering. Fatigue is a complex phenomenon and it represents large number of facts, some independent and some interrelated. Several conceptual approaches like material degeneration, debonding, damage accumulation, dislocation tangles and dislocation arrays etc. have been suggested in the past. But these been qualitative have been unable to provide a definite answer to predict the fatigue behaviour in metals. This research work makes a step ahead in predicting and selecting the proper material in design phase for fatigue loading conditions by proposing a generalized relationship between effective stress intensity range ration and work hardening exponent for Aluminium Alloys under different kind of fatigue loading conditions.

The research in fatigue has continued for more than a century as more than a century as more than 60% of all types of mechanical failures are due to their working under alternating stresses. In scientific research the physical concepts often develop from the experimental and statistical data. The studies regarding fatigue behaviour of materials have grown in a similar way.

It is not always practicable to limit the fluctuating stresses on components and structures so that fatigue cracks never occur. It is sometimes necessary therefore to carry out periodic inspections of service parts to insure that fatigue cracks do not propagate to cause complete failure. In these circumstances, information is required about the rate at which fatigue cracks are likely to propagate. There is no simpler answer to the problem. The development of a quantitative approach to fatigue crack propagation requires the following information:

(i) Physical behaviour of the material in the vicinity of the fatigue crack,

(ii) Mechanism of fatigue crack propagation,

(iii) Effect of loading conditions on fatigue crack propagation,

(iv) Knowledge of the existing propagation laws

(v) Dependence on mechanical properties of the material

In recent past, a large number of theoretical and experimental relations have been developed to predict fatigue crack growth rate. These relations have to invariably

consider important aspects like material properties and type of geometry of the component. Since many variables are involved, the problem becomes more and more complex. One single relationship found and derived for one material may not represent the behaviour of other materials in general. A generalized approach to the problem is therefore required.

Engineering fracture mechanics is concerned with the analysis and design of structures when there is a likelihood of cracks. When a crack is present in the structure under consideration it tends to grow with time due to the application of repeated or increasing loads. If the structure has been designed for a particular strength the residual strength decreases monotonically with time due to crack propagation. Fracture mechanics attempts to provide answers for the problems of residual strength reduction, determination of critical crack size, estimation of time for the crack to reach the critical size and determination of frequency of inspection for cracks. While several analytical method have been used for the determination of stress intensity factors in linear elastic fracture mechanics and the general behaviour in elastic-plastic fracture mechanics, finite element method has been found to be very versatile in handling all types of problems in fracture and fatigue.

There is some contradiction regarding the effect of different parameters on crack closure (Effective Stress Intensity Range Ratio) U. A large amount of work, both theoretical & experimental is required to correlate strain hardening exponent (n), material properties (σ_y) and loading parameters$\Delta\sigma$ and R for finding a general relationship with the above background in mind following proposal makes a step forward in this regard.

(i) Effect of load parameters on effective stress intensity range ratio (U)

- **a)** Effect of change of stress ratio R
- **b)** Effect of change of overload ratio
- **c)** Effect of block loading

(ii) Effect of change of material Properties on effective stress intensity range ratio (U)

- **a)** Change of Material Properties- Five Materials were taken 3003, 5052, 6061-T6, 6063-T6, 6351 Al-alloys.

To verify the application of expression of effective stress intensity range ratio (U) and crack growth rate (da/dN) found by above study the experimental results are compared with those found by applying the model.

The objective of the proposed research work are to determine the crack opening and closing stresses and find out the dependency of the material properties on the crack growth in fatigue loading. This proposes the effect of work hardening exponent on crack closure and crack growth rate in different types of fatigue loading.

It has been found to be possible to measure accurately the crack closure loads using the Finite Element Method. The FEM investigation on side edge notched specimens show a monotonic increase of crack closure loads up to a/b ratio of approximately which crack closure loads stabilize for constant amplitude loading. This is probably due to mode transition. The effect of work hardening on crack closure under various loading shows the following trends:

In constant amplitude loading Crack opening and closing loads are particularly equal. Effective stress intensity range ratio increases with increases work hardening exponent. U increases with crack length, yield strength and stress ratio also. A generalized empirical formula has been developed and validated for Aluminium Alloy which gives very good agreement with the experimental results. The presented model equations are applicable for Al Alloy only and only SEN. Effect of strain hardening on crack growth were noticed as for lower R-ratios, i.e., R=0, R=0.1, R=0.3, crack growth rate decreases with the increasing work hardening effect and for R= 0.5, crack growth rate increases with the increasing strain hardening effect. The modified Paris Law has been proposed for Aluminium Alloys and SEN.

Increasing overload ratio decreases the effective stress range ratio U. The decrease is related to overload ratio. Change in U is related to overload ratio by power law. For all overload ratios, the cyclic life is found to decrease with increase in strain hardening- the effect is more on larger stress ratios. The effect of strain hardening is realized on yield strength of the material. The increase in strain hardening gives larger yield strength. A generalized relationship was formed for evaluation of U accordingly and modified Paris Law was obtained having limitation to Al Alloy only.

After an overload band, the value of U decreases as was found for the case of single overload. At constant amplitude loading, this value of crack closure remains

almost constant till the load again increases. During subsequent cycles after an overload band, U reaches a minimum value. This shows that crack propagation during a number of cycles takes place at minimum U, resulting in considerable increase in life. A generalized equation has been developed that gives very good agreement with the values obtained from experiments. Below 2% error was recorded in values obtained by generalized equation obtained after regression analysis on the data obtained by FEM analysis.

NOMENCLATURE

Greek Symbols	Description
α	A variable factor
σ	Normal stress
σ_a	Average (mean) stress in a cycle
σ_m	Maximum stress in a cycle
σ_n	Minimum stress in a cycle
σ_o	Optimum stress
σ_p	Stress amplitude in a cycle
σ_u	Ultimate stress
σ_y	Yield stress
$\Delta\sigma$	Stress range
ω_p	Monotonic plastic zone size
$\Delta\omega_p$	Cyclic plastic zone size

English Symbols	Description
a	Crack length
A	A constant
B	Specimen thickness
C	Constant of crack growth equation
$d_{1,}$ $_{d2}$, $d_3 \ldots d_7$	Constants of seven point method
$\frac{da}{dN}$	Crack growth rate
D	A constant
E	Young's modulus of elasticity

f	A variable factor
K	Stress intensity factor
K_C	Fracture toughness of the material
K_m	Maximum stress intensity factor of a cycle
K_n	Minimum stress intensity factor of a cycle
K_o	Optimum stress intensity factor of a cycle
K_t	Threshold stress intensity factor
ΔK	Stress intensity range
ΔK_Θ	Effective stress intensity range
m	Exponent of crack growth rate equation
n	Exponent of crack growth rate equation
N	Number of cycles
N_f	Number of cycles to failure
N_p	Number of readings in a set of readings
p	A ratio $\frac{\Delta\sigma}{\sigma_y}$
P	Simple load
P_a	Average load in a cycle
P_m	Maximum load in a cycle
P_n	Minimum load in a cycle
ΔP	Load range in a CAL cycle
R	Stress ratio in CAL cycle ($\frac{P_m}{P_n}$)
S_1	Relationship constant
S_2	Relationship constant
T_1	Relationship constant
T_2	Relationship constant

W	Width of the specimen

Abbreviation	**Description**
CA	Constant amplitude
CAL	Constant amplitude loading
CGR	Crack growth rate
CL	Crack length
ESIR	Effective stress intensity range
ESIRR	Effective stress intensity range ratio
LEFM	Linear elastic fracture mechanics
MSIF	Maximum stress intensity factor
SEN	Single edged notched
SIR	Stress intensity range
UTS	Ultimate tensile stress

TABLE OF CONTENTS

LIST OF TABLES

LIST OF FIGURES

CHAPTER: 01

1 INTRODUCTION

1.1 INTRODUCTORY REMARKS

The research on fatigue has continued for more than a century as more than a century as more than 60% of all types of mechanical failures are due to their working under alternating stresses. In scientific research the physical concepts often develop from the experimental and statistical data. The studies regarding fatigue behavior of materials have grown in a similar way.

Fatigue is a complex phenomenon and it represents large number of facts, some independent and some interrelated. Several conceptual approaches like material degeneration, debonding, damage accumulation, dislocation tangles and dislocation arrays etc. have been suggested in the past. But these been qualitative have been unable to provide a definite answer to predict the fatigue behavior in metals.

It is not always practicable to limit the fluctuating stresses on components and structures so that fatigue cracks never occur. It is sometimes necessary therefore to carry out periodic inspections of service parts to insure that fatigue cracks do not propagate to cause complete failure. In these circumstances, information is required about the rate at which fatigue cracks are likely to propagate. There is no simpler answer to the problem. The development of a quantitative approach to fatigue crack propagation requires the following information:

(i) Physical behavior of the material in the vicinity of the fatigue crack,

(ii) Mechanism of fatigue crack propagation,

(iii) Effect of loading conditions on fatigue crack propagation,

(iv) Knowledge of the existing propagation laws

(v) Dependence on mechanical properties of the material

In recent past, a large number of theoretical and experimental relations have been developed to predict fatigue crack growth rate. These relations have to invariably consider important aspects like material properties and type of geometry of the component. Since many variables are involved, the problem becomes more and more complex. One single relationship found and derived for one material may not represent the behavior of other materials in general. A generalized approach to the problem is therefore required. A general theory developed will be of very much help to aerospace and power generating industry. In this chapter a brief introduction to the different aspects of fracture and fatigue is presented.

1.2 FRACTURE MECHANICS FUNDAMENTAL

Engineering fracture mechanics is concerned with the analysis and design of structures when there is a likelihood of cracks. When a crack is present in the structure under consideration it tends to grow with time due to the application of repeated or increasing loads. If the structure has been designed for a particular strength the residual strength decreases monotonically with time due to crack propagation.[**1**] Fracture mechanics attempts to provide answers for the problems of residual strength reduction, determination of critical crack size, estimation of time for the crack to reach the critical size and determination of frequency of inspection for cracks. Some elementary ideas of linear elastic fracture mechanics and elastic plastic fracture mechanics are described in section 1.2.1 and 1.2.2.

1.2.1 Linear elastic fracture mechanics:

In linear elastic fracture mechanics the material is assumed to be in a linear elastic state or if plastic deformation takes place the size of crack tip zone is small. The stress concentration in the neighborhood of the crack tip for different opening modes

can be obtained through analytical solutions[**2**]. The stress components at the crack tip possess $\sqrt{\mathbf{r}}$ singularity at the crack tip where "r" is the distance from the crack tip. Thus with the help of the appropriate "stress intensity factor" the whole stress field at the crack tip is known. The elastic solution does not prohibit the stresses from being infinite at the crack tip. However, in actual practice plastic deformation at the crack tip keeps the stresses finite. The size of the crack tip plastic zone can be obtained as suggested by Irwin [**3**]**.** The crack tip plastic zone is a function of the stress intensity factor and the yield stress. Crack extension will occur when the stresses and strains at the crack tip reach a critical value. In other words, mode I fracture will occur when K_I reaches a critical value K_{Ic} which is a material parameter.

1.2.2 Elastic Plastic Fracture Mechanics:

When the size of the plastic zone at the crack tip is large the LEFM approach described above is not satisfactory. Irwin [**3**]reasoned that the occurrence of plasticity makes the crack behave as if it was longer than its physical size from which the expression for crack opening displacement (COD) and crack tip opening displacement (CTOD) can be obtained. Dugdale[**5**] adopted a slightly different approach to find the extent of the plastic zone. The concept of J integral has been introduced by Rice [**6**]where

$$J = \int_{\Gamma} w dy - T_i \frac{\partial u_i}{\partial s} ds \qquad (1.1)$$

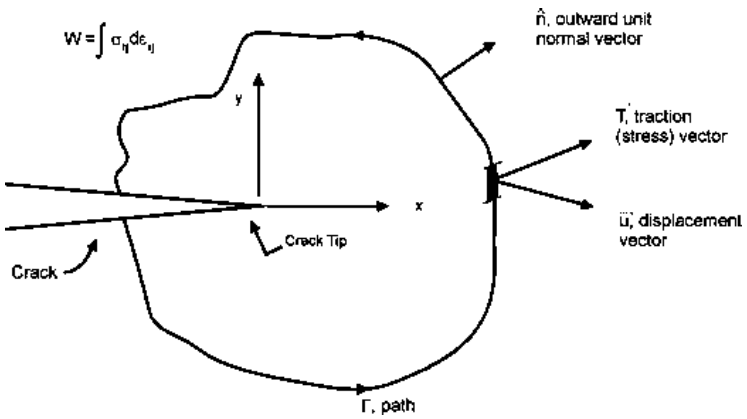

Fig 1.1 Definition of J-Integral[**6**]

Where Γ is a closed contour followed counter clockwise in surrounding an area in a stressed solid (**Fig**. 1.1). {T}is the tension vector perpendicular to Γ in the direction of the exterior normal and {U} is the displacement vector and w is the strain energy density. For the elastic case J- integral is equal to the strain energy releases rate. Rice [**6**]has shown that the J- integral is path independent. The determination of J-integral for arbitrary boundary conditions and loading can be done using numerical method.

1.3 FATIGUE LOADING AND CRACK PROPAGATION

Fatigue load varies between a maximum and a minimum value if stress-intensity factors corresponding to the maximum and minimum K_{max} and K_{min} respectively the stress intensity factor cycles over a range $\Delta K=K_{max} - K_{min}$. The rate of crack propagation per cycle $\frac{da}{dN}$depends on the stress intensity rangeΔ K.

$$\frac{da}{dN} = f(\Delta K) \tag{1.2}$$

When the result of several tests for various stress amplitudes are plotted in a log-log plot the form of equation 1.2 is

$$\frac{da}{dN} = C(\Delta K)^n \tag{1.3}$$

Where "C" and "n" are material constants. The above relation has been recommended by Paris[**7**]**.** Several other relations have been suggested by various other investigators which will be reviewed in the Chapter 02. At low ΔK values the crack propagation is extremely slow and there is a threshold value of ΔK below which there is no crack growth at all.

Fatigue crack growth rate is affected by several factors among which the major ones are material thickness, presence of surface flaws, anisotropy arising out of forming method, heat treatment, cold deformation, temperature, manufacturing method, environment and load cycling frequency. The application of overload results in retardation of crack growth rate.

Elber[**8**]observed that even in tension cycling the crack closes during unloading. This is attributed to the presence of residual plasticity in the wake of the crack tip. Since the crack is open only during a portion of the load cycle modification in the crack growth law has been proposed by him. Thus the modified law is of the form

$$\frac{da}{dN} = C(\Delta K_{eff})^n \qquad (1.4)$$

Where $\Delta K_{eff} = K_{max} - K_o$, where Ko is the stress intensity factor corresponding to crack opening load which is generally very near to crack closure load. The crack closure behavior has been found to be sensitive to environmental factors.

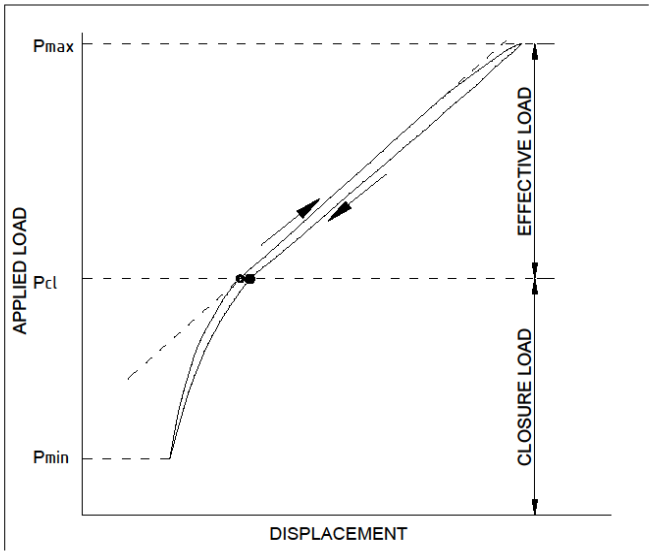

Fig 1.2 Typical applied load-displacement curve[**8**]

1.4 PROBLEM STATEMENT

Elber[**8**]observed that the crack is closed at the tip over a lower portion of the loading cycle and is opened only after the applied stress exceeds σ_{op} and suggested that the fatigue crack growth can occur only during that portion of the cycle in which the crack is fully open. Based on this suggestion effective stress range, $\Delta\sigma_{eff}$ and effective intensity range ratio, U were defined,

$$U = \frac{\Delta\sigma_{eff}}{\Delta\sigma} = \frac{\sigma_{max} - \sigma_{op/cl}}{\sigma_{max} - \sigma_{min}} \qquad (1.5)$$

He further suggested that the crack growth relationship should be written in the following form

$$\frac{da}{dN} = C(\Delta K_{eff})^n = C(U\Delta K)^n \qquad (1.6)$$

Where "C" and "n" are the material constants.

For 2024-T3 Aluminum alloy sheet the effective stress range U was found to be independent of σ_{max} or K_{max} and was expressed as

$$U = 0.5 + 0.4\,R \qquad -0.1 < R < 0.7$$

Equation 1.6 was found to provide a better fit to the experimental data than equation 1.3.

Other workers also considered that for a given material, U is only a function of R and is independent of other parameters. Katcher and Kaplan [**10**], Bell and Creager[**11**], Madaox et al.[**12**], Schijve[**13**] and Newman[**17**]developed U as a function of R only.

According to some other workers, U depends on K_{max} and R. Unangst et al [**21**], Adams [**25**]and Shih & Wei [**26**]showed that U tends to decrease with increase in K_{max} and increase in specimen thickness. Bachmann and munz[**31**]developed a model for U for Ti-6Al-4V and found it to be a function of R and K_{max} and a/w. They found that if K_{max} is increased, this model predicted an increase in U. the results of Bachmann and Munz[**31**]and Shih & Wei[**26**]are contradictory.

Homa and Nakazawa[**40**]showed U as a function of maximum stress (σ_{max}), stress ratio (R), yield strength (σ_y) and crack length. Lal et al [**46**]showed that U depends on $\Delta\sigma$, R, σ_y and n, but the effect of n is less as compared to other parametres. Literature shows that the crack growth rate can be related to ΔK or $U\Delta K$. There is some contradiction regarding the effect of different parameters on crack closure U as seen above. A large amount of work, both theoretical & experimental is required to correlate strain hardening exponent (n), material properties (σ_y) and loading parameters$\Delta\sigma$ and R for finding a general relationship with the above background in mind following study was carried out with regard of da/dN and U.

(i) Effect of load parameters

- **a)** Effect of change of stress ratio R
- **b)** Effect of change of overload ratio
- **c)** Effect of block loading

(ii) Effect of change of material Properties

- **a)** Change of Material Properties- Five Materials were taken 3003, 5052, 6061-T6, 6063-T6, 6351 Al-alloys.

To verify the application of expression of U and da/dN found by above study the experimental results are compared with those found by applying the model.

1.5 APPROACH

For meeting the objective described above it was decided to review the work available (Chapter 02) and developed an experimental setup for studying the phenomenon of crack closure using finite element method and conduct different type of tests on all five materials (3003, 5052, 6061, 6063, 6351 Al alloy)using side edge notch specimen (SEN). Experimental and FEM results on side edge notched specimens subjected to fatigue loading were collected and compared with each other to study as discussed in Chapter 04. Implementation of FEM application Abaqus® 6.10 for determining the crack opening and closing stresses were discussed in Chapter 05. Effects of work hardening exponent on crack growth rate and crack closure were studied in Chapter 05 and Chapter 06.

1.5.1 Scope and Limitations

All the experiments were performed on thin sheet SEN therefore plane stress condition dominated in the tests. Also the tests were carried out for stress ratios 0, 0.1, 0.2, 0.3, 0.5 only. The values of peak loads are given with experimental details describing each type of test.

1.6 DEFINITIONS

1.6.1 Stress Intensity Factor and Stress Intensity range

The stress intensity factor may be interpreted as parameters that reflect the redistribution of the stress ion a body resulting from the introduction of a crack. It is a function of load, the specimen geometry size and location of the crack. Two configurations have been used in this work.[**4**]

(i) A finite plate containing a central crack of length 2a under Mode-I loading, for which

$$K = \sigma\sqrt{\alpha\pi a} \tag{1.7}$$

$$\alpha = (\sec\frac{\pi a}{2w})^{\frac{1}{2}} \tag{1.8}$$

(ii) A single edge notched specimen

The expression of K for this case is

$$K = \sigma\left[1.99 - 0.41\left(\frac{a}{w}\right) + 18.7(\frac{a}{w})^2 - 38.48(\frac{a}{w})^3 + 53.85(\frac{a}{w})^4\right]\sqrt{a} \tag{1.9}$$

1.6.2 Stress Intensity Range

From definition $\Delta K = \Delta\sigma\sqrt{\alpha\pi a}$, it follows that a cyclic variation of σ will cause a similar cyclic variation of K [**4**, **5**].The stress intensity in the crack tip region will thus be characterized by maximum stress intensity, K_{max} and minimum stress intensity, K_{min}. The stress intensity range ΔK is defined below

$$\Delta K = \Delta\sigma\sqrt{\alpha\pi a} \tag{1.10}$$

For the same cycle

Stress ratio, $R = \frac{\sigma_{min}}{\sigma_{max}} = \frac{K_{min}}{K_{max}}$(2.1)

$$K_{max} = \frac{\Delta K}{1-R} \tag{1.11}$$

$$K_{min} = \frac{R\Delta K}{1-R} \quad (1.12)$$

Where

ΔK is the stress intensity range.

$$\Delta K = K_{max} - K_{min} \quad (1.13)$$

1.6.3 Effective Stress Intensity Range Ratio

In an elasto-plastic analysis of the crack tip under cyclic tension loading, Rice[**6**]showed that crack remains fully open above minimum load. Elber[**8**]has shown that a fatigue crack closes during unloading before zero load because crack surfaces having residual plastic deformations get pressed together. The phenomenon of fracture surfaces coming closure together before complete unloading is referred as crack closure. Fatigue crack propagation can occur only during that portion of the loading cycle in which the crack is fully open. It is therefore evident that in a crack extension, the load beyond crack opening is effective. Elber[**8**]defined this useful portion of the load cycle as the effective stress range. These effective stress range and crack closures are explained[**8**]in typical stress vs crack opening displacement. (see **Fig** 1.2). The curve EC'B'A is for unloading and ABCE is for loading. During unloading part, the crack starts to close at C' and closes completely at B'. From B' to A elastic compression takes place during loading. The starts to open at B and becomes fully open at C. from C to E, the crack extension takes place. Thus the effective stress ($\Delta\sigma_{eff}$)to extend the crack is the difference between the stress at E and Stress at C. i.e ($\sigma_{max} - \sigma_{op}$)

The stress from A to C is used to overcome the compressive stresses and in opening the crack tip. Point C and Point C' almost coincide at the same stress level.

On the basis of the above observations, the effective stress range is defined as [**8**]

$$\Delta\sigma_{eff} = \sigma_{max} - \sigma_{op}\ (\sigma_{cl}) \quad (1.14)$$

Since cyclic variation of K corresponds to cyclic variation of σ, the effective stress intensity range, ΔK_{eff} is defined

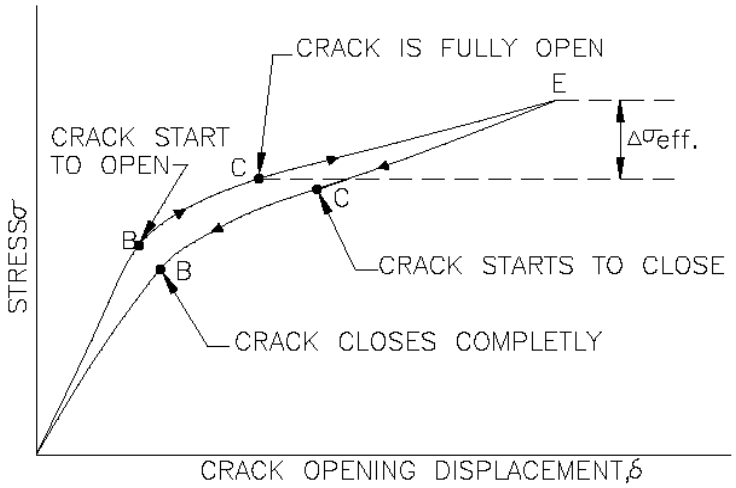

Stress vs crack opening dispacement

Fig 1.3 Stress Vs Crack opening displacement[8]

$$\Delta K_{eff} = \Delta\sigma_{eff}\sqrt{\alpha\pi a} = K_{max} - K_{op} \quad (1.15)$$

Where $K_{max}$and K_{op} represent maximum stress intensity and stress intensity at crack opening stress level respectively.

Elber[**8**]defined a parameter, effective stress range ratio, U as given by eqn. (1.16).

$$U = \frac{\Delta\sigma_{eff}}{\Delta\sigma} \quad (1.16)$$

$$U = \frac{\sigma_{max} - \sigma_{op}(or\ \sigma_{cl})}{\sigma_{max} - \sigma_{min}} \quad (1.17)$$

Writing eqn. (1.17) in terms of stress intensity factor, U is called as effective stress intensity range ratio. (eqns. 1.18 and 1.19).

$$U = \frac{\Delta K_{eff}}{\Delta K} \quad (1.18)$$

$$U = \frac{K_{max} - K_{op}\ (or\ K_{cl})}{K_{max} - K_{min}} \tag{1.19}$$

Using this parameter, the CGR eqn.(1.3) is modified as given below

$$\frac{da}{dN} = C(\Delta K_{eff})^n \tag{1.20}$$

Where

$$\Delta K_{eff} = U\Delta K \tag{1.21}$$

In the present work, the model of effective stress intensity range ratio (U) was developed for constant amplitude loading pattern.

The crack opening load is measured from the load displacement record and is taken at the point at which nonlinearity starts. It is schematically shown in **Fig.** 1.1.

1.6.4 Fatigue Failure

The fatigue refers to the behavior of the materials subjected to cyclic loading. ASTM defines fatigue as [**18**]

The process of progressive localized permanent structural change occurring in the material subjected to conditions which produce fluctuating stresses and strains at some points and which may culminate in crack complete failure after a sufficient number of fluctuations.

1.6.5 Monotonic and Cyclic Plastic zone Sizes

Rice[**6**]has shown that crack advance is related to the size of the zone in which the material becomes fully plastic during loading part of the cycle. During loading up to maximum stress with stress intensity factor K_{max}, a plastic zone of width w_p is developed at crack tip (**Fig** 1.3). when the direction of loading is reversed, the local stress is reduced to a level corresponding to stress intensity K_{min}. Since the elastic stress distribution associated with K_{max} is truncated at yield stress by local yielding, reduction of elastic stress distribution from K_{max} to K_{min} leaves residual compressive

stresses at the crack tip. These compressive stresses exceed the compressive yield strength of the material. At K_{min} a small plastic zone experiences alternate tensile and compressive yielding and is known as reversed plastic zone. This reserved plastic zone accompanies the original loading.

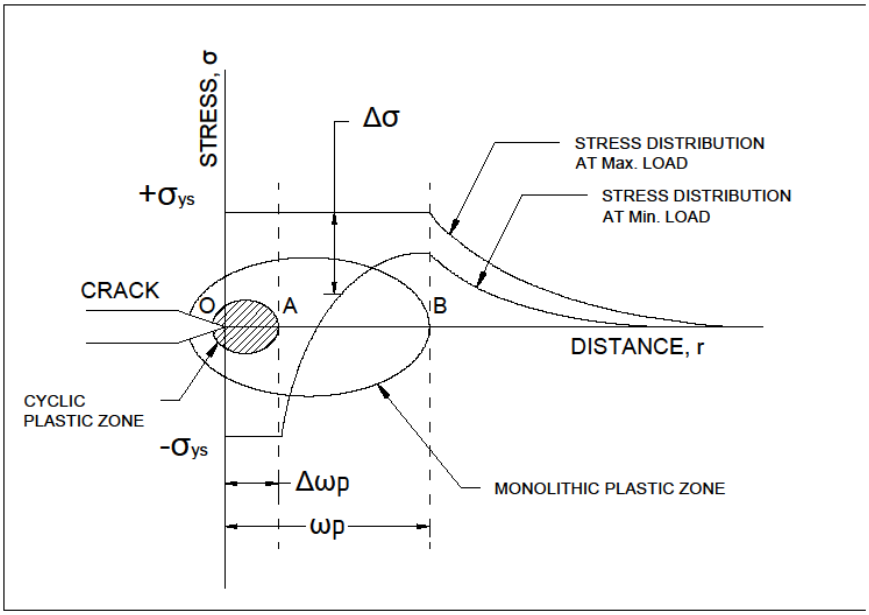

Fig 1.4 Schematic illustration of the monotonic and cyclic plastic zone[**6**]

Rice[**6**] showed that for a perfectively elastic- plastic material having yield stress numerically equal in tension and compression, the size plastic zone can be given by

$$\omega_p = \frac{1}{2\pi}\left(\frac{K_{max}}{\sigma_y}\right)^2 \tag{1.22}$$

$$\Delta\omega_p = \frac{1}{\pi}\left(\frac{\Delta K}{2\sigma_y}\right)^2 \tag{1.23}$$

According to Schijve[**6**], the monotonic plastic zone is significantly larger than the reversed plastic zone. The size of plastic zone is inversely proportional to the square of yield stress. During unloading the stress increment to cause yielding in the reversed direction may be assumed to be equal to twice the yield stress during unloading. The size of cyclic plastic zone can be given by eqns.(1.24) and (1.25).

Reversed plastic zone size = ¼ (monotonic plastic zone)

For plane stress

$$(\omega_p)_{cyclic} = \frac{1}{2\pi}(\frac{K}{2\sigma_y})^2 \quad (1.24)$$

For plane strain

$$(\omega_p)_{cyclic} = \frac{1}{6\pi}(\frac{K}{2\sigma_y})^2 \quad (1.25)$$

1.6.6 Overload Ratio

Overload ratio is defined as the ratio of maximum load is an overload cycle to the maximum load in steady state cycle (see **Fig**. 1.5[**17**])

$$OLR = \frac{P_{OL(max)}}{P_{s(max)}}$$

$$P_{OL(max)} = \text{Tensile overload}$$

$$P_{s(max)} = \text{Maximum Constant Steady Load}$$

1.6.7 Load Parameters

A constant stress amplitude fatigue cycle is shown in **Fig**. **1.5**. Block sequence loading is shown in **Fig 1.6.**The various terms defined are also given in the same **Fig**ure.

1.6.8 Ramberg-Osgood Stress- Strain Relation

This relation is given in the form

$$\varepsilon = \frac{\sigma}{\varepsilon} + K(\frac{\sigma}{\sigma_y})^n \quad (1.26)$$

Where K is the factor related to yield stress of the material. Some times in some material it is difficult to identify the point of yielding.

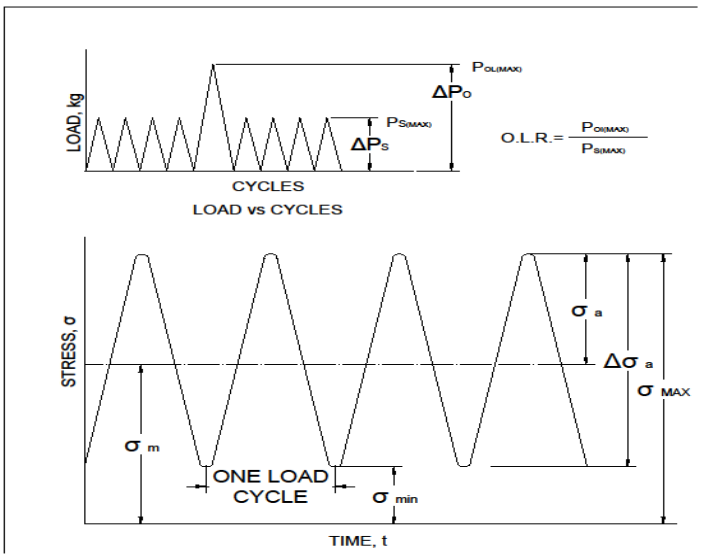

Fig 1.5 A Typical Constant Stress Amplitude and Over load Fatigue Cycle[17]

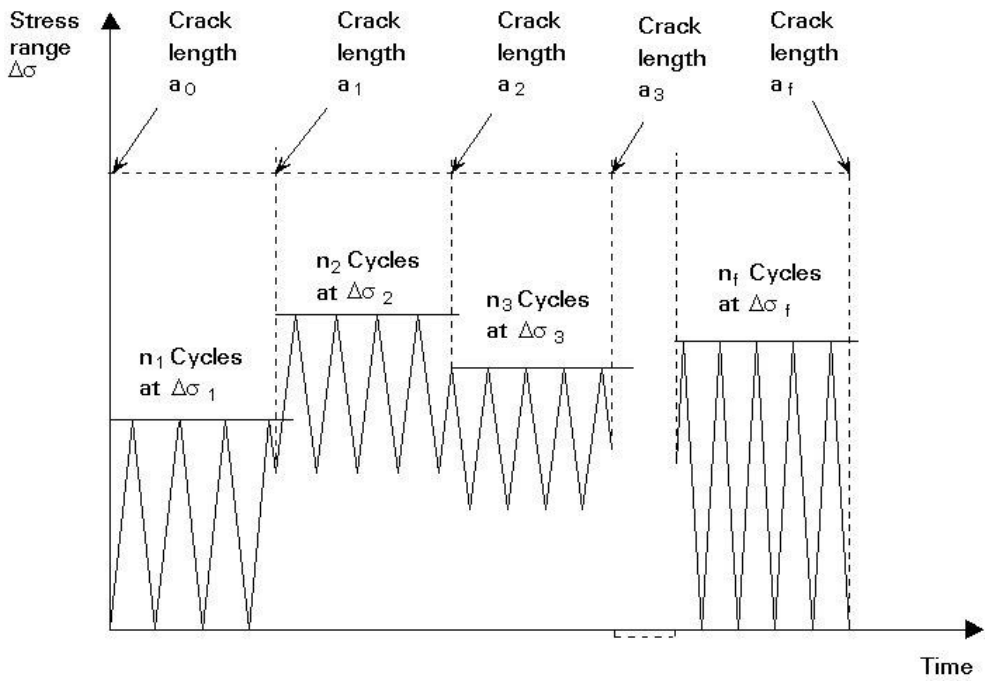

Fig 1.6 Sequence of Block Loading

1.6.9 Fatigue Crack Closure Mechanism

Elber [**8**]observed the tip of fatigue crack to close while a specimen was still subjected to a tensile loading. The load at which crack tip was found to close approximately 50% of the maximum load applied under zero to tension loading. The compressive stresses (Contact stresses associated with closure) transmitted across the crack surfaces during closure were found to alter the state of straining at the crack tip and consequently affected the subsequent crack growth.

In fatigue growth the residual deformation are left in the wake of advancing fatigue crack. This is illustrated in **Fig**. 1.7 which shows the plastic zone and crack tip deformation for a fatigue crack. The dashed curve in **Fig**. 1.7 shows the crack tip deformation for the 'ideal' crack. The residual deformation (The difference in solid and dashed curve in **Fig**. 1.7 affecting reduces the amount of crack opening displacement from that of an ideal 'crack'. When plate is unloaded, the residual deformation cause the crack tip to close at higher load that of an ideal crack. This behavior is shown schematically in **Fig** 1.8. On further unloading, the crack surfaces come in contact more extensively and the material may go under compressive yielding. Upon subsequent reloading the crack opening load is found to be lower than the previous closure load as the compressive stresses alter the crack surfaces residual deformation

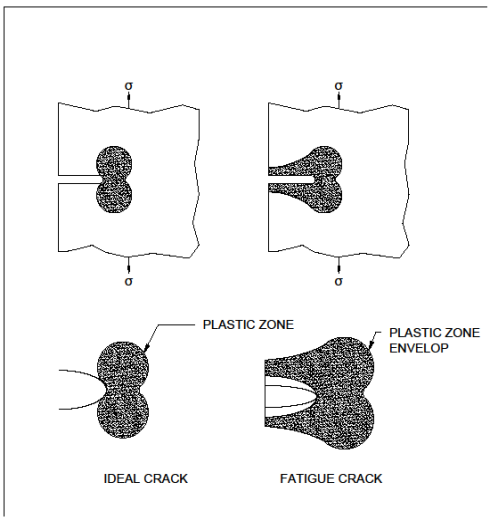

Fig 1.7 Plastic Zones and crack tip deformations for an ideal crack and a fatigue crack

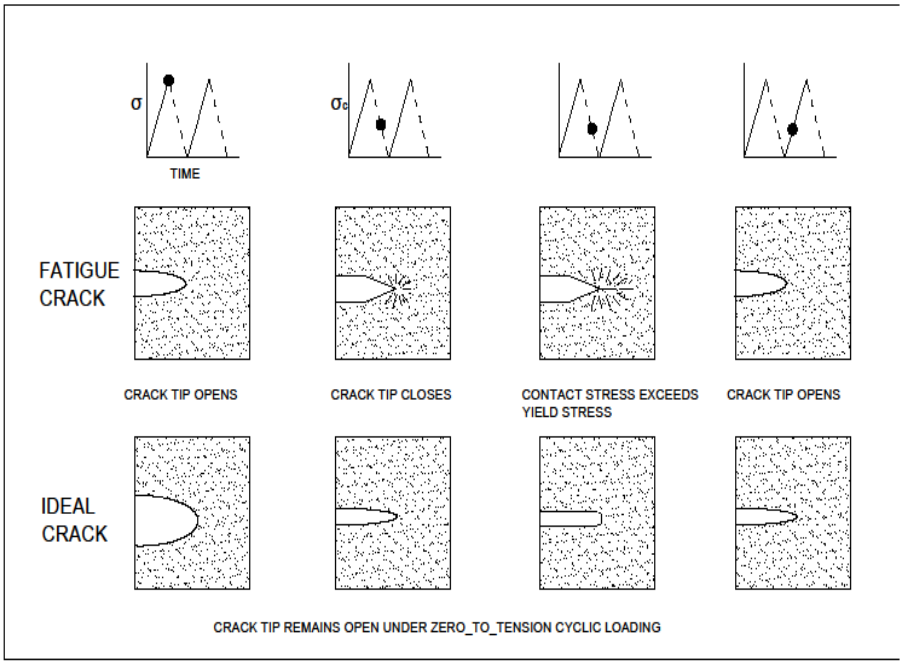

Fig 1.8Schematic of the fatigue crack closure mechanism[8]

1.7 CONCLUSION

A brief introduction to the study of fracture mechanics and the behavior of materials under fatigue has been presented. Crack propagation behavior and crack closure effects under fatigue loading have been discussed.

CHAPTER: 02

2 LITERATURE REVIEW AND THE SCOPE OF THE PRESENT INVESTIGATION

2.1 INTRODUCTION

During fatigue crack propagation, the crack closure is affected by material properties, environment loading and geometry of the specimen. A review of the application of these parameters is presented in this chapter.

It is well established that large stresses produced due to stress concentration at the crack tip are responsible growth. Stress intensity rang (ΔK) at the crack tip is therefore a dominant parameter. Though use of ΔK is a well-established phenomenon in correlating crack growth curves, its use requires experimental determination of constant amount of empiricism. One of the main causes of this deficiency is that derivation of ΔK solely depends upon equilibrium equation.

2.2 FATIGUE CRACK PROPAGATION-STRESS INTENSITY FACTOR APPROACH

Ever since it was realized that crack extension takes place due to stress concentration at the crack tip and due to failure of the material [133] during cycling loading, an effort has being made to relate the crack growth with stress intensity factor at the crack tip. Though the above physical basis has limitations for elasto-plastic

materials due to the presence of large plastic deformation at the crack tip, Paris an Erdogan [86] gave the following relation for fatigue crack growth rate

$$\frac{da}{dN} = C(\Delta K)^n \tag{2.1}$$

Here "C" and "n" are considered to be material dependent. After this relation, a sudden surg in the activity occurred for finding out this form of relationship by evaluating "C" and "n" for different material. A large number of accumulated data showed considerable variation in c and n for different materials. These value were also found to change different loading conditions. It is found that for the different value of "R" for the same materials, a large deviation in data is obtained from the curve fitted by Eqn.2.1.

2.3 EFFECTIVE STRESS INTENSITY RANGE RATIO APPROACH

Elber [**8**] suggested that the use of "ΔK" implies that a crack is closed under the influence of compressive stress and open under tensile tresses. This Assumption is based on the behavior of a saw cut crack of zero width. The fatigue crack differs from a saw cut crack primarily because during crack propagation, a zone of residual tensile deformation is left in the wake of a moving crack tip.

In fatigue crack due to the presence of residual tensile deformation, the load versus crack opening displacement records are quite different compared to those of saw out crack, The Load versus crack opening displacement for saw cut and fatigue crack are shown schematically in [**106**].

The saw cut load/COD records show a linear variation while fatigue load/COD Records is nonlinear. Beyond point A. the applied load is found to vary to vary linearly with crack length suggesting that the crack is fully open. Load corresponding to point A is called the opening load (Pop). Repeated COD records usually show some hysteresis, but occurrence of full crack opening at A and the onset for crack closure at A followed by linear part is easily observed, measurements suggest That points A and A' coincide with each other. Experience however shows that the uploading branch A' gives a slightly better reproduction. From the above discussion

change of load from A to B is called the effective load range (ΔP_{eff}) and crack propagation is assumed to occur during this load change. The Crack opening tress Level is therefore used as reference stress level from which an effective stress rang is obtained. The effective stress range is therefore defined here as

$$\Delta\sigma_{eff} = \sigma_{max} - \sigma_{op} \tag{2.2}$$

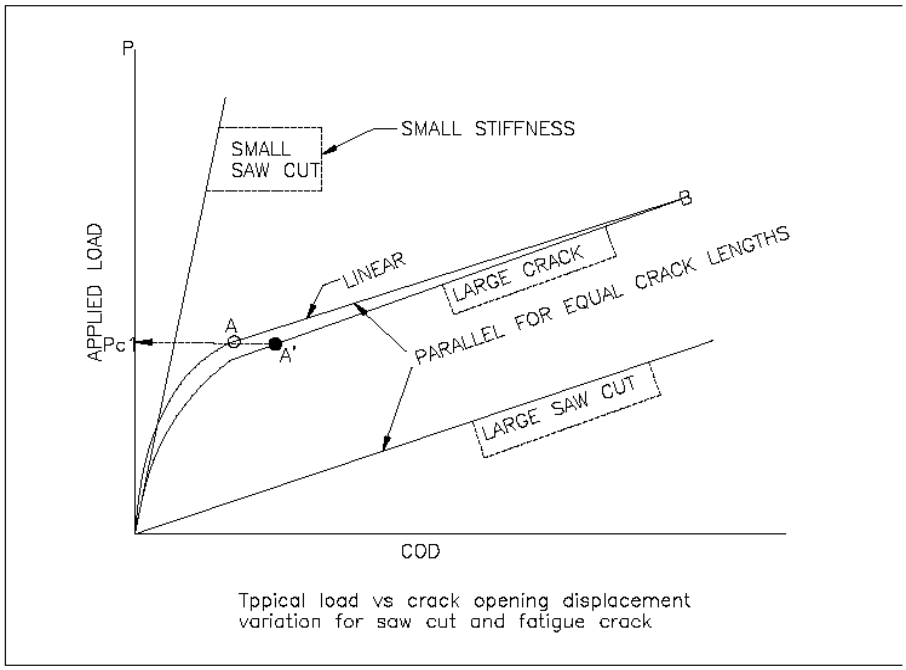

Fig 2.1Load Vs Crack Opening Displacement[8]

The ratio of $\Delta\sigma_{eff}$ to total stress range is defined as effective stress Intensity Range ratio U and is given by following equation:

$$U = \frac{\sigma_{max} - \sigma_{op}(\text{or } \sigma_{cl})}{\sigma_{max} - \sigma_{min}} = \frac{\Delta\sigma_{eff}}{\Delta\sigma} = \frac{1 - \frac{\sigma_{op}}{\sigma_{max}}}{1 - R}$$
$$= \frac{\Delta K_{eff}}{\Delta K} = \frac{K_{max} - K_{op}}{K_{max} - K_{min}} \tag{2.3}$$

Where $K_{eff} = U\Delta K$

The crack propagation rate equation is therefore written in terms of ΔK_{eff} instead of Δk.

The factors which have been reported to influence U are Stress ratio. In the work of Elber However U is shown to depend only as stress ratio, R. (Table2.1 a)

Since Elber introduced this concept, a large amount of work has been done for finding U as a function of stress ratio. R, k_{max} Stress range ($\Delta\sigma$),material properties (σ_y, σ_f) crack length and strain hardening exponent (n). A review of this work is presented here.

2.4 CRACK CLOSURE STUDIES

Most of the work on crack closure is experimental and only a few have suggested analytical approach. We will review here both analytical and experimental works for both constant amplitude loading and variable amplitude loading.

2.4.1 Crack Closure Studies under Constant Amplitude loading

2.4.1.1 Analytical Studies

Lal and Garg [**46**] have suggested a simple mathematical model to evaluate factor U, the crack tip displacement during loading was obtained by assuming material to be elasto-plastic assumed to behave elastically. This method in some details is discussed here:

Fig.2.2 shows a typical fatigue cycle having the constant stress range ($\Delta\sigma$) and stress ratio $R=\sigma_{min}/\sigma_{max}$.The fatigue specimen is loaded first in the tensile portion of the Stress cycle from O to A causing concentration tensile stresses near the crack tip. The loading O and A give crack displacement V_c which is brought to zero at B during unloading. The Crack tip opening displacement can be determined by Dugdale plane Stress analysis [**9**].

In this analysis it is assumed that material outside the plastic zone obeys Rambarg-Osgood [**26**] stress-strain relation. The Dugdale model of fatigue crack is shown in the Griffith analysis [**104**] is applicable to linear fracture mechanics. The crack

closing displacement due to loading from C to D is found from Griffith theory [**104**]. Lal and Garg[**63**] have suggested that the plastic zone width are given by

$$\frac{\omega_p}{a} = \left(\frac{\sigma_{OA}}{\sigma_y}\right)^{1+n} \tag{2.4}$$

$$\frac{\omega_p{}'}{a} = \left(\frac{\sigma_y{}^t}{\sigma_y}\right)^{1+n} \tag{2.5}$$

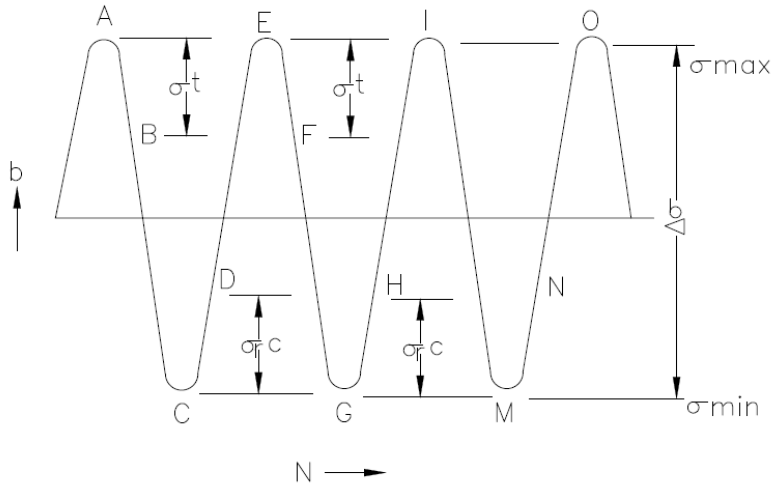

Fig 2.2A General Stress Cycle Pattern[**17**]

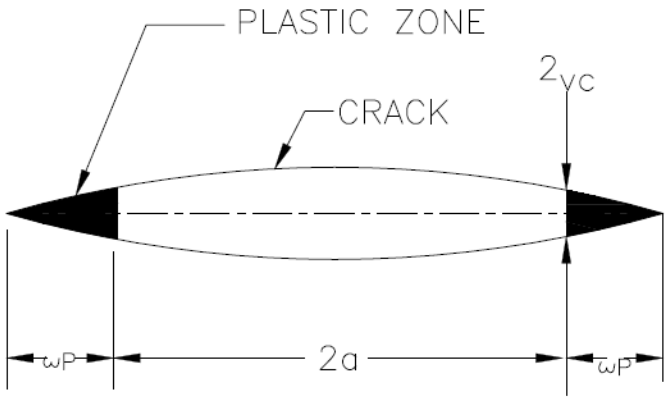

Fig 2.3Dugdale's Model of Fatigue Crack[**9**]

The effective stress intensity range ratio,U_1 after the first cycle, is given by equation 2.6 (see **Fig**.2.2).

$$U_1 = \frac{\sigma_{DE}}{\Delta\sigma}\left(\frac{\Delta\sigma - \sigma_r^C}{\Delta\sigma}\right) \quad (2.6)$$

This above analysis can be applied to successive stress cycles. The tensile and compressive relaxation range σ_{EF} and σ_{GH} for the second stress cycle is given by equation 2.7 and 2.8.

$$\sigma_{EF} = \sigma_y\left[0.45\ln\left\{1 + \left(\frac{\sigma_{DE}}{\sigma_y}\right)^{1+n'}\right\}\right]^{2/(3+n')} \quad (2.7)$$

$$\sigma_{GH} = \sigma_y\left[0.45\ln\left\{1 + \left(\frac{\sigma_{FG}}{\sigma_y}\right)^{1+n'}\right\}\right]^{2/(3+n')} \quad (2.8)$$

The effective stress range for fatigue crack growth and applied stress range $\Delta\sigma$ is denoted U_2 which is given by

$$U_2 = 1 - U_2^C(1 - U_1U_2^t) \quad (2.9)$$

Where

$$U_2^t = \frac{\sigma_{EF}}{\sigma_{DE}} \text{ and } U_2^C = \frac{\sigma_{GH}}{\sigma_{FG}}$$

Similarly, the value of effective stress intensity range ratio for and successive stress are obtain as

$$U_3 = 1 - U_3^C(1 - U_2U_3^t) \quad (2.10)$$

$$U_n = 1 - U_n^C(1 - U_{n-1}U_n^t) \quad (2.11)$$

Where $U_n$is the effective stress range ratio after n cycles.

It is clear from the above analysis that the values of U_n are independent of instantaneous crack length. It has been concluded that stabilized value of effective stress intensity the component.

Newman [**88**] using finite element technique, analyzed a fatigue cycle and found that crack closing load gets stabilized after a few loading cycle.

2.4.1.2 Experimental Studies

In the past various methods have been used for establishing the crack opening and closing points. Most of the methods depend upon indirectly the opening and closing points from load displacement diagrams obtained from the loading curve. A displacement gauge is usually mounted either across the crack or at the mouth and the load displacement curve is taken. The change in the slope of the load/displacement curve gives an indication of certain amount of judgment is essential.

Some workers have tried ultrasonic and electric potential methods also. But because of difficulties in interpreting the results the COD method is still considered superior to other method. A review of work reported in the literature using above methods is given in Tables 2.1a b and c.

2.4.1.3 Classification of Crack Closure Work

The review work on crack closure is divided in the following categories.

- **i)** Constant Amplitude Loading (Table 2.1a)
- **ii)** Single peak loading (Table 2.1b)
- **iii)** Programmed loading (Tables 2.1c)

2.4.1.4 Constant Amplitude loading

This work is further divided in the following categories

- **i)** Dependence of crack closure on stress ratio,R
- **ii)** Dependence of crack closure on stress ratio R, K_{max} and ΔK.
- **iii)** Dependence of crack closure on material properties
- **iv)** Dependence of crack closure on environment and instantaneous crack length.
- **v)** Classification on the basis of the crack closure measurement techniques.

2.4.1.5 Dependence of Crack closure on Stress ratio, R

A large number of research workers have that for a given material; U is Only a function of R and is independent of other parameters. This work is given in Table 2.1a from 1 to 5 serial numbers, Elber [**28**], Katcher and Kaplan [**59**], Sachjve [**107**] and Maddox et al.[**67**] developed model for U as function of R Only. The Elber's Model is valid for -0.1<0.7. Katecher and Kaplan observed no crack closure after stress ratio 0.3. Sachjve's [**107**] model is based on analytical work of Newman [**78**]. He [**107**] found U to be a function of second order polynomial in R. The model is valid for both positive and negative Value of R. Buck et al. [**11, 12**] found that U increases from 0.30 to 0.62 for increasing R values. As R increases crack closure load decreases in all the cases. **Fig**.2.4 shows the relation between U for various materials tested by many authors [**28, 54,107**].

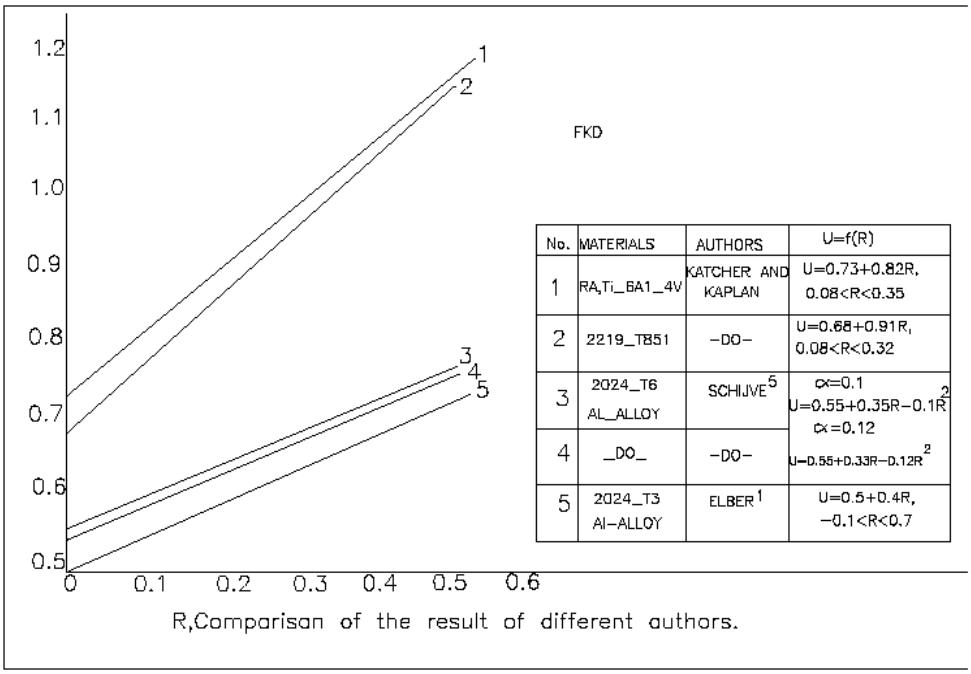

No.	MATERIALS	AUTHORS	U=f(R)
1	RA,Ti_6A1_4V	KATCHER AND KAPLAN	U=0.73+0.82R, 0.08<R<0.35
2	2219_T851	-DO-	U=0.68+0.91R, 0.08<R<0.32
3	2024_T6 AL_ALLOY	SCHIJVE[5]	α=0.1 $U=0.55+0.35R-0.1R^2$
4	_DO_	-DO-	α=0.12 $U=0.55+0.33R-0.12R^2$
5	2024_T3 Al-ALLOY	ELBER[1]	U=0.5+0.4R, -0.1<R<0.7

Fig 2.4U Vs R for various materials tested by many authors

2.4.1.6 Dependence of Crack closure on Stress ratio R, K_{max} and ΔK

According to some other workers U depends on R, K_{max} and ΔK. Bachmann and Munz [**4,6**] and Chand[**17**] developed model for U as a function of K_{max} and R. Srivastava [**105**] developed model for U as function of ΔK and R. Bachman and Munz [**6**], Staal and Elen [**116**]. Chand [**107**] and Irvin et al.[**21, 23, 35, 36, 37, 39 53,54**] show that U tends to increase for increasing $K_{max.}$

Srivastava [**105**] shows that U is a function of ΔK and R. U tends to increase with increase with increasing ΔK. Shih and Wei [**101,102**] Franden et al. [**32**], Adoms [**11**] and Unangst et al.[**106**] show that U tends to decrease for increasing K_{max}.

The results of these works are contradictory to Bechmann and Munz [**6**] and other researchers [**17, 20, 22, 24, 26, 28, 40, 54,106**]. Clark and Cassat [**20**] found that for specimen thickness 6.35 and 25.40 mm U increased with increasing with increasing K_{max} but for thickness 12.70mm it decreased. Sharpe et al. [**100**] found difference in crack closure load due to use of difference crack closure measuring techniques.

2.4.1.7 Dependence of crack closure on Material Properties

Some research workers found that U is a function of stress ratio and material properties. Lal and Garg [**65**], Homma & Nakazawa [**78**] and Bell and Creeger [**8**] developed model for U as function of R and material properties like yield stress, cyclic hardening exponent etc. Elber [**29**] and Schijive [**104,106**] showed that crack closer load is lesser in presentation material in comparison to as received material due to higher yield strength.

2.4.1.8 Dependence of crack closure on environment and geometry

Bechmann and Munz [**5**], Irving et al. [**54**], Homma &Nakazawa [**47**], Moris & James [**75**], Ohta et al.[**35**] and Ho et al. [**45**] found change in U with gauge location along the crack line. Schijive [**106**], Srivastava [**105**] and Lal and Garg [**65**] found that crack closure load is independent of instantaneous crack length. Schijive

[**105**] also showed the crack closure load was same in all three environments (Vacuum, air, and salt water).

Buck [**13**] found lower crack closure loads in moist in comparison to dry atmosphere. Schijve [**106**] found lesser crack closure load in thick material. Unangst et al. [**106**] and Clark and Cassat [**20**] showed that crack closure depends on thickness of the material. If thickness of material increases crack closure load decreases.

2.4.1.9 Classification on the basis of crack closure Measurement Techniques

The methods used in experimental studies are classified into two broad categories; surface measurement techniques and bulk measurement techniques.

(i) The surface measurement techniques include strain gauges, optical means of monitoring surface displacements and Elber type crack tip compliance gauge.

(ii) The bulk measurement techniques include acoustic, potential and photoelectric method.

Out of all the methods used, COD gauge technique has been found to be most reliable [**6, 43, 45, 48, 49, 60, 62, 64, 67, 70, 72, 78, 80, 83, 87, 90, 94, 106**].

2.4.1.10 Conclusions

From the above review following conclusions are drawn:

1. According to some workers [**8, 28, 59, 67, 95, 107**] U is a function of R only and is independent of other parameters.

2. According to some others [**1, 4, 20, 101, 102, 103, 104, 105, 106, 107, 108**] the value of U increases with increase in R but the effect of K_{max} on U is not well established. In some cases [**6, 32, 101,106**] it has been reported that U increases with increase in K_{max} while in others [**1, 101,102**] it is found to decrease.

3. Crack closure is not observed at higher values of R [**32, 54, 101, 102**]

4. Crack closure measurement technique is found to influence the result of crack closure stress, σ_{c1} [**5**].

5. Material properties are found to affect crack closure [**10, 47, 104**]

6. Specimen geometry is found to affect the crack closure [**20, 32, 106**].

Crack closure is found to be influence by thickness of the material (i.e. plane stress or plane strain case), and environmental effects.

Table 2.1Researches on Constant Amplitude Loading

Sl. No.	**Author**	**Equation for U**	**Material and geometry Of Fatigue Specimen Used.**	**Experimental Techniques Used**	**Remark, Factors affecting crack closure or U**
1.	Elber, wolf [**28**]	$U=\frac{\sigma_{max}-\sigma_{cl(\sigma op)}}{\sigma_{max}-\sigma_{min}}$ $U=\frac{\sigma_{max}-\sigma_{cl}(\sigma_{op})}{\sigma_{max}-\sigma_{min}}$ U= 0.5 + 0.7 Where -0.1<R<0.7	2024-T3 Al-alloy Centre cracked panel of 5mm thickness and 130mm width	Crack tip compliance gauge (or Elber gauge) with gauge lenth 5mm	He observed the dependence of U on stress ratio R only (for 80.5<ΔK<96 .6 kg/mm$^{3/2}$)

2.	Katchera nd Kaplan[**59, 80, 82, 84**]	U=0.68+0.91 R, Where 0.08<R<0.32 U=0.73+0.82 R, Where 0.08<R<0.35	i) 2219-T851 Al-alloy ii) RA Ti-6A1-4V Titanium alloy compact tension specimen H/W=0.6 i) B=25.3mm ii) B=18.3mm	i) LVDT, strain gauge ii) Elber type gauge	They found U to depend on R and a/w, but independent of K_{max} , They also observed that U>1.0 (no crack closure) for maximum limiting value of R.
3.	Schijve [**10, 7**]	U=0.55+(0.45-α) R+Ω R^2 Where α values varying from 0.10 to 0.15	2024-T3 Al-alloy	Based on analytical work, of Newman [78]	He found U to be a function of R (second order polynomial). The model of U is valid for both positive and negative R values(as low as R= -1). For 2024-T3 Al-alloy

					α=1.12 fits all data.
4.	**[105, 106]**	Plane strain $\omega_p = \frac{1}{6\pi}(\frac{K_{max}}{\sigma_y})^2$ Plane stress $\omega_p = \frac{1}{2\pi}(\frac{K}{\sigma_y})^2$	2024-T3 and 7075-76 Al-alloy center cracked specimen	COD Measurement GL= 4 mm at, a=5,10,15, 20.	He found **i-** U is independent of crack length. **ii-** Lesser crack closure in thicker material, due to smaller plastic zone. **iii-** Crack closure is not dependent on tensile mode or shear mode. **iv-** Crack closure stress is same in all three

					environments (vacuum, air and salt water) **v-** Crack closure load gets stabilized for CAL Loading.
5.	Maddox et al. [**67**]	U=0.75+0.25 R, and U=0.722+0.278 R,	Steel A σ_y=435 N/mm^2 σ_u=546 N/mm^2 Steel c σ_y=379 N/mm^2 σ_u=479 N/mm^2 Centre cracked Specimen	i- Electrical potential drop. ii- Strain gauge. gauge length 2 or 3 mm	They found U to depend on stress ratio R only.
6.	Bachmann and Munz [**4**]	K_{op}=6.67R+4.27 $U=\frac{1}{1-R}\left[1-\frac{6.67R}{K_{max}}-\frac{4.27}{K_{max}}\right]$	Ti -6Al-4V Titanium alloy CT-specimen	Extensometer developed by Nowack [82] with	They found no consistent effect of a/w on U, but did observe U to

				gauge length 1.5mm	increase with K_{max} (U=0.7 to 0.9 for K_{max} increasing 41.9 to 90.29 kg/mm$^{3/2}$). Finally they concluded U is dependent on both R and K_{max}.
7.	Chand, Satish [**117**]	$U=\frac{K_{max}}{1000}(8.80R+60)$	6063-T6 Al-alloy Centre cracked specimen	COD gauge GL=4mm	Crack closure load is found to decrease as K_{max} increase. For larger value of R no crack closure is observed. He found U to be a function of K_{max} and R.
8.	Srivast-ava [**115**]	$U=\{(13.5R+5.925)/1000\}\Delta K+1.15R+0.22$	6063-T6 Al-alloy Centre cracked specimen	COD gauge (GL=6mm, 2mm)	He found that U is function of R and ΔK. He also found

					that crack opening load is independent of instantaneous crack length.
9.	Lal and Garg [**62,65**]	$U = \frac{R}{60} + \frac{2}{3}\left(\frac{\Delta\sigma}{\sigma_{ys}}\right)^{\frac{1-n'}{4}}$	6063-T6 Al-alloy 6061-T6 Al-alloy Centre cracked Specimen	Eddy current technique	They found U to depend on the applied stress range $\Delta\sigma$, stress ratio R, yield strength σ_y and strain hardness exponent of the material. They also concluded that the value of U reachesasTable value after about 10 cycles. This Table value of effective stress range factor

					remains constant throughout the cyclic life of the component.
10	Newm-an [**106**]	$U=(1+qR)^n$ C,q and n are material constant	2291-T851A Al-alloy	Finite element technique	He found that crack opening and crack closing loads are same.These loads reach asTable value after few cycles For closure pattern.
11	Bell and Creager [**12**]	$U=(1-C_f)/1-R$ where $C_f=\sigma_{op}/\sigma_{max}$ $C_f=C_f\ -1^+$ $(C_{fo}-C_{f-1})$ $(1+R)^p$ Where $C_{f-1}=C_f$ at R=-1 and $C_{fo}=C_f$ at R=0 And p is exponent	I)2219-T851 Al-alloy and II)Ti-6Al-4V titanium alloy	Strain gauge and mechanical displaceme nt gauge	According to him the crack closure depends on stress ratio and material properties. The values of the constants are given below I) For 2219-T851 Al-

					alloy C_{fc}=0.347,C_{fo}=0.40, P=3.93, C=7.39X10^{-10} And m=3.34 II)For Ti-6al-4v titanium alloy C_{f-1}=0.332,C_{fo}= 0.40, p=3.3, C=3.08X10^{-10} m=3.08
12	Morris,James and Beck [**75, 86**]	$U \propto \sigma\sqrt{cx}$	Ti-6Al-2Sn-4zn-6Mo alloy	Scanning Electron microscope	A model is proposed which describes the effect of fracture surface roughness
13	Roberts and Schmidt [**95**]	He could not give the model for U	2024-T3 and 7075-T6 Al-alloy compact Tension	Strain gauge Technique	The authors observed a value of U=0.8 for R=0 and

			specimen H/W=0.6 W=63.5 mm B =3.2mm for First material and B=6.36 for second material		K_{max} ranging from 28.38 to 53.3 kg-$mm^{3/2}$ in contrast to U=0.5 found earlier by Elber [**8**]
	R.Ku-mar [**78**]	$U=\frac{\sigma_y}{42}+0.5R$	6061 T6 Al Alloy & 6063 T6 Al Alloy SEN specimen were used at different prestrains.	Strain gauge Technique	In CA loading Crack closure and crack opening points are found equal. After stabilized for all cases.

2.4.2 Effect of single overload on crack closure

The research on crack closure for simple variable amplitude loading & single overload can be studied under two categories (Table 2.2)

- Studies using Finite Element
- Experimental observation

Table 2.2Researches under CAL with Single overload

Sl. No.	Author	Equation for U(ESIRR)	Material and geometry Of Fatigue Specimen Used.	Experimental Techniques Used	Remark, Factors affecting crack closure or U
1	Newman [**80**]	$\Delta K_o = \frac{1-\frac{\sigma_o}{\sigma_{max}}}{1-R}\Delta K_{th}$	2219-T851 Al –Alloy CT Specimen	Finite Element Method	It was concluded that the retardation and acceleration phenomenon in variable amplitude loading are closely related with crack closure phenomenon.
2	Newman [**81**]	$\frac{da}{dN} = G\Delta K_{eff} C_2 \left\{\frac{1-(\frac{\Delta K_e}{\Delta K_{eff}})^2}{1-(\frac{K_{max}}{CJ})^2}\right\}$	2119-T851 Al-Alloy CT Specimen	Finite Element Method	An analytical crack closure model proposed crack growth

					law predicted crack growth in all spectrum load tests quite well.
3	Chanani Mays[**16**]	No Expression was given	7075-T6 Al Alloy SEN Specimen	Strain Gauge	The delay depends upon specimen geometry, thickness and sensitivity of the instruments. This work shown that the crack closure hypothesis is not universally applicable and needs more investigation.

2.4.3 Finite Element Method

The result [**78,84**] show that in a CAL test with single peak high load cycle, the crack closure load rises to a maximum level and after a certain closure load rises to a maximum level and after a certain crack extension, it decreases asymptotically corresponding to constant amplitude load test as the magnitude of a single peak high load increases, the closure load also riser. The same characteristic behavior of the crack closure load was observed for Hi-Lo load sequence In Lo-HI load sequence test, the value of crack closure decreases to a high level and then start to increase and later gets stabilized for high load level.

A peak low load cycle just after the peak high load cycle relaxes the peak high load cycle effect on the crack closure. No effect of peak low load cycle just before the peak high load cycle on crack closure was observed.

2.4.4 Experimental Observation

Elber [**8**] observed that crack closure phenomenon could account for acceleration and retardation effect in crack propagation ,Further, Brown and Weertman [**107**] conducted crack closure experiments using an extensometer placed across the crack during CAL test with intermediate single and multi-peak high loads The stress ratios of CAL loads in these tests were chosen as 0.05,0.075 and 0.050 After removal of peak high load (CAL,R=0.05),it was found that the crack closure load rose to a maximum value at about the same crack length at which crack growth rate become minimum For CAL, R=0.5,no closure was observed before and after the application of peak high load cycle through crack growth rate retardation was observed .A large compressive spike also depressed the crack closure load.

Chanani and Mays [**16**] found no significant change in crack closure load after the application of single and multiple peak high load cycles in a CAL test. Arkema [**91**] conducted crack closure experiments on 2024-T Al-alloy in a CAL test (R=0.67) with an intermediate single peak high load cycle. The crack closure load in a CAL test, before the applications of intermediate peak high load cycle was below the minimum

load level. Later it started to increase and reached a maximum value which after some cycle started to decrease and reached below minimum load level.

Sharpe at al [**100**] found the crack closure load to increase with the application of an overload and then decrease to the original value. They found different crack closure loads by laser technique and strain gauge technique Musil and Stepphens [**76**] observed delay in crack growth after single tensile overload. They found good agreement between crack closure predicted delay and experimental observed delay.

Schijve [**106**]found that after an intermediate peak load the closure load increased significantly. Thereafter, when the test was cycled with a constant amplitude loading, the crack closure load started to decrease and then reached its previous stabilized value. Same pattern was found in Hi-Lo load sequence. In Lo-Hi load sequence the closure load first increased and then reached as Table value during the second sequence load.

2.4.5 Conclusions

1. The finite element analysis shows that the calculated crack-closure and crack opening load under either constant amplitude or simple block person loading were consistent with experimental observation.

2. The experimental crack closure data available in the literature is limited and only few workers have tried to correlate the crack closure with load parameters. The trend of experimental of crack growth delay is explained by crack closure concept.

3. If the amplitude of single peak load is increased, the crack closure load is also increased. After a few cycles however, it tends to reach as Table value.

4. The trends of crack growth rates for the different tests have different value of stress ratios of constant amplitude load is same, although the crack closure is not observed between the minimum and maximum loads.

2.4.6 Effect of Programmed and block loading on Crack Closure

The review work of the type of loading is given in Table 2.3, The crack closure load data in block and programmed loading is hardly available in the literature, expect that some crack closure record were taken during flight simulation tests [**102,103**] using COD gauge .It was observed that crack closure load were qualitatively in agreement with the results of simple pattern.

Table 2.3 Researches under block loading

Sl. No.	**Author**	**Equation for U**	**Material and geometry Of Fatigue Specimen Used.**	**Experimental Techniques Used**	**Remark, Factors affecting crack closure or U**
1	Pelloux et al.[**85**]	No expression was given	2124-T35 Al Alloy CT Specimen	Electron Fractrography	Crack closure effect are relatively small in the plane strain region. The crack retardation effect was due to peak loads. Closure stresses increased after peak

					load.
2	Lindely & Richards [66]	No Expression was given	Various Steel SEN Specimen of different thickness	COD	Closure does not occur under plane strain condition.
3	Sunder & Dash[21]	$\sigma_{op} = \sqrt[q^{1-n}]{f_0^1(1-S_{op}(z)^m\alpha_z}$ Where $z=\frac{2z}{\tau}$ $S=\frac{\sigma_{op}}{\sigma_{max}}$	DDT-546 Al-Cu Alloy SEN Specimen	COD	Electro Fractrography confirms the existence of crack closure. U stabilize after some crack growth

2.4.7 General Conclusion

1. In constant amplitude loading crack opening/closing load remains constant. Its value is found to depend upon R, S_y and K_{max} as found by many workers using different techniques for finding crack opening loads.

A large number of workers using Elber type gauge however suggest that for a particular material crack closing load is a function of R only. In some cases work with D.C. potential and ultrasonic transmission techniques suggest the dependence of crack closure on k_{max} also.

2. If an overload is given during Constant Amplitude Loading, the crack closure load first decreases, but further cycling it is found to slowly increase and approaches a value corresponding to that obtained for CA loading.

3. In Hi-Lo load sequence, the crack opening load slowly approaches a value corresponding to lower value of load.

4. In Lo-Hi load sequence, the crack opening loading slowly approaches a value corresponding to high value of load.

2.5 FINITE ELEMENT METHOD

While several analytical method have been used for the determination of stress intensity factors in linear elastic fracture mechanics and the general behavior in elastic-plastic fracture mechanics, finite element method has been found to be very versatile in handling all types of problems in fracture and fatigue. A brief review of finite element based literature relevant to the present investigation is presented below. Early studies on fracture have been carried out by Swedlow [**56**] **,** Chan el at [**57**] and Kobyashi [**58**]. A direct application of the method for the determination of stress intensity factors by these investigation and others raised certain questions about convergence and reliability. Several crack tip elements with embedded singularity have been proposed. The advisability and convenience of the use of such elements have also been questioned by different investigators. An exhaustive discussion of these investigations can be found in the reviews by Hilton and Sih[**60**]and Gallagher[**61**] . The application of computational procedures for the simulation of non-linear fracture mechanics has been reviewed by Rice [**8**]. The problem of steadily growing crack under constant or monotonically increasing load has been treated by Kobyashi et al [**70**]**.** Anderson [**75**] analysed the steadily growing crack in an elastic plastic material. Crack growth was modeled in his work by simultaneously relaxing the crack tip nodal force and moving the finite element mesh. Newman [**103**]in his extensive work studied the crack closure behavior under constant and variable amplitude loading on a moving crack under cyclic load. He adopted a quasi-static approach wherein the crack tip was advanced through one element width along the crack path for each cycle. The material was assumed to be elastic and ideally plastic. Ogura & Ohji et al [**89**]used a similar

approach and studied the behavior of a moving crack under cyclic loading. All the works reported above on crack closure report the general trends of behavior under specific loading and boundary conditions on some standard specimens and no comparison between numerical and experimentally results have been attempted. The works of Luxmoore et al [**90**]is the only investigation in this direction.

The present investigation is concerned with the determination of crack opening and closing stresses under constant amplitude fatigue loading conditions for materials having different work hardening exponent both theoretically, experimentally and analytically.

2.6 SCOPE OF PRESENT INVESTIGATION AND ORGANIZATION OF THE THESIS

2.6.1 The main purpose of the present investigation is fourfold

- **i)** Development of an experimental set up for the study of crack propagation behavior using a fatigue testing machine and indigenous instrumentation.
- **ii)** Extensive experimental results for side edge notched specimen in plane stress under different loading conditions.
- **iii)** Finite element method application Abaqus® for the study of crack closure behavior under fatigue of side edge notched specimen.
- **iv)** Comparison of experimental results with the analytical result for various types of materials.

The thesis has been divided into seven chapters. The Chapter 01 presents an introduction to the subject of fracture under fatigue loading. Chapter 02 presents a detailed literature survey of the experimental and finite element based research on fatigue and the scope of present work. The Chapter 03 presents the details of the development of an FEM procedure for studying the phenomenon of crack closure. Chapter 04 presents implementation of FEM application Abaqus® 6.10 describes implementation of FEM application Abaqus® 6.10 for determining the effect of work hardening exponent on side edge notched specimens subjected to CAL fatigue loading.

Finite element results for fatigue crack propagation and comparison with experimental trends have been studied. Chapter 05 describes implementation of FEM application Abaqus® 6.10 for determining the effect of work hardening exponent under CAL with single over load fatigue loading. Finite element results for fatigue crack propagation and comparison with experimental trends have been studied. Chapter 06 describes implementation of FEM application Abaqus® 6.10 for determining the effect of work hardening exponent under block loading conditions. Detailed comparison of experimental and analytical results is presented. The thesis ends with conclusions and suggestions for future work in Chapter 07.

2.7 CONCLUSION

The importance of research on fatigue crack growth behavior has been emphasized. A review of experimental and finite element based research has been presented. The aim and scope of the present investigation has been discussed.

CHAPTER: 03

3 FINITE ELEMENT METHOD

3.1 INTRODUCTION

This chapter describes the elasto-plastic finite element method based computer application Abaqus® 6.10 to analyze the mechanics of a propagating fatigue crack in a side edge notched (SEN) panel.Features like non-linear strain hardening behavior of the material in the plastic range, the crack closure effects, effects of residual stress changing boundary conditions with crack propagation, block loading etc. are taken care of in the analysis. The accuracy of the application has been tested with known solutions. Results for copper sheet specimen with a symmetric central hole having fixed grips at both ends under monotonic loading upto the plastic range have been compared with experimental values. The computer application is applicable to a center notched specimen with symmetric configuration with crack propagating transverse to the loading axis, the loaded boundary being parallel to the direction of the notch.

3.2 FINITE ELEMENT METHOD

In finite element analysis an approximate solution to a complicated problem can be obtained by subdividing the region of interest into a finite number of discrete elements and representing the solution within each element by a simple function. In the

displacement formulation of FEM for problem of elasticity and plasticity, the displacement components in each element are expressed as simple polynomials.

For practical purposes the polynomial must be truncated to a finite number of terms. Thus the number of elements in a structure must be large enough so that the displacement function for each element closely approximates the exact displacements in that particular region. The numerical solution should converge to the exact solution as the size of the elements became small. For the displacement formulation, it has been shown that under certain conditions the solution provides a lower bound to the exact displacements[45]. For this convergence to be assured, certain conditions must be met:

1) The displacement function must be chosen so that rigid body displacements do not cause straining of the element.

2) The function must be chosen so that a constant state of strain is obtained as the element size approaches zero.

The simplest polynomial function which satisfies these two requirements and also maintains compatibility between adjacent elements is the linear displacement function.

A typical triangular element, M, is shown in Fig.(5.1) with nodes I,j and k numbered in an anticlockwise direction. The Linear displacement function which defines the displacements within this element is given by

$$U = \alpha_1 + \alpha_2 x + \alpha_3 y \tag{3.1}$$

$$V = \alpha_4 + \alpha_5 x + \alpha_6 y \tag{3.2}$$

Where the constants $\alpha_1 \ (i = 1 \dots \dots \dots 6)$ are determined from the nodal displacements and nodal coordinates as

$$\begin{Bmatrix} \alpha_1 \\ \alpha_2 \\ \alpha_3 \end{Bmatrix} = \frac{1}{2A_M} \begin{bmatrix} a_i & a_j & a_k \\ b_i & b_j & b_k \\ c_i & c_j & c_k \end{bmatrix} \begin{Bmatrix} U_i \\ U_j \\ U_k \end{Bmatrix} \tag{3.3}$$

$$\begin{Bmatrix} \alpha_4 \\ \alpha_5 \\ \alpha_6 \end{Bmatrix} = \frac{1}{2A_M} \begin{bmatrix} a_i & a_j & a_k \\ b_i & b_j & b_k \\ c_i & c_j & c_k \end{bmatrix} \begin{Bmatrix} V_i \\ V_j \\ V_k \end{Bmatrix} \tag{3.4}$$

Where A_M is the cross-sectional area of the element. The coefficientsa_i, b_i, c_i are given by

$$a_i = X_j Y_k - X_K Y_j \tag{3.5}$$

$$b_i = Y_j - Y_k \tag{3.6}$$

$$c_i = X_k - X_j \tag{3.7}$$

Where X_i and Y_i are the co-ordinates of the nodal points. The other coefficients are obtained by cyclic permutation of the subscript I, j and k.

The strain at any point within an element is defined in terms of the displacement derivatives as

$$\{\varepsilon\} = \begin{Bmatrix} \varepsilon_x \\ \varepsilon_y \\ \gamma_{xy} \end{Bmatrix} = \begin{Bmatrix} \frac{\partial U}{\partial x} \\ \frac{\partial V}{\partial y} \\ \frac{\partial U}{\partial y} + \frac{\partial V}{\partial x} \end{Bmatrix} \tag{3.8}$$

From equations 3.1 to 3.5 the strains are written in terms of nodal displacements and co-ordinates as

$$\{\varepsilon\} = [B]\{U\} \tag{3.9}$$

Where $\{U\}$ is the generalized nodal displacement vector ($\{U\}^T = \{U_i,\ V_i,\ U_j,\ V_j, U_k, V_k\}$) and

$$[B] = \frac{1}{2A_M} \begin{bmatrix} b_1 & 0 & b_j\, 0 & b_k & 0 \\ 0 & c_1 & 0\ c_j & 0 & c_k \\ c_1 & b_1 & c_j\, b_j & c_k & b_k \end{bmatrix} \tag{3.10}$$

The superscript ‘T’ denotes the matrix transpose.

For linear-elastic and isotropic materials, the relationship between stresses$\{\sigma\}$,$\{\varepsilon\}$ and any initial stresses $\{\sigma^o\}$ which may exist in the element is given by

$$\{\sigma\} = \begin{Bmatrix} \sigma_x \\ \sigma_y \\ \tau_{xy} \end{Bmatrix} = [D_e]\{\varepsilon\} + \{\sigma^o\} \tag{3.11}$$

Where $[D_e]$ is the elasticity matrix. The matrix $[D_e]$for plane stress

conditions ($\sigma_z = 0$) is given by

$$[D_e] = \frac{E}{1-PR^2}\begin{bmatrix} 1 & PR & 0 \\ PR & 1 & 0 \\ 0 & 0 & (1-PR)/2 \end{bmatrix} \tag{3.12}$$

where E and PR are the modulus of elasticity and poison's ratio respectively.

3.3 ELASTIC ANALYSIS

For elastic analysis, the equilibrium equation for the finite element assembly can be derived

$$[K_e]\{U\} = \{P\} + \{Q\} \tag{3.13}$$

Where $[K_e]$ is the global stiffness matrix of the finite element assembly obtained as the sum of the element stiffness matrices-

$$[K_e] = \sum_{M=1}^{N'} \int_{V_M} B^T\ [D_e]\ B\ dV_M + K_S \tag{3.14}$$

Further P is the external load vector and

$$Q = \sum_{M=1}^{N'} \int_{V_M} B^T\ \{\sigma^o\}\ dV_M \tag{3.15}$$

Where $\{\sigma^o\}$ is the initial stress vector,

3.4 ELASTIC PLASTIC ANALYSIS

For the elastic plastic problems the coefficients in the stiffness matrix vary as a function of loading. Thus the displacements are usually obtained by applying small load increments to the structure and updating the co-efficient of the stiffness matrix or applying an "effective" plastic load vector after each load increment. Here, the equations associated with incremental plasticity and those used to account for the elastic plastic material behavior (in place stress) in the FEM. are given. In any elastic plastic analysis the finite element equations for elasticity can be used prior to plastic yielding.

There after it is necessary to have a yield criterion to determine the state of stress at which yielding occurs. The Von-Mises yield criterion assumes that yielding is caused by the maximum distortion energy [**44**]. The yield criterion for plane stress conditions is given by-

$$F = F\{\sigma\} = (\sigma_x^2 + \sigma_y^2 - \sigma_x\sigma_y + 3\tau_{xy}^2)^2 - \sigma \tag{3.16}$$

Where σ is the equivalent stress or the uniaxial yield stress. If the state of stress is such that F<0, the material is still in the elastic range. When F=0, a plastic state is obtained and one of the flow theories of plasticity must be used to determine subsequent plastic behavior under increasing stress or strain.

One of the basic assumptions in the theory of plasticity is that the total strain $\{\varepsilon\}$ or total strain increment $\{d\varepsilon\}$ can be decomposed into elastic and plastic strain components as follows:

$$\{\varepsilon\} = \{\varepsilon_e\} + \{\varepsilon_p\} \tag{3.17}$$

Or incrementally

$$\{d\varepsilon\} = \{d\varepsilon_e\} + \{d\varepsilon_p\} \tag{3.18}$$

In the incremental theory of plasticity the plastic strain increment vector$\{d\varepsilon_p\}$ is a function of the current state of stress and is related to the yield criterion through Drucker's normality principle as

$$\{d\varepsilon_p\} = \lambda\left\{\frac{\partial F}{\partial \sigma}\right\} \tag{3.19}$$

Where λ is a positive scaler quantity. This flow rule is known as the normality principle because the plastic-strain increment vector is stipulated to be normal to the yield surface when the von-mises yield criterion is used with Equation (3.16) the resulting expression for$\{d\varepsilon_p\}$ is indentical to that proposed by Prandt1 and Reuss. The total strain increment vector can now be written as

$$\{d\varepsilon\} = [D_e^{-1}]\{d\sigma\} + \lambda\left\{\frac{\partial\varepsilon}{\partial\sigma}\right\} \quad (3.20)$$

Where the elastic strain increment vector has been related to the stress increment $\{d\sigma\}$ through the elasticity matrix. Therefore, if λ is known, the desired stress strain relation for an elastic plastic material would be obtained. When yielding occurs, the total differential of equation (3.13) gives-

$$dF = \left\{\frac{\partial F}{\partial\sigma}\right\}^T \{d\sigma\} - d\overline{\sigma} = 0 \quad (3.21)$$

The increment in equivalent stress $d\overline{\sigma}$ was obtained from a uniaxial tensile test as

$$d\overline{\sigma} = d\sigma^U = \left(\frac{d\sigma^u}{d\varepsilon_p^u}\right) d\varepsilon_p^u = H' d\varepsilon_p^u \quad (3.22)$$

Where H' is the slope of the uniaxial stress-plastic strain curve, $d\sigma^u$ is the uniaxial stress increment and $d\varepsilon_p^u$ is the uniaxial plastic strain increment. Using Drucker's normality principle for the uniaxial case gives $d\varepsilon_p^u = \lambda$ Thus equation (3.18) becomes

$$\left\{\frac{\partial F}{\partial\sigma}\right\}^T \{d\sigma\} - H'\lambda = 0 \quad (3.23)$$

Eliminating λ from equations (3.17) and (3.20) we get

$$\{d\sigma\} = \left[D_{e_p}\right]\{d\varepsilon\} \quad (3.24)$$

Where

$$\left[D_{e_p}\right] = [D_e] - [D_e]\left\{\frac{\partial F}{\partial\sigma}\right\}\left\{\frac{\partial F}{\partial\sigma}\right\}^T [D_e]\left[H' + \left\{\frac{\partial F}{\partial\sigma}\right\}^T [D_e]\left\{\frac{\partial F}{\partial\sigma}\right\}\right]^{-1} \quad (3.25)$$

The matrix $\left[D_{e_p}\right]$ is elastic plastic matrix and replaces the elasticity matrix $[D_e]$ in incremental analysis. For an elastic perfectly plastic material H' is taken as zero. For a linear strain hardening material H' is a constant and if the material is non-linear strain hardening H' is a function of plastic strain.

3.5 NON-LINEAR ANALYSIS PROCEDURE

Initial stress method as developed by Zienkiewicz, Valliappan and King [96] is used for performing the non-linear analysis. Detailed description of the procedure described here is similar to the one described by Newman. It, however, differs from the fact that the method has been extended to handle non-linear strain hardening behaviour. The application also handles modified boundary conditions.

The equation which governs the response of a discretized structure under loads which cause plastic deformation [93] is

$$[K'_e]\{U\}_I^i = \{P\}^i + \{Q\}_{I-1}^{i-1} \tag{3.26}$$

Where K'_e is the elastic stiffness matrix, $\{U\}$ is the displacement vector, $\{P\}$ is the applied load vector and $\{Q\}$ is the "effective" plastic load vector which takes care of the elements in plastic state. In the initial stress method the solution is carried out for an elastic-plastic the continuum until the desired load is reached ($\{P\}^i = \{P\}^{i-1} + \{dP\}$).The superscript i denotes the current increment and i-1 denotes the preceding increment. After a load increment an iterative process is required to stabilize the plastic load vector. The subscript I denotes the current iteration and I-1 denotes the preceding iteration. During the i^{th} increment a purely elastic problem is solved and the increment in total strain $\{d\varepsilon\}$ and corresponding elastic stress $\{d\sigma_e\}$ are computed from the displacement increments $\{dU\}$ for every element. Because of the non-linearity the stress increments are not,in general, correct. If the correct stress increment for the corresponding strain increment is $\{d\sigma\}$ then a set of body forces or plastic-load vectors $\{dQ\}$ caused by the "initial" stress $\{d\sigma^0\} = \{d\sigma_e\} - \{d\sigma\}$ is required to maintain the stress components on the yield surface. The correct stress increment $\{d\sigma\}$ is computed from equation (3.23). The plastic load increments are computed from

$$\{dQ\} = \sum_{M=1}^{N'} \int [B]^T \{d\sigma^o\} dV_m \tag{3.27}$$

Where N' is the number of elements.

In the next section the equations necessary to compute the plastic-load increment $\{dQ\}$

are given. For elements which are in an elastic state,$\{d\sigma^o\} = 0$. The total plastic load vector is then computed as

$$\{Q\}_I^i = \{Q\}_{I-1}^{i-1} + \{dQ\} \tag{3.28}$$

At the second stage of computation the new force system $\{Q\}_I^i$ is added to the applied load vector and a new set of displacements is obtained.. The iteration process is repeated until the change in the plastic load vector is small. Usually this process requires 5 to 12 iterations for convergence.

3.6 DETERMINATION OF THE PLASTIC LOAD VECTOR BY USING INITIAL STRESS METHOD

During the incremental loading process, whenever the conditions $F\{\sigma\}^i \geq 0$ are met, the plastic-load increment is computed from the "initial" stress increment $\{d\sigma^o\}$. The initial stress is necessary to maintain the element stresses on the yield surface. The equation to compute the plastic-load increment due to the initial stress on element M is

$$\{dQ\} = \int [B]^T \{d\sigma^o\}\, dV_m \tag{3.29}$$

Where

$$\{d\sigma^o\} = \{d\sigma_\varepsilon\} - \{d\sigma\} = \left([D_e] - [D_{ep}]\right)\{d\varepsilon\} \tag{3.30}$$

The matrix [B] is given by equation (3.7). The thickness of each element is assumed to be t. Thus, the differential volume is $dV_m = tA_m$. Because the stresses on the element are constant and matrix B is only a function of nodal co-ordinates, the plastic-load increment becomes

$$\{dQ\} = [B]^T \begin{Bmatrix} d\sigma_x^o \\ d\sigma_y^o \\ d\tau_{xy}^o \end{Bmatrix} A_M.t \tag{3.31}$$

Where A_M is the cross-sectional area of the element. Expanding equation (3.26), with

the use of equation (3.7), the plastic load increments for the element are given by-

$$dQ = \frac{1}{A_m^2}\begin{Bmatrix} b_i & 0 & c_i \\ 0 & c_i & b_i \\ b_j & 0 & c_j \\ 0 & c_j & b_j \\ b_k & 0 & c_k \\ 0 & c_k & b_k \end{Bmatrix}\begin{Bmatrix} d\sigma_x^o \\ d\sigma_y^o \\ d\tau_{xy}^o \end{Bmatrix} A_M t \tag{3.32}$$

$$dQ_{xi} = \frac{t}{2}[b_i \quad d\sigma_x^o + c_i \quad d\tau_{xy}^o] \tag{3.33}$$

$$dQ_{yi} = \frac{t}{2}[c_i \quad d\sigma_y^o + b_i \quad d\tau_{xy}^o] \tag{3.34}$$

$$dQ_{xj} = \frac{t}{2}[b_j \quad d\sigma_x^o + c_j \quad d\tau_{xy}^o] \tag{3.35}$$

$$dQ_{yj} = \frac{t}{2}[c_j \quad d\sigma_y^o + b_j \quad d\tau_{xy}^o] \tag{3.36}$$

$$dQ_{xk} = \frac{t}{2}[b_k \quad d\sigma_x^o + c_k \quad d\tau_{xy}^o] \tag{3.37}$$

$$dQ_{yk} = \frac{t}{2}[c_k \quad d\sigma_y^o + b_k \quad d\tau_{xy}^o] \tag{3.38}$$

The stress increments $\{d\sigma^o\}$ are obtained from equation 3.28 in terms of total strain increments and are given by-

$$d\sigma_x^o = \frac{E}{\emptyset(1-PR^2)}\left[A_{11}d\varepsilon_x + A_{12}\varepsilon_y + A_{13}d\gamma_{xy}\right] \tag{3.39}$$

$$d\sigma_y^o = \frac{E}{\emptyset(1-PR^2)}\left[A_{21}d\varepsilon_x + A_{22}\varepsilon_y + A_{23}d\gamma_{xy}\right] \tag{3.40}$$

$$d\tau_{xy}^o = \frac{E}{\emptyset(1-PR^2)}\left[A_{31}d\varepsilon_x + A_{32}\varepsilon_y + A_{33}d\gamma_{xy}\right] \tag{3.41}$$

Where $\emptyset = F_x^2 + 2PRF_xF_y + F_y^2 + \frac{1-PR}{2}F_{xy}^2 + \frac{1-PR^2}{E}H'$

Non-linear strain hardening is incorporate by using Ludwik's stress, plastic strain relationship of the type

$$A_{11} = F_x^2 + 2PRF_xF_Y + PR^2F_y^2 \tag{3.42}$$

$$A_{12} = A_{21} = F_xF_y + PR\left(F_x^2 + F_y^2\right) + PR^2F_xF_y \tag{3.43}$$

$$A_{13} = A_{31} = \frac{1-PR}{2}F_{xy}(F_x - PRF_y) \tag{3.44}$$

$$A_{23} = A_{32} = \frac{1-PR}{2}F_{xy}(F_y - PRF_x) \tag{3.45}$$

$$A_{23} = A_{32} = \frac{1-PR}{2}F_{xy}(F_y - PRF_x) \tag{3.46}$$

$$A_{33} = \left(\frac{1-PR}{2}\right)^2 F_{xy}^2 \tag{3.47}$$

For the von-mises yield criterion

$$F_x = \frac{\partial F}{\partial \sigma_x} = \frac{1}{\sigma}\left[\sigma_x - \frac{1}{2}\sigma_y\right] \tag{3.48}$$

$$F_y = \frac{\partial F}{\partial \sigma_y} = \frac{1}{\sigma}\left[\sigma_y - \frac{1}{2}\sigma_x\right] \tag{3.49}$$

$$F_{xy} = \frac{\partial F}{\partial \tau_{xy}} = \frac{3}{\sigma}\tau_{xy} \tag{3.50}$$

The stresses $\sigma_x, \sigma_x$and τ_{xy} are the current stress components.

For the situation in which $F\{\sigma\}^i \geq 0$ and $F\{\sigma\}^{i-1} < 0$, on intermediate stress value at which yielding begins is obtained and the plastic-load increment is computed from the modified stress increment$\{d\sigma'\}$. The intermediate stress value and the corresponding plastic load increment are determined as given below. To obtain the intermediate stress value, a multiple of the elastic stress increment is added to the preceding stress state as

$$\{\sigma'\} = \{\sigma\}^{i-1} + \beta\{d\sigma_e\} \tag{3.51}$$

This equation is substituted into the yield condition,

$F\{\sigma'\} = 0$ to determine β The stress increment $\beta\{d\sigma_e\}$ and the corresponding strain increment are purely elastic and do not produce a plastic load increment. Only the stress increment which causes the stress state to exceed the yield criterion produces a plastic load increment. This stress increment is given by

$$\{d\sigma'\} = (1 - \beta)\{\sigma^o\} \tag{3.52}$$

Equations (3.28) are used to compute$\{d\sigma^o\}$. The plastic-load increments are obtained by using equation (3.29) where $\{d\sigma^o\}$ is replaced by $\{d\sigma'\}$.

3.7 NUMERICAL ALGORITHM

The steps in the numerical algorithm are as follows:

1) Perform an elastic analysis for a uniform prescribed displacement.

2) Find out the element in which the induced stress is maximum. Determine the ratio 'R' between yield stress and the maximum stress.

3) Find the impressed displacement at the boundary and load applied for initial yield.

4) Add load/displacement increment to the preceding displacements (U^{*i-l}) or loads $P^{(i-1)}$ to obtain current displacement (U^{*i}) or load $P^{(i)}$

5) Compute the displacement $\{U\}^i$. Initially $\{Q\}_o^{i-1}$ using Equation 3.22.

6) Set M (element-No)=1 initially. Compute the increment in the total strain $\{d\varepsilon\}_M^i$From the relation

$$\{d\varepsilon\}_M^i = [B]_M (\{U\}^i - \{U\}^{i-1})$$

And $\{d\varepsilon\}_M^i$to the preceding total strain vector to get current total strain $\{\varepsilon\}_M^i$

$\{\varepsilon\}_M^i = \{\varepsilon\}_M^{i-1} + \{d\varepsilon\}_M^i$

Where M indicates the element number.

7) Compute element stress increment

$$\{d\sigma_e\}_M^i = [D_e]\{d\varepsilon\}_M^i$$

And current stress vector

$$\{\sigma\}_M^i = \{\sigma\}_M^{i-1} + \{d\sigma_e\}_M^i$$

8) Check for yield condition

If $F\{\sigma\}_M^i < 0$ Indicates only elastic strains state proceed to step (x).

If $F\{\sigma\}_M^i > 0$ proceed to step (9).

9) **(a)** Two possibilities exist:

$F\{\sigma\}_M^i > 0$

$F\{\sigma\}_M^{i-1} = 0$

Compute initial stress increment $\{d\sigma^o\}_M^i$From equation (3.28) and (3.29)

Replace $\{\sigma\}_M^i$ by $\{\sigma\}_M^i - \{d\sigma^o\}_M^i$

Compute

$$\sigma_M^i = \left\{\left(\sigma_{XM}^i\right)^2 + \left(\sigma_{YM}^i\right)^2 - \sigma_{XM}^i\sigma_{YM}^i + 3(\tau_{XYM}^i)^2\right\}^{1/2}$$

And store it.

(b) If

$F\{\sigma\}_M^i > 0$ and $F\{\sigma\}_M^{i-1} < 0$

Find the intermediate stress value of the stress components at which yielding begins and the stress increment $\{d\sigma'\}_M^i$ above the yield surface to compute $\{d\sigma^o\}_M^i$ and $\{dQ\}$ For this proceed according to equations (3.30) and (3.31)

(10) Compute element plastic load vector $\{dQ\}_M = [B]^T\{d\sigma_M^o\}A_M^t$

(11) Repeat steps (6) (10) for all the elements and compute the plastic load vector

$$\{Q\}^i = \{Q\}^{i-1} + dQ$$

Where

$$\{dQ\} = \sum_{M=1}^{N'} \{dQ\}_M$$

(12) Use equation (3.22) and carry out the solution for the unknown displacements corresponding to the next iteration.

(13) Repeat steps (5) to (12) until the displacements converge or {dQ} becomes small.

(14) Repeat steps (4) to (14) until the desired load or impressed displacement is reached.

3.8 ABAQUS® 6.10

Abaqus® FEA is a software based on finite element analysis, originally released in 1978. The Abaqus® product consists of three softwares.

1- Abaqus/CAE® is used for both the modeling and analysis of mechanical components and assemblies and visualizing the finite element analysis results

2- Abaqus/Standard® is a general-purpose finite element analysis module.

3- Abaqus/Explicit®, a special purpose finite element analysis module that is used for explicit integration scheme to solve highly nonlinear systems with many complex contacts under transient loading conditions.

3.9 SOLUTION PROCEDURE

In the FEM method, we encounter the solution of a large system of symmetric bounded matrix equation. For reasons of economy in computing time and core memory, it is necessary to use an efficient solution algorithm. In this investigation Choleski factorization of the coefficient matrix is carried out and the displacements are

obtained through back substitution. Details of the method can be found in ref. [**56**].

The imposition of prescribed displacements and the computation of nodal reactions were carried out by simple numerical procedures.

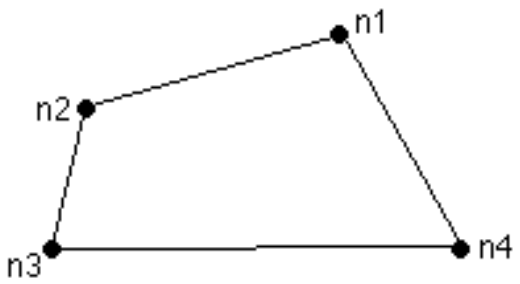

Fig 3.1 Quadrilateral Element [56]

3.10 FEM ANALYSIS OF FATIGUE CRACK PROPAGATION

The present investigation on fatigue behavior though similar to that of Newman [**56**] differs in the following aspect:

a) The material is considered to be non-linear strain hardening.

b) The ends of the specimen are considered to be uniformly displaced instead of being uniformly stressed.

c) A modified method of incorporating the changing boundary conditions due to intermittent crack closure opening and growth has been used.

d) The criterion for crack growth as suggested by Ogura et al [**58,59,60**] which appears to be more realistic is incorporated into the application.

3.11 FEM RESULTS FOR CRACK OPENING AND CLOSING STRESSES

The computer application using the steps described in section (3.4) to (3.8) has been used to study the fatigue crack propagation in a specimen with a side edge notch of 6 mm length. Load acts in a direction transverse to that of the notch. Constant

amplitude loading has been considered. Result shows the crack propagation load varies with the crack length. The general trend of results is the same as reported by other authors [**58,59,60**] for a uniformly stressed boundary. Crack profile at different loads during unloading and loading at a crack length of 11.25 mm. The distribution of stresses around the crack tip at a crack length of 11.00 mm for increasing and decreasing loads.

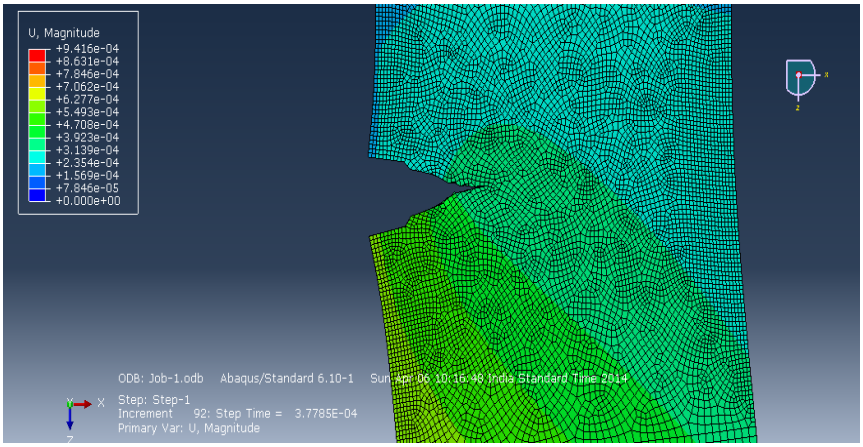

(a)

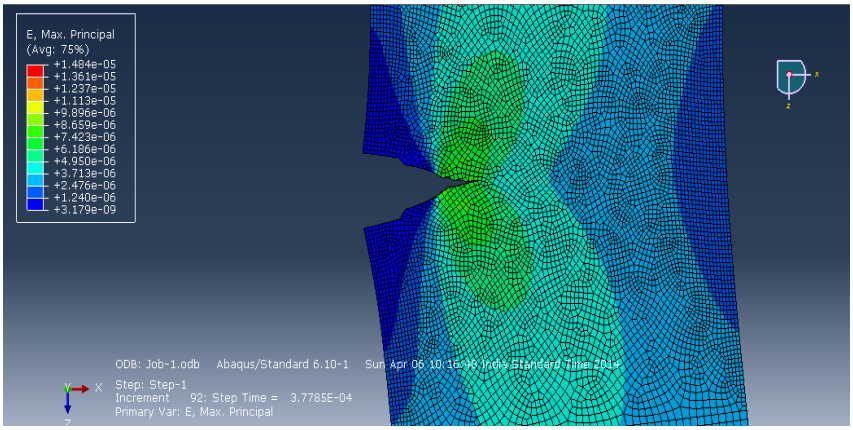

(b)

Fig 3.2(a), (b) FEM Results

The following curves were plotted to verify the results with the experimental results and authenticity of the application as shown in **Fig 3.3 & Fig 3.4**. 6063T6 Al Alloy was used for these tests. The variation of crack propagation, crack opening load and crack closure load are presented as shown in **Fig 3.3** and **Fig 3.4**. It is

observed that crack closure load stabilizes at about 5300 Newton. The initial portion of the crack Length Vs crack closure curve shown the approximate procedure in chapter 4, 5, 6 for different loading conditions. The crack propagation and crack opening loads also demonstrate similar trends. It is interesting to note that frequently a crack starts to close first at a node further from the crack tip and not at the node nearest to the crack tip during the unloading process.

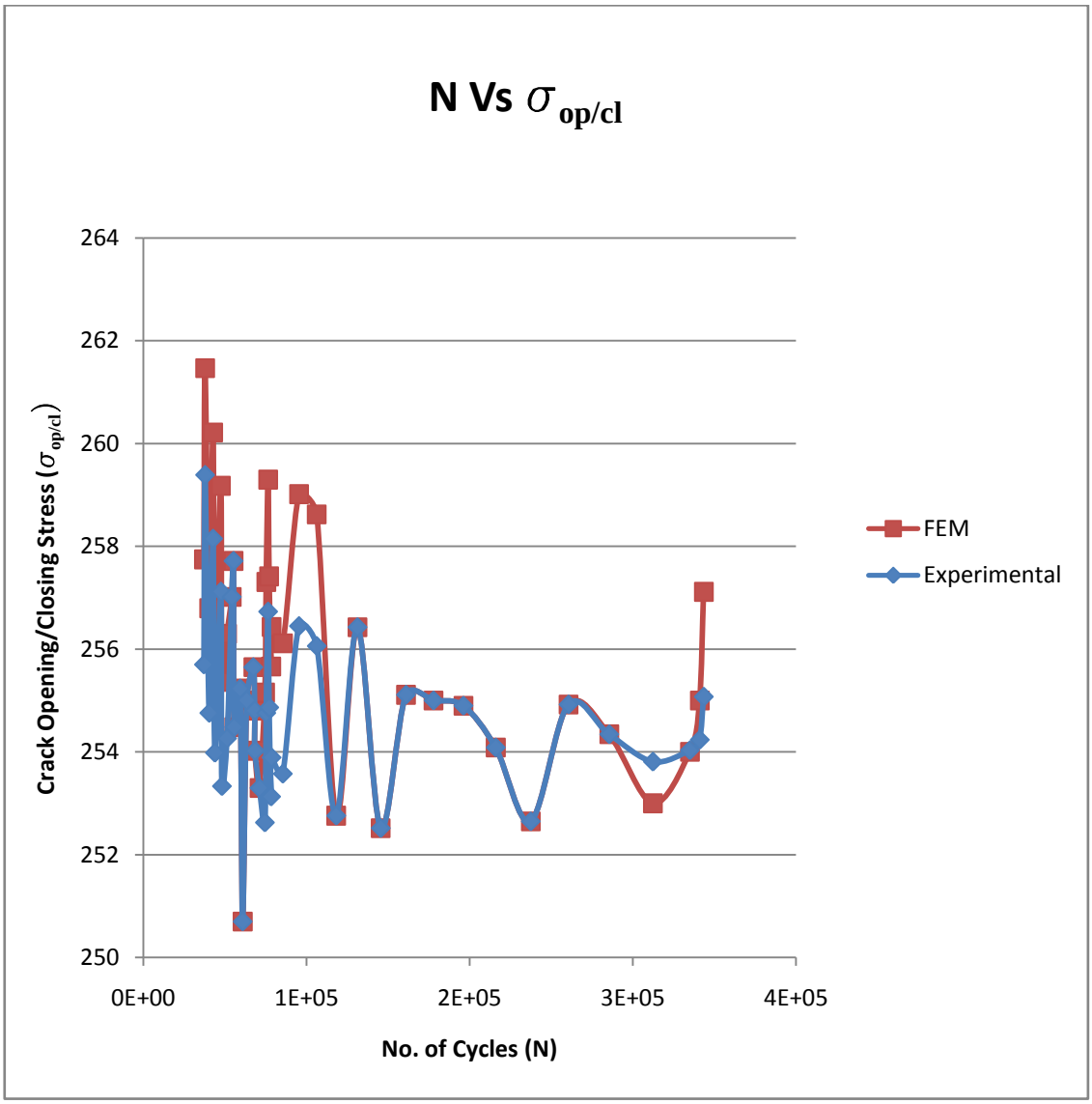

Fig 3.3 No. of Cycle Vs Crack Opening/Closing Stresses

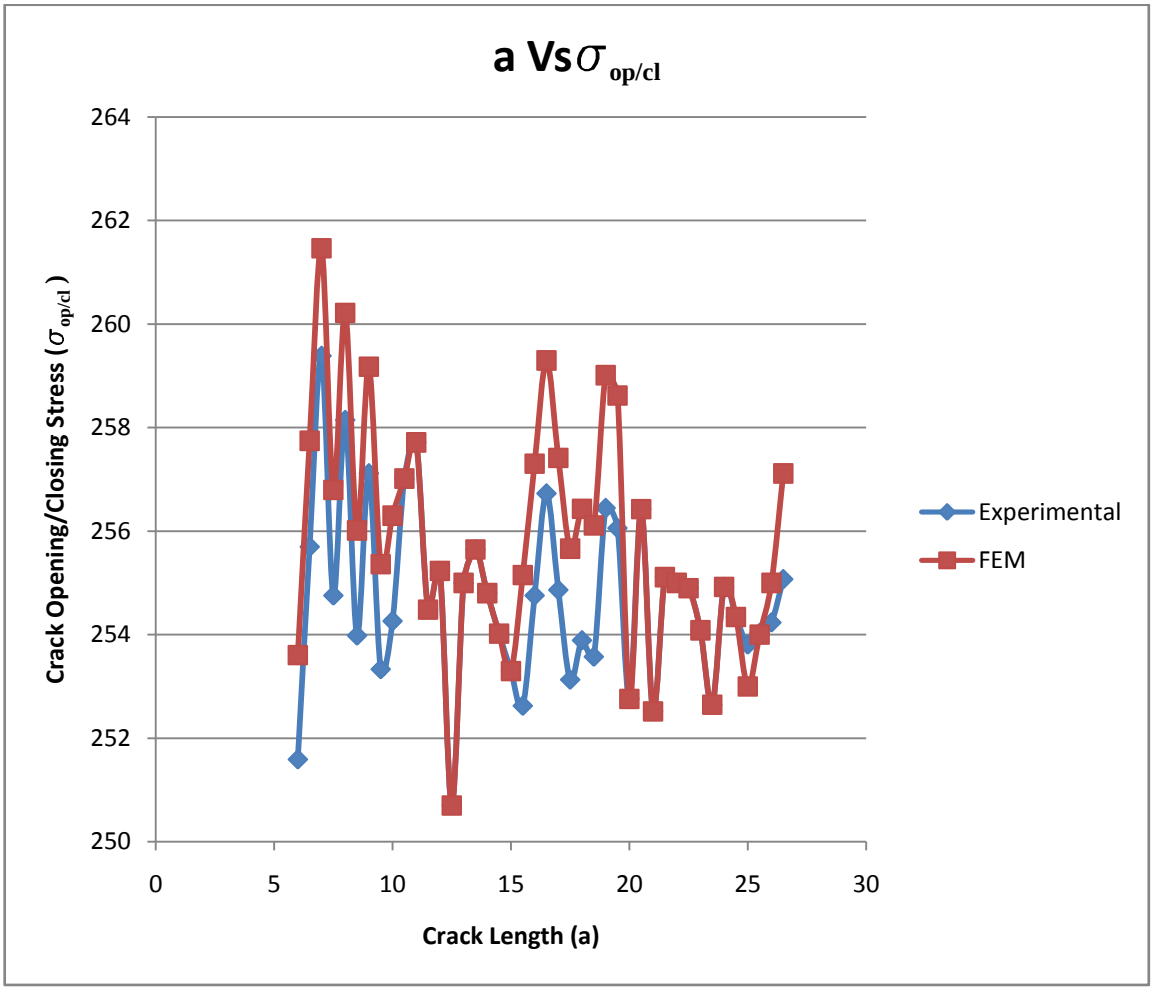

Fig 3.4 Crack Length Vs Crack Opening/Closing Stress

CHAPTER: 04

4 EFFECT OF WORK HARDENING EXPONANT IN CONSTANT AMPLITUDE LOADING

4.1 INTRODUCTION

The aim of the thesis is to study the crack opening and closing loads under various types of loading conditions and for materials having different work hardening exponent. Five materials 3003, 6061, 6063, 5052, 6351 Aluminum Alloys were used for getting results on different work hardening exponents. Table 4.1, 4.2 give the details of chemical and mechanical properties of all the materials. in this chapter we will present & discuss the results obtained for all the materials for effect of work hardening exponent in fatigue crack propagation in constant amplitude loading condition. Al though the technique described in Chapter 03 for analyzing the crack for crack opening and closing load using FEM. All experiments were done on Abaqus® 6.10.The review in Chapter 02 makes it necessary to have further studies on effect of material properties on crack growth rate and effective stress intensity range ratio.

It was realized that crack extension takes place due to stress concentration at the crack tip and due to failure of material during cyclic loading; an effort has been made to relate the crack growth with stress intensity factor “K” at the crack tip. A well-established relationship was given by Paris and Erdogan [**11**] and takes the following form:

$$\frac{da}{dN} = C(\Delta K)^n \quad (1)$$

Where C, and n depend on material, specimen geometry and loading.

It is found that for different values of stress ratios, R, for the same material a large deviation in data was obtained from the curve fitted by eq.(1). The use of the range of cyclic stress intensity factors to describe fatigue crack growth rate is based on the assumption that the crack tip starts to open as soon as load is completely relaxed. In 1968 on the basis of results of experiments, Elber [**14**] predicted that cyclic plasticity gives rise to the development of residual plastic deformation in the vicinity of the crack tip causing the fatigue crack to close under a positive load. He described this as crack closure phenomenon and suggested that the fatigue crack growth can occur only during the portion of the loading cycle in which the crack is fully open. Based on this suggestion, an effective stress range is defined:

$$\triangle\sigma_{eff} = \sigma_m - \sigma_o \ (\text{or } \sigma_{cl}) \quad (2)$$

The ratio of $\triangle\sigma_{eff}$ to the total stress range ($\triangle\sigma$) is defined as the stress intensity range ratio, U, and is given by

$$U = \frac{\triangle\sigma_{eff}}{\triangle\sigma} = \frac{\sigma_m - \sigma_o (\text{or } \sigma_{cl})}{\sigma_m - \sigma_n} \quad (3)$$

Elber [**15**] further suggested that the crack growth relationship be written in the following form:

$$\frac{da}{dN} = C(\Delta K_{eff})m = C(U\Delta K)^m \quad (4)$$

The crack propagation equation is written in terms of "ΔK_{eff} , instead of "ΔK". the factors which have been reported to influence U are stress intensity range ($\triangle\sigma$), material properties (σ_y , σ_f) , crack length (a) and stress ratio R. In the work of Elber [**15**], however, U is shown to depend only on stress ratio R. Many laws are available which give crack growth rate as a function of $\triangle$K and material properties. In this regards many other researchers [**1, 2, 7, 16, 17, 18, 19, 21, 22, 25, 32, 37, 44**] had given their contribution to formulate the crack growth. In the present study, effort has

been made to show the effect of strain hardening on crack growth rate for 5052 Aluminum alloy. Side Edge Notch (SEN) Specimen is considered in this study.

4.2 MATERIAL PROPERTIES

The material used to prepare specimen is 5052 Al alloy that's chemical and mechanical properties are given in table no.1 & 2 respectively.

Table 4.1Chemical composition of Aluminum Alloys

	Element								
Material									
	Si	Fe	Cu	Mn	Mg	Cr	Zn	Ti	Other
6061 T6 Al	0.4-0.8	0.7	0.15-0.40	0.15	0.8-1.2	0.04-0.35	0.25	0.15	0.4
6063 T6 Al	0.30-0.70	0.6	0.1	0.3	0.40-0.90				0.4
6351 Al	0.7-1.3	0.5	0.1	0.4-0.8	0.4-0.8		0.2	0.2	
3003 Al	0.6	0.7	0.05-0.20	1.0-1.5			0.1		
5052 Al	0.25	0.4	0.1	0.1	2.2-2.8	0.15-.35	0.1		-

Table 4.2Mechanical properties of Aluminum Alloys

	Element					
Material	**σ_y**	**σ_u**	**σ_f**	**Ex10^6**	**Elongation%**	**Reduction in Area %**
6061 T6 Al	30.14	32.5	45	7	10.5	28.3
6063 T6 Al	21	24.2	64	7	10.6	60
6351 Al	174.7	179.31	129.3	14.76	17	50
3003 Al	153	157	8	16	8	18.7
5052 Al	195	230	105		32	

4.3 SPECIMEN GEOMETRY

Specimen has been modeled with the dimensions of

Length (H)- 180 mm

Width (W) - 50 mm

Thickness (t) – 3 mm

Initially a notch of 6 mm had been made at en edge for crack propagation under the load applications on the specimen during the fatigue test. The geometry is shown in **Fig**: 01.

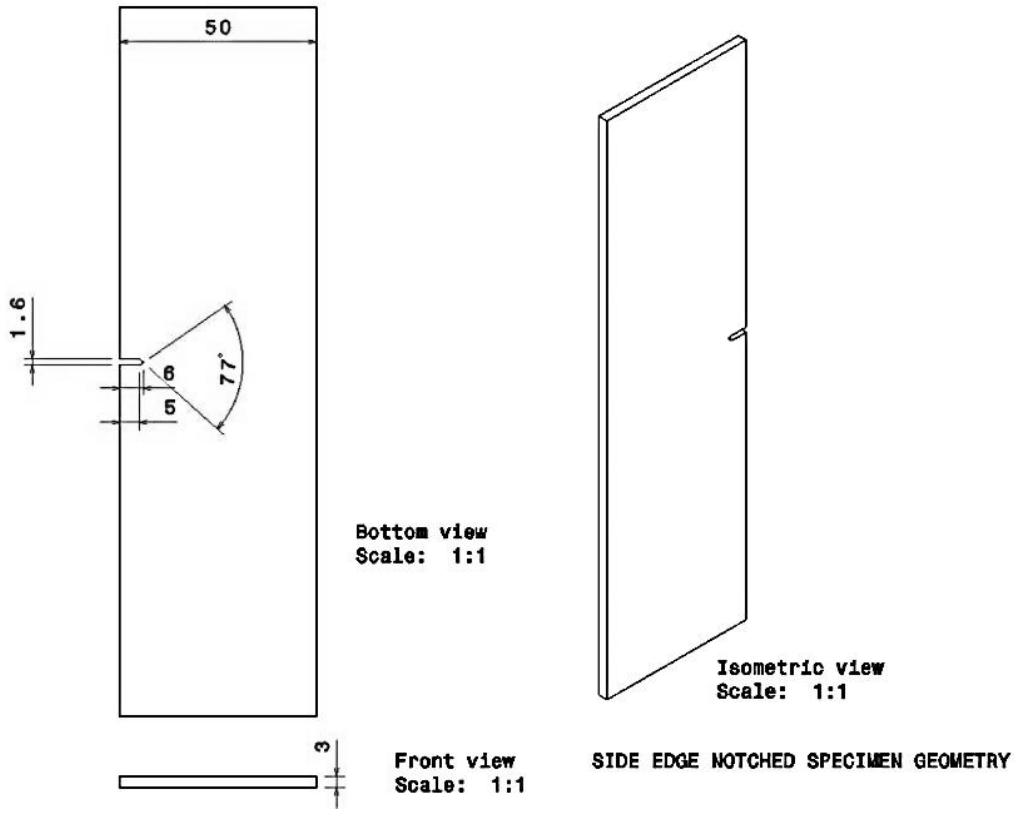

Fig 4.1Specimen Geometry

4.4 METHODOLOGY FOR DETERMINATION OF CRACK GROWTH RATE

The methodology adopted for this study has certain specific steps which start from experiments for fatigue testing of the specimen given in **Fig**: 4.1 on MTS machine and result data collected for the validation with analytic approach finite element method were used after tabulating all result parameters together regression analysis were to be performed to determine the dependency of strain hardening on fatigue crack growth. All steps are shown in **Fig**:4.2

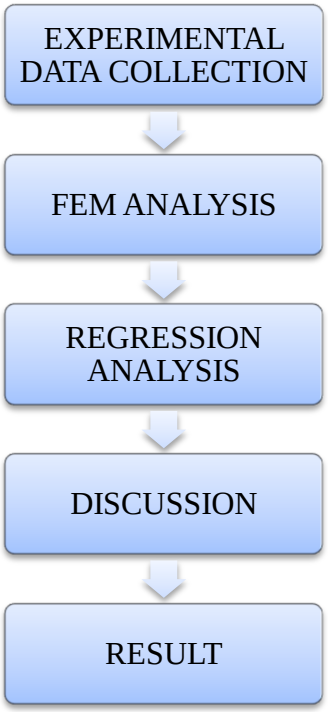

Fig 4.2Flow Diagram of Methodology

4.5 FINITE ELEMENT ANALYSIS FOR DETERMINATION OF CRACK GROWTH RATE

4.5.1 3D Modeling Using Catia V5 R19:

3D modeling of specimen had been done on CATIA® V5 R19 as shown in **Fig**: 01 the dimensions of the specimen were based ASTM standard for fatigue testing and then it has been imported to Abaqus® 6.10 as a deformable solid part.

4.5.2 FEM Modeling

A crack had been developed in Abaqus® 6.10 itself as a shell deformable part. After modeling both the instances were called in assemble module to insert the crack in the specimen. C3D8R elements were used to mesh the specimen but not the crack. Crack remains unmeshed throughout the analysis. Because the whole analysis were done for **Mode I** as **Fig**: 4.2 so that one side of the specimen were kept fixed and other end was loaded.

XFEM module was used to study the onset and propagation of cracking in quasi-static problems. XFEM allows us to study crack growth along an arbitrary, solution-dependent path without needing to remesh our model. We can choose to study a crack that grows arbitrarily through our model or a stationary crack. We defined an XFEM crack in the Interaction module. We specified the initial location of the crack. Alternatively, we allowed Abaqus® to determine the location of the crack during the analysis based on the value of the maximum principal stress or strain calculated in the crack domain.

4.5.3 Initial Conditions

Initial values of stresses, temperatures, field variables, solution-dependent state variables, etc. specified as follows.

4.5.4 Boundary Conditions

Specimen has been kept in mode I fracture mode that is called as crack opening mode as shown in **Fig**: 4.3 in this mode tensile forces are exerted on the top and bottom face of the specimen in this case displacement will be normal to the crack surface.

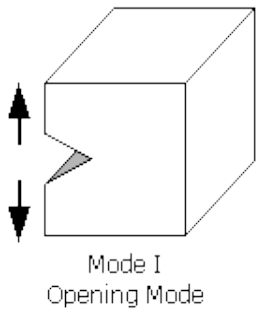

Fig 4.3Mode I Fracture Modes

Boundary conditions applied to the displacement or rotation degrees of freedom for the SEN Specimen. One side kept fixed (use Encastre Boundary condition) and on other side stress applied. During the analysis, boundary conditions had an amplitude definition that is cyclic over the step.

4.5.5 Loads

Following loading conditions were considered:

Table 4.3 CAL Conditions for 3003 Al Alloy

R	P_{min} (KN)	P_{max}(KN)	ΔP
0	0	6.2	6.2
0.1	0.69	6.89	6.2
0.3	2.66	8.66	6.2
0.5	4.13	10.33	6.2

R	P_{min}(KN)	P_{max}(KN)	ΔP
0	0	8.25	8.25
0.1	0.825	8.25	7.425
0.3	2.47	8.25	5.78
0.5	3.30	8.25	4.95

Table 4.4CAL Conditions for 5052 Al Alloy

R	P_{min}(KN)	P_{max}(KN)	ΔP
0	0	14	14
0.1	1.4	15.4	14
0.3	4.2	18.2	14
0.5	7	21	14

R	P_{min}(KN)	P_{max}(KN)	ΔP
0	0	14	14
0.1	1.4	14	12.6
0.3	4.2	14	9.8
0.5	7	14	4.95

Table 4.5 CAL Conditions for 6061 Al Alloy

R	P_{min}(KN)	P_{max}(KN)	ΔP
0	0	14	14
0.1	1.4	15.4	14

0.3	4.2	18.2	14
0.5	7	21	14

R	P_{min}(KN)	P_{max}(KN)	ΔP
0	0	9	9
0.1	0.9	9	8.1
0.3	2.7	9	6.3
0.5	4.5	9	4.5

Table 4.6 CAL Conditions for 6063 Al Alloy

R	P_{min}(KN)	P_{max}(KN)	ΔP
0	0	8.2	8.2
0.1	0.82	8.2	7.38
0.3	2.46	8.2	5.74
0.5	4.1	8.2	4.1

R	P_{min}(KN)	P_{max}(KN)	ΔP
0	0	5.85	5.85
0.1	1.36	7.21	5.85
0.3	3.9	9.75	5.85
0.5	8.77	14.62	5.85

Table 4.7 CAL Conditions for 6351 Al Alloy

R	P_{min}(KN)	P_{max}(KN)	ΔP
0	0	14	14
0.1	1.4	15.4	14
0.3	4.2	18.2	14
0.5	7	21	14
R	P_{min}(KN)	P_{max}(KN)	ΔP
0	0	9	9
0.1	0.9	9	8.1
0.3	2.7	9	6.3
0.5	4.5	9	4.5

4.5.6 Fields Output

Fields output variables 'PHILSM', 'PSILSM' and STATUSXFEM under the Failure/Fracture and Status category respectively are selected to calculate crack length with no of load cycle.

4.6 FEM RESULTS& DISCUSSION

Results obtained from FEM analysis of fatigue crack in SEN specimen of five different Al Alloy under constant amplitude loading at different stress ratios, R=0, 0.1, 0.3 and 0.5 at every 2 mm crack length. These records are shown in **Fig 4.5** to **Fig 4.24.**

For various loading given in Table 4.3 to 4.7 the value of U and da/dN were determined.**Fig 4.5** to **Fig 4.15** show that da/dN increases with increases of "n" and "n" increases with increases of stress ratio for all the materials. σ_y increases the crack closure load is reduced. If σ_y is increased the plastic zone size is decreased at the crack tip. The curves plotted between U & n at P_{max}= constant & ΔP= Constant shown in **Fig 4.16 to Fig 4.24**show scatter plot for some extent and after that it stabilizes and follow a straight line, this happens due to larger plastic zone generated at the crack tip after increasing the crack length.It is found that for a given value of "n" the value of effective stress intensity range ratio (U) increases in lower stress ratio up to 1mm fatigue length.In the end when the crack has become sufficiently large and crack propagation rate has increased to a fairly large value and the area available for tension has decreased to considerable extent effective stress intensity range ratio (U) increases. "U" increases with "n" at all stress ratio (R) for all the materials.The above results lead us to the conclusion that da/dN and U are dependent upon "n".

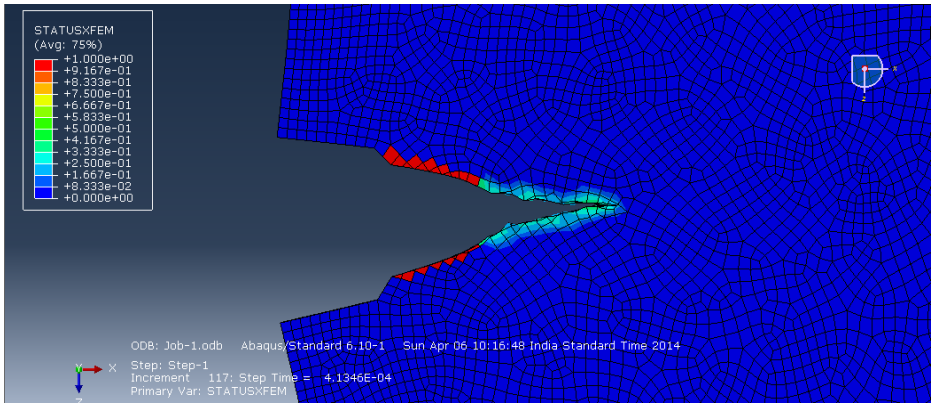

Fig 4.4Results Visualization

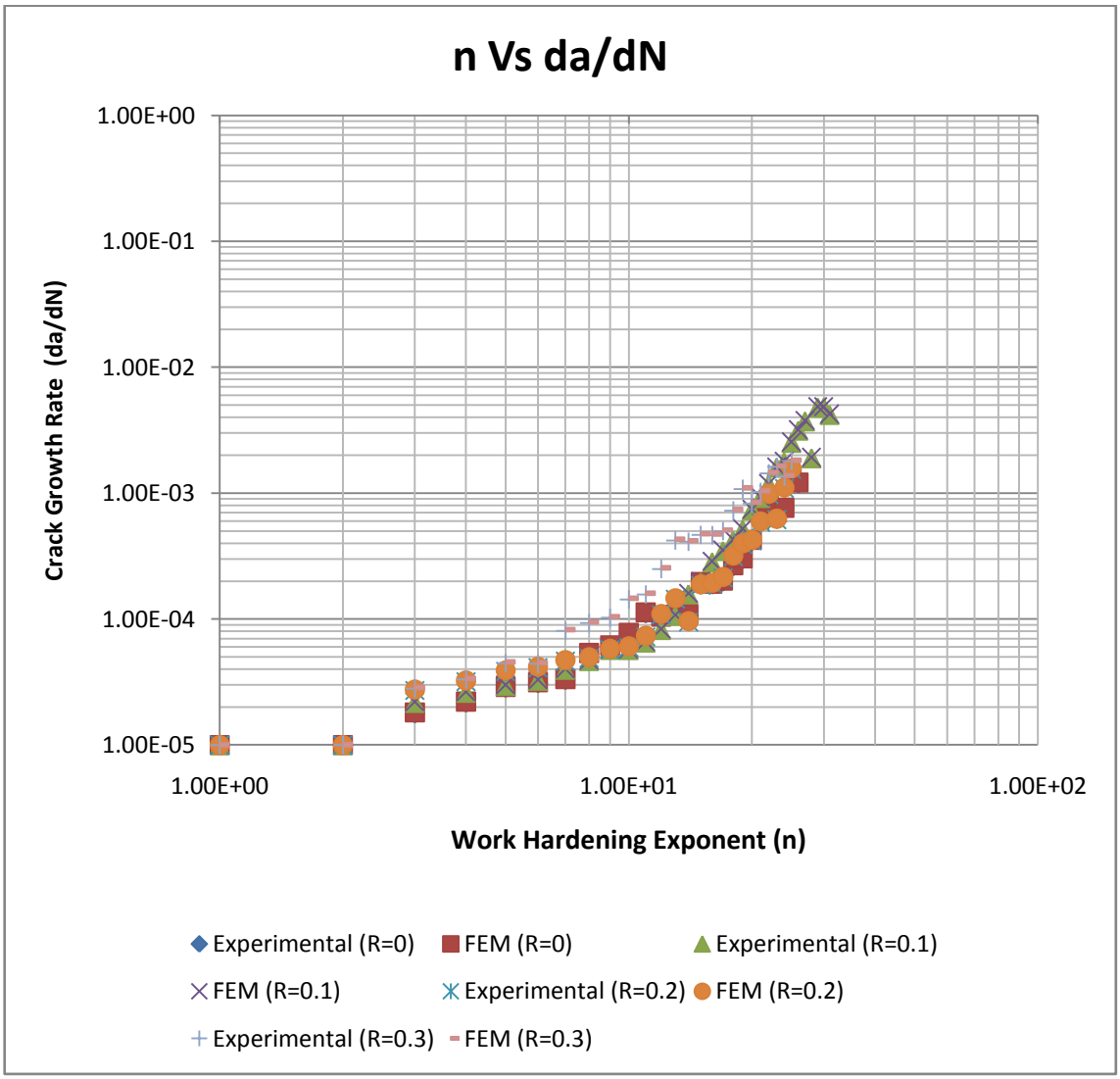

Fig 4.5For ΔP = Constant (3003 Al)

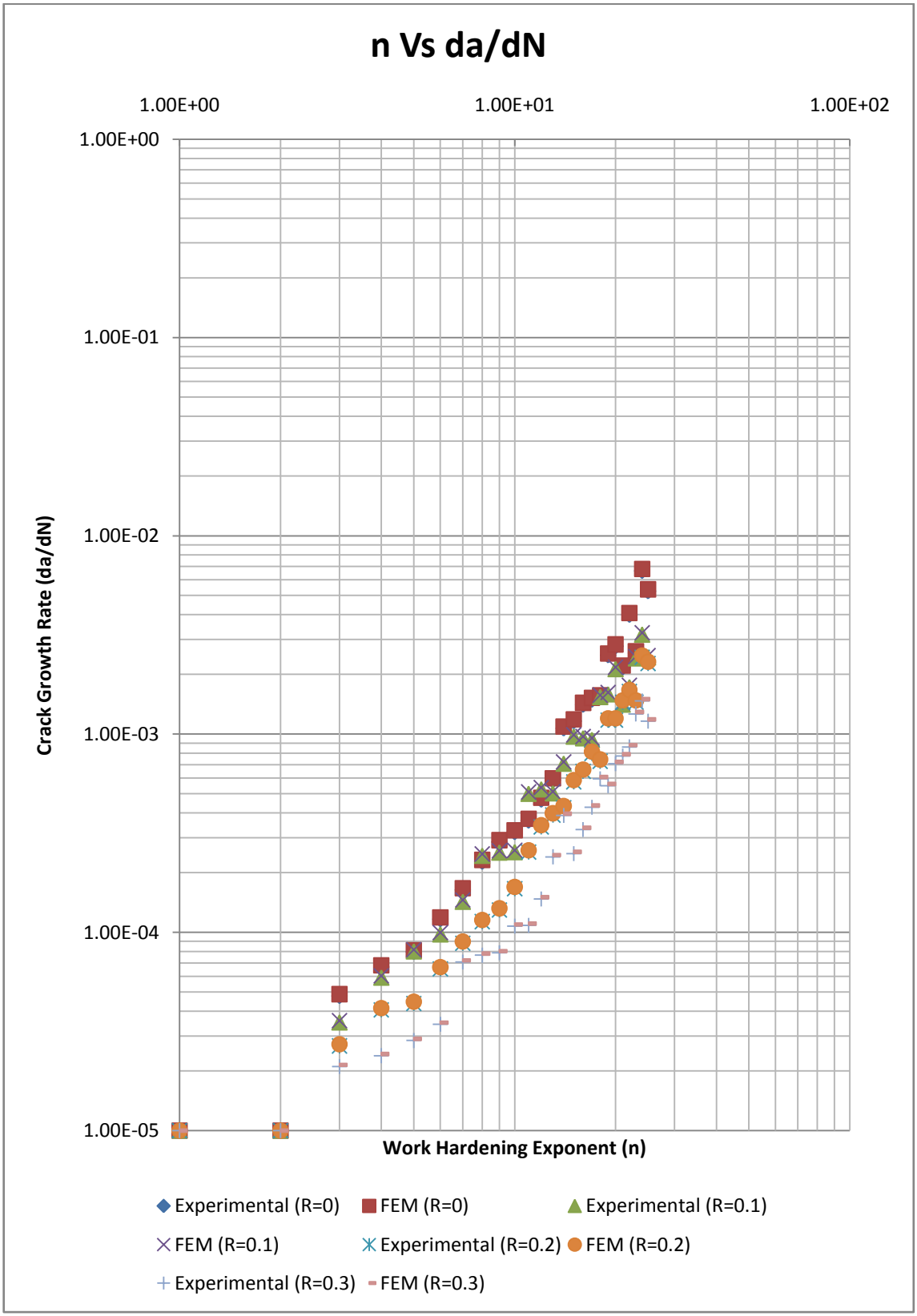

Fig 4.6For Pmax=Constant (300Al)

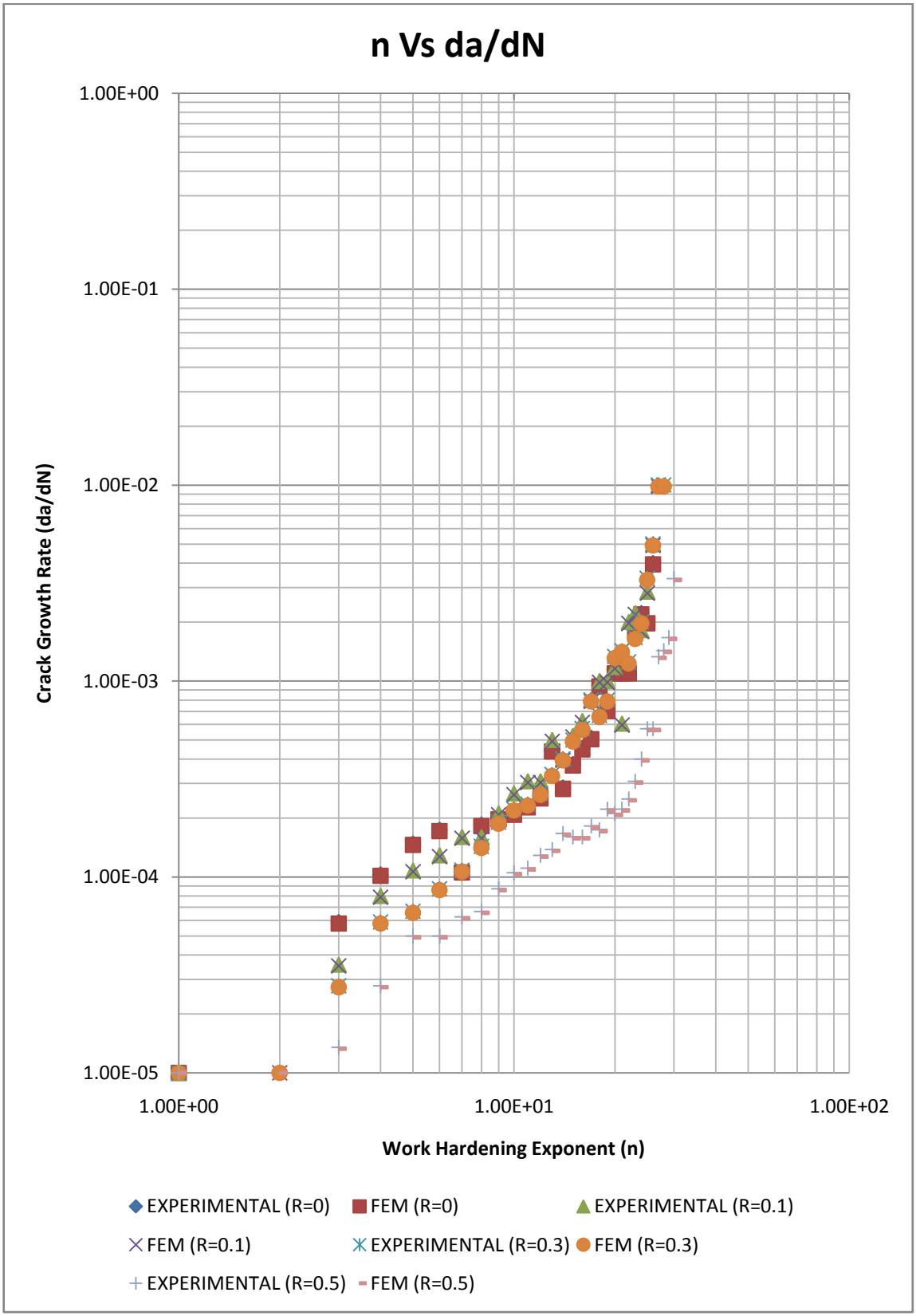

Fig 4.7 For ΔP= Constant (5052 Al)

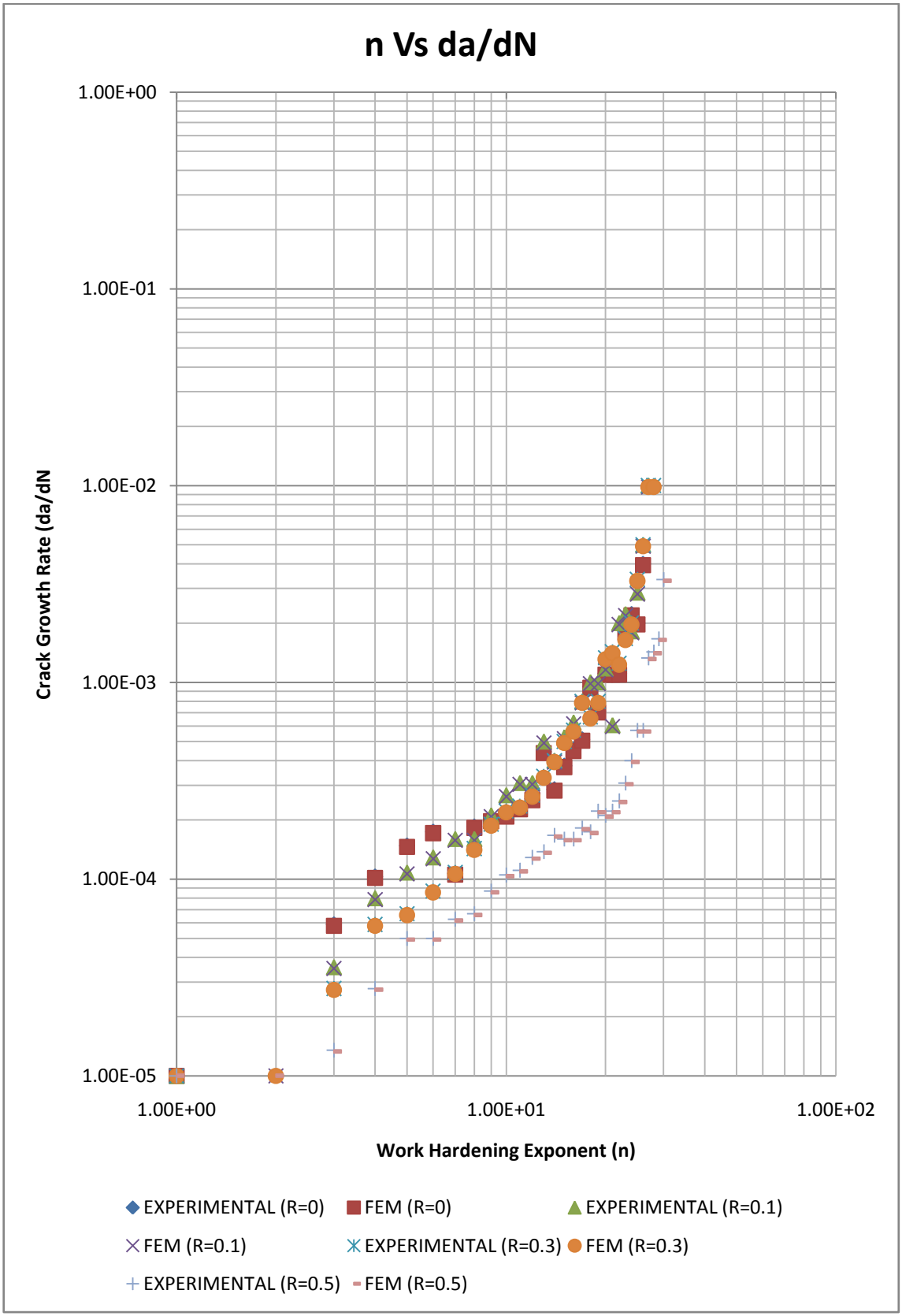

Fig 4.8 For Pmax= Constant (5052 Al)

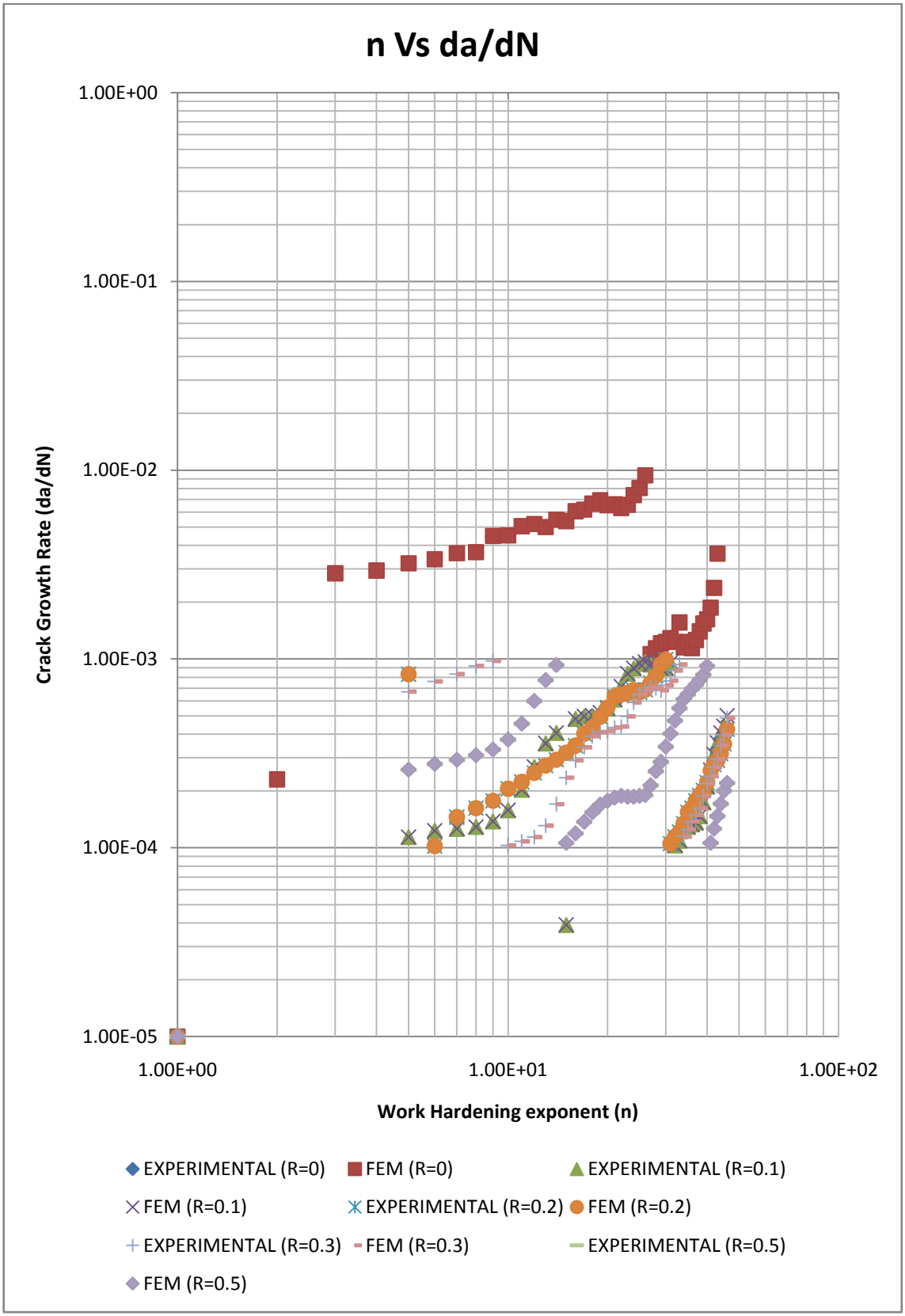

Fig 4.9 For ΔP= Constant (6061-T6 Al)

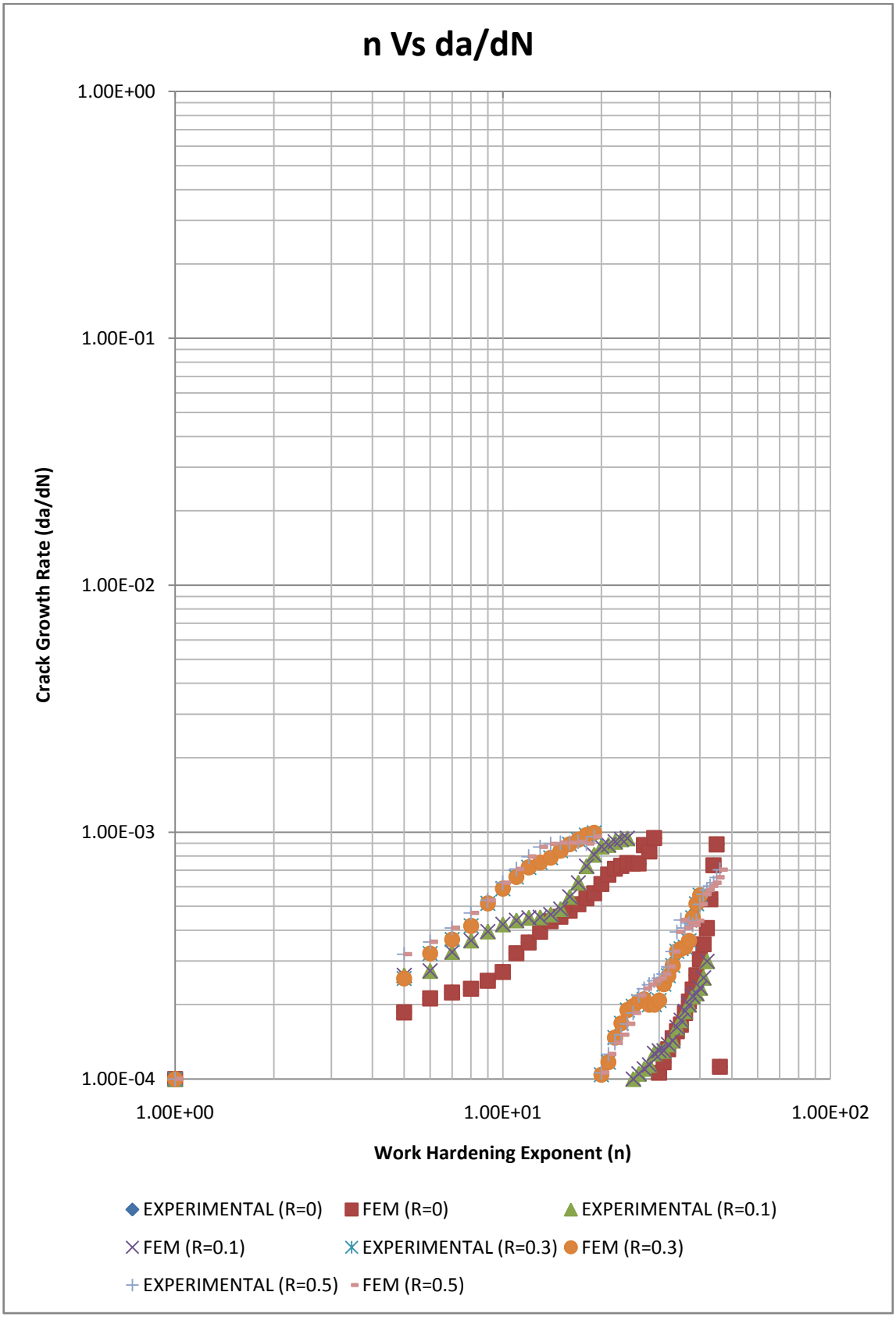

Fig 4.10 For Pmax=Constant (6061-T6 Al)

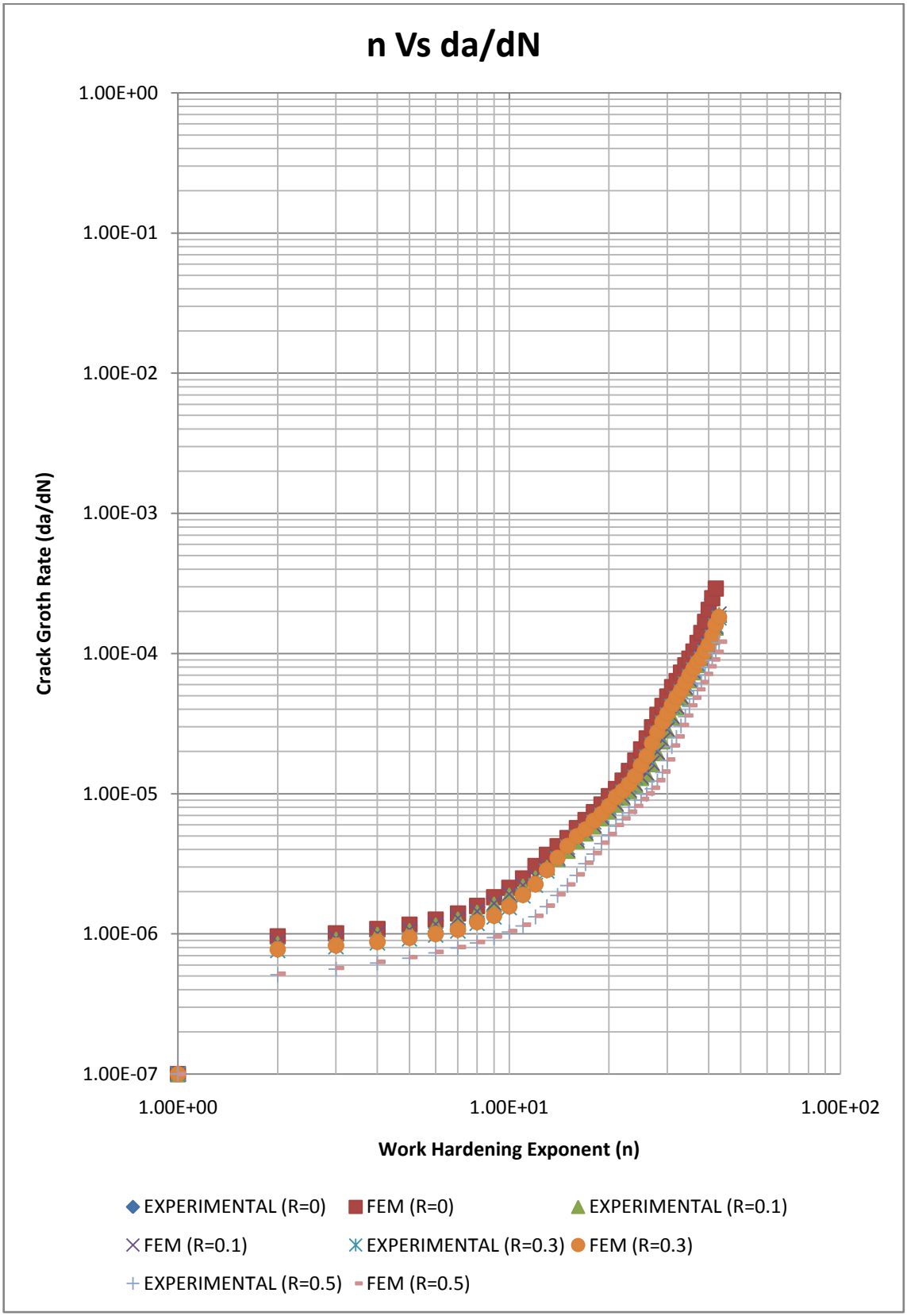

Fig 4.11For Pmax= Constant (6063-T6 Al)

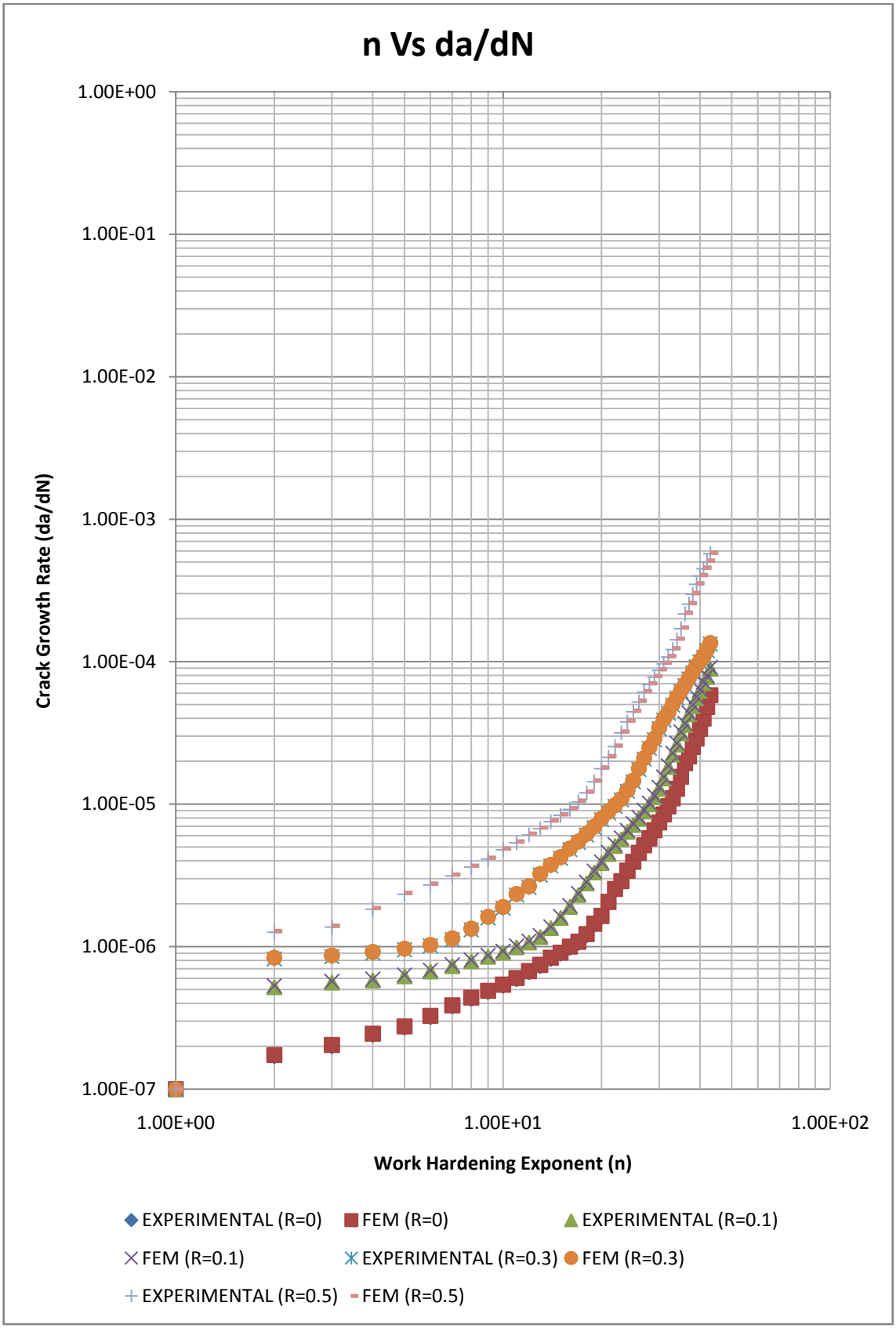

Fig 4.12 For ΔP=Constant (6063-T6 Al)

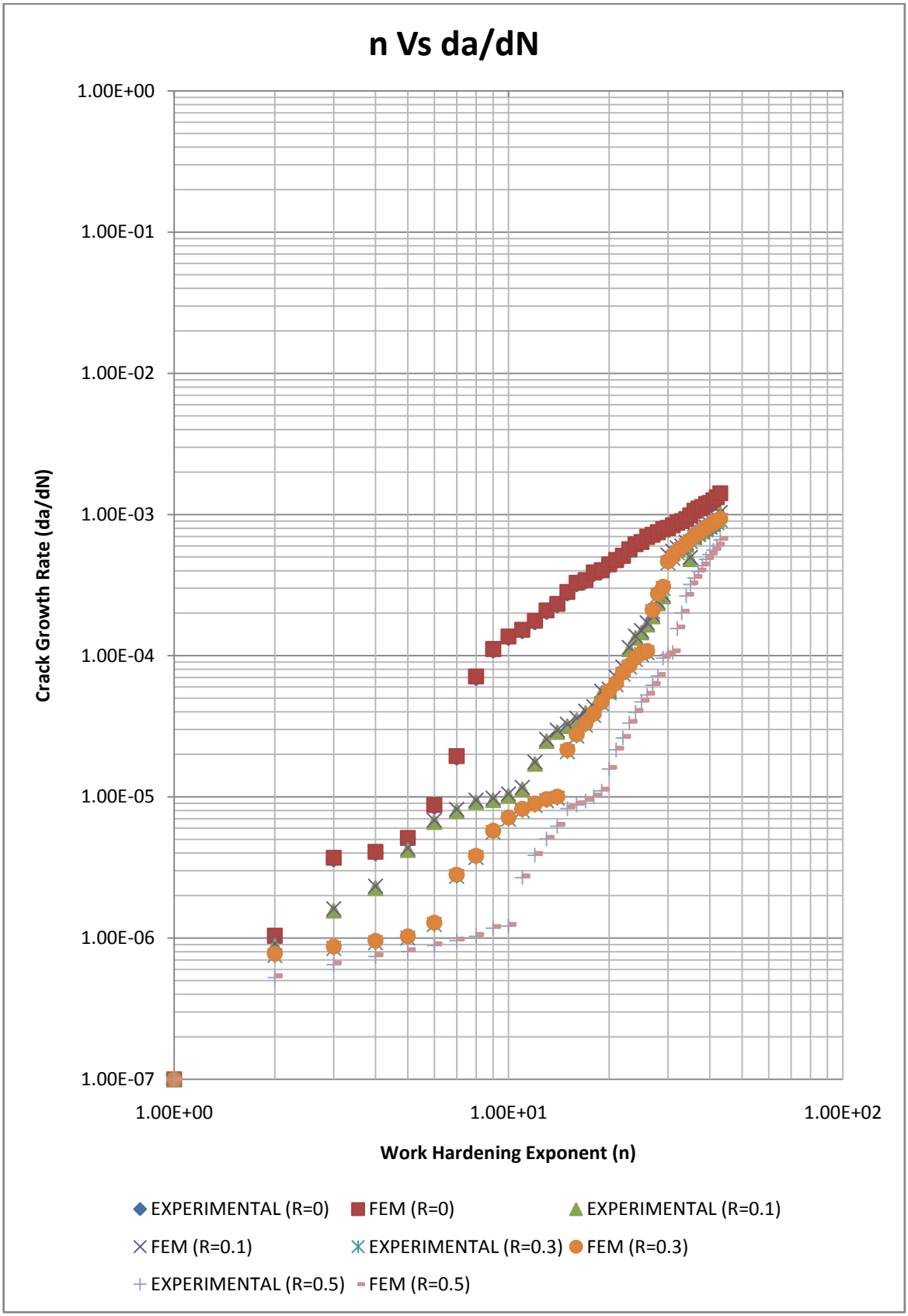

Fig 4.13 For ΔP=Constant (6351-T6 Al)

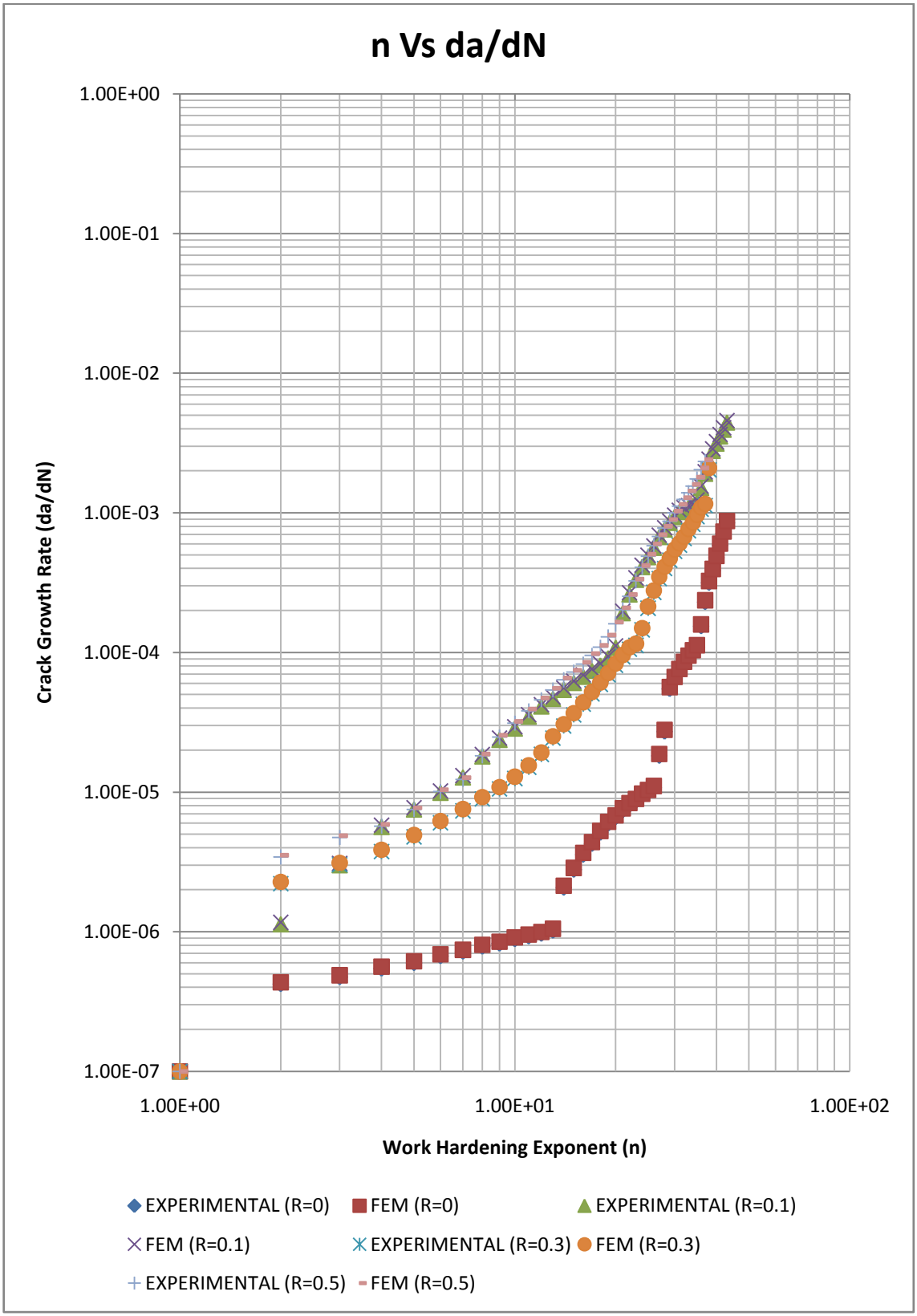

Fig 4.14 For Pmax=Constant (6351-T6 Al)

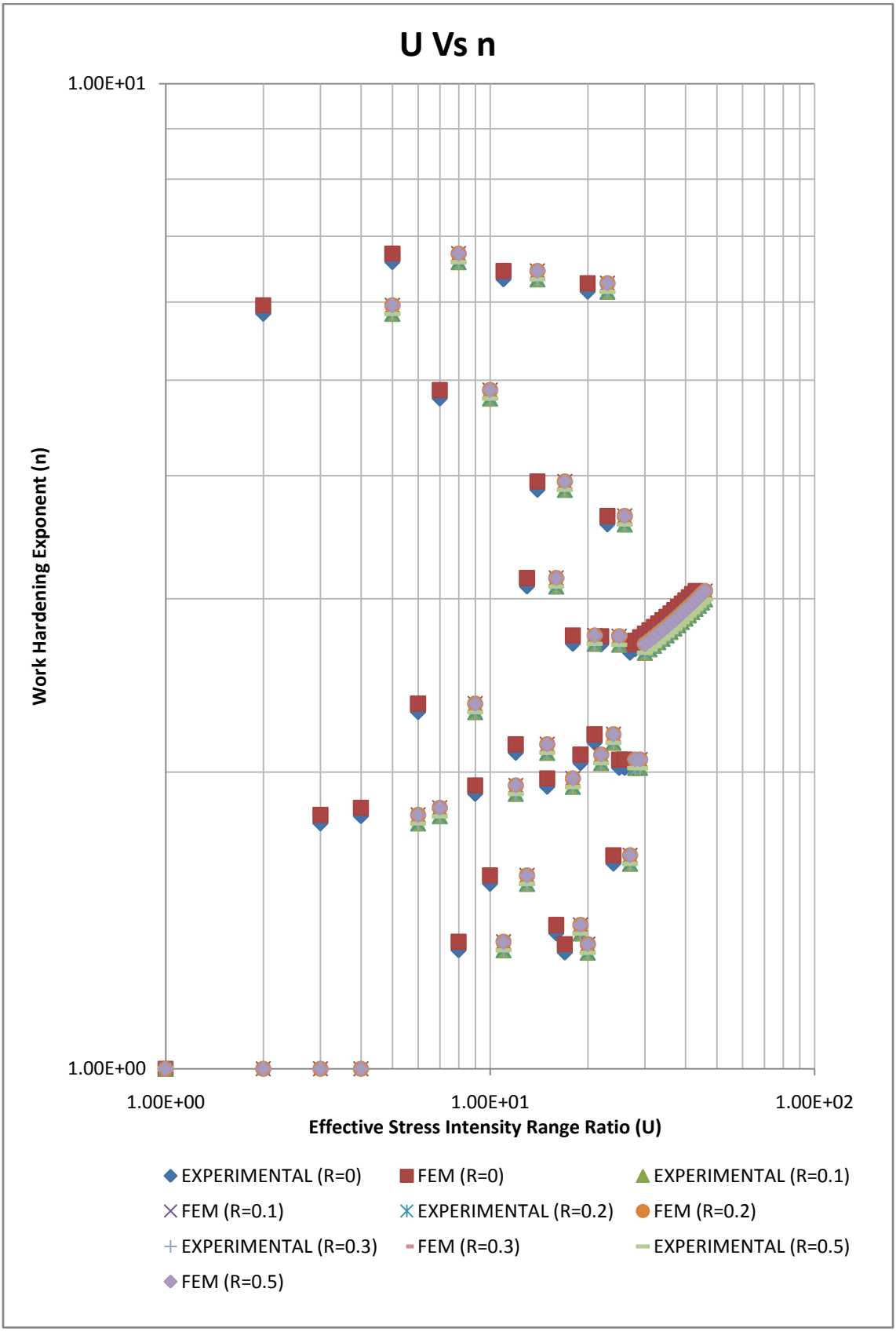

Fig 4.15 For ΔP = Constant (3003 Al)

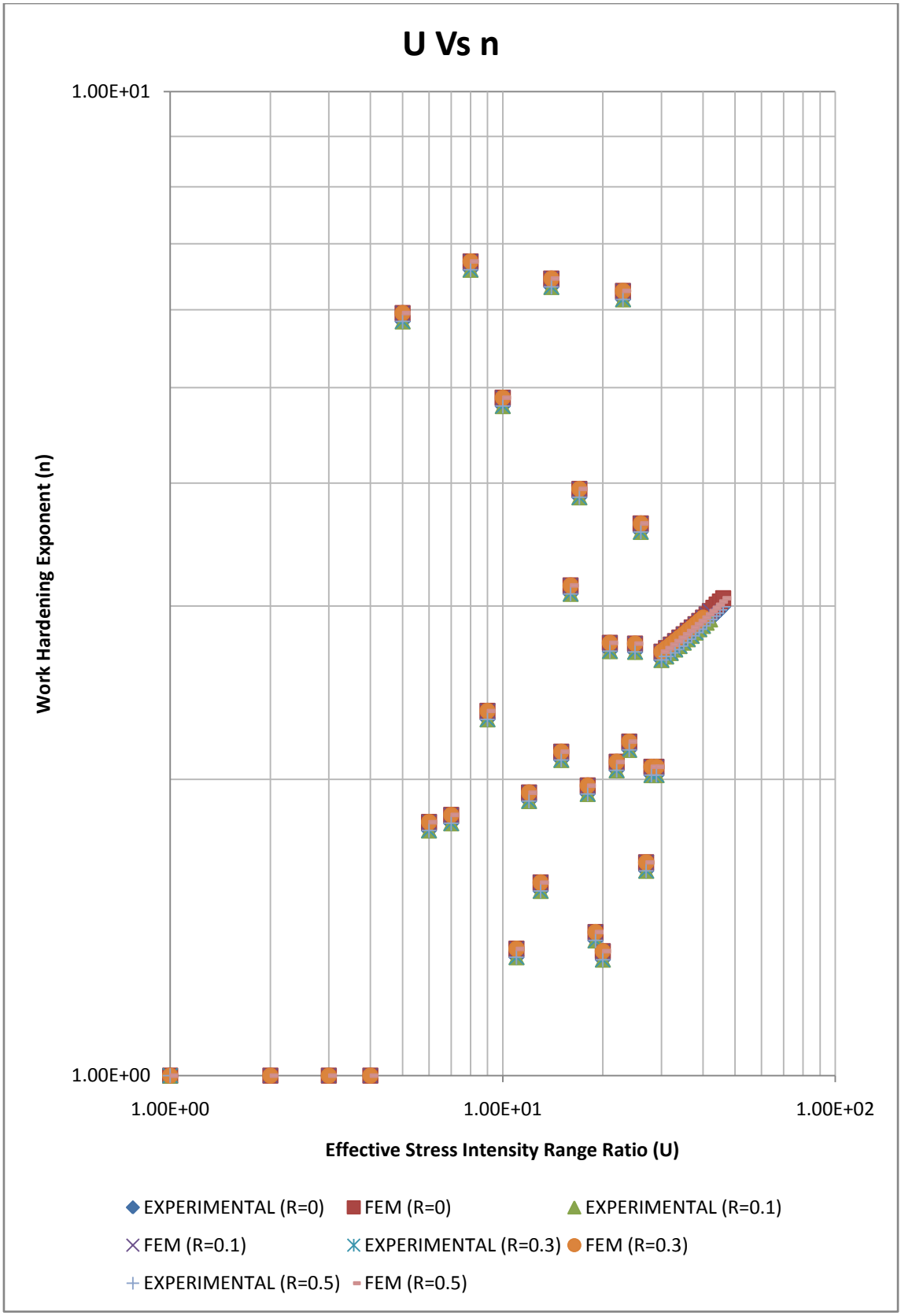

Fig 4.16 For Pmax=Constant (3003 Al)

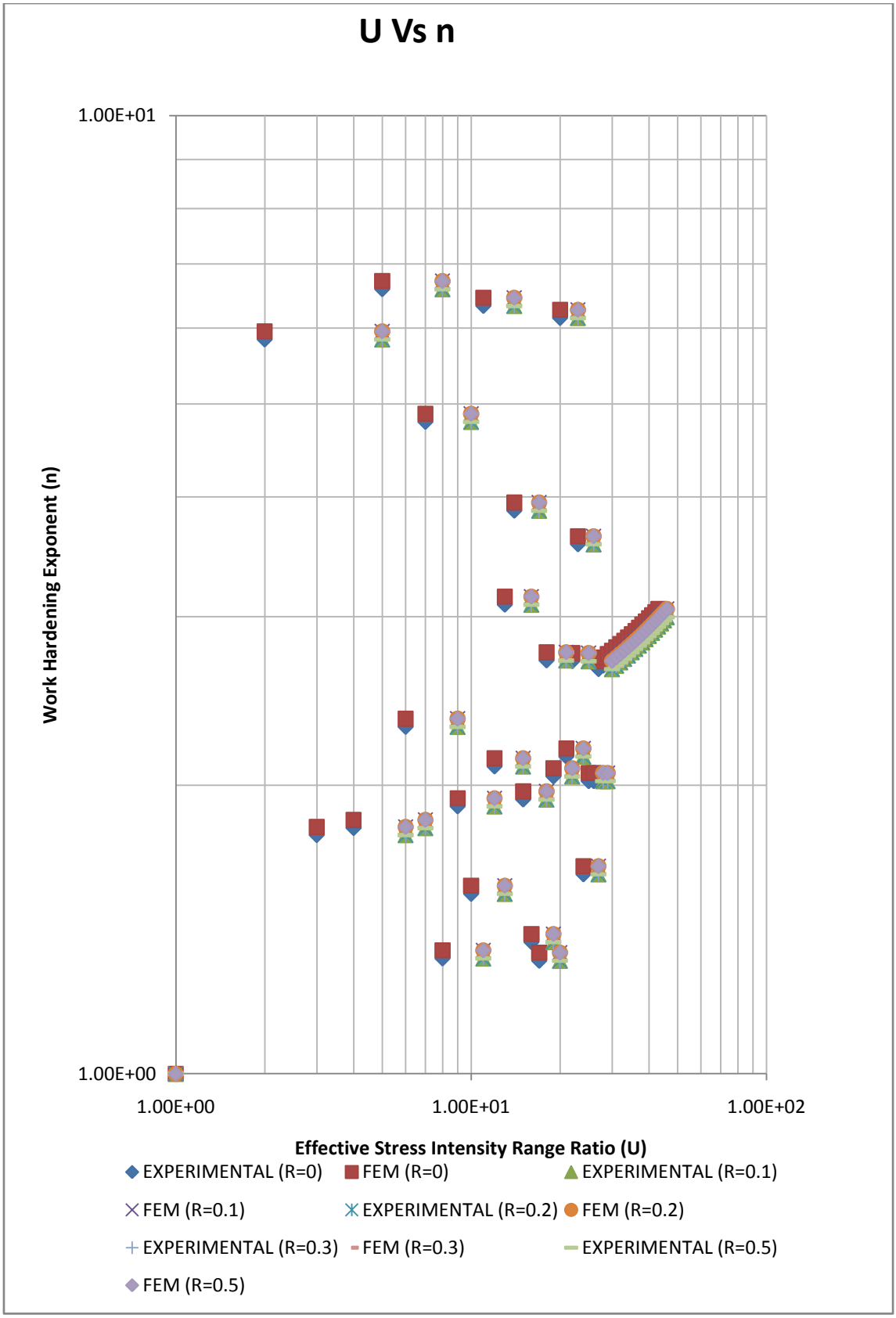

Fig 4.17 For ΔP= Constant (5052 Al)

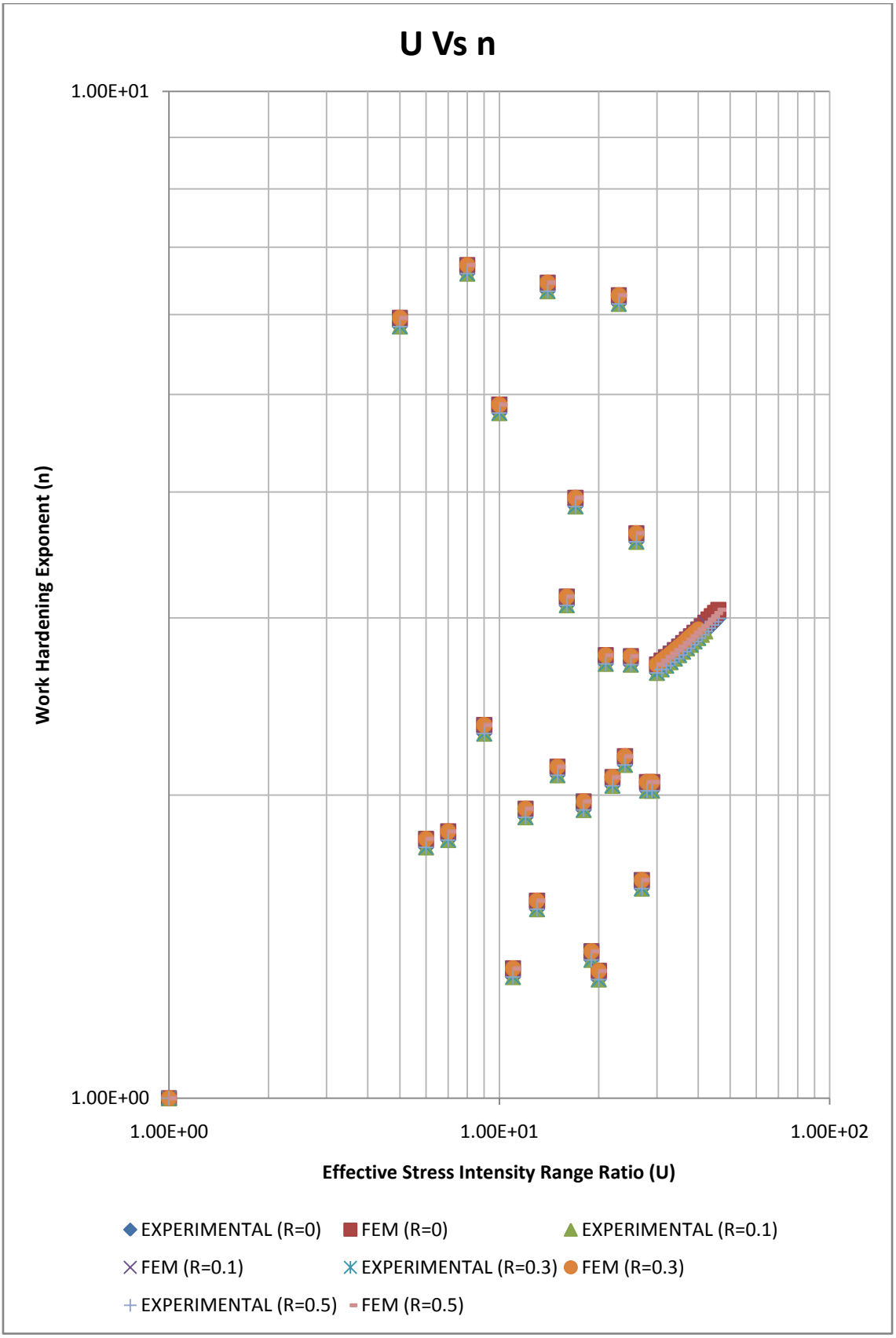

Fig 4.18 For Pmax= Constant (5052 Al)

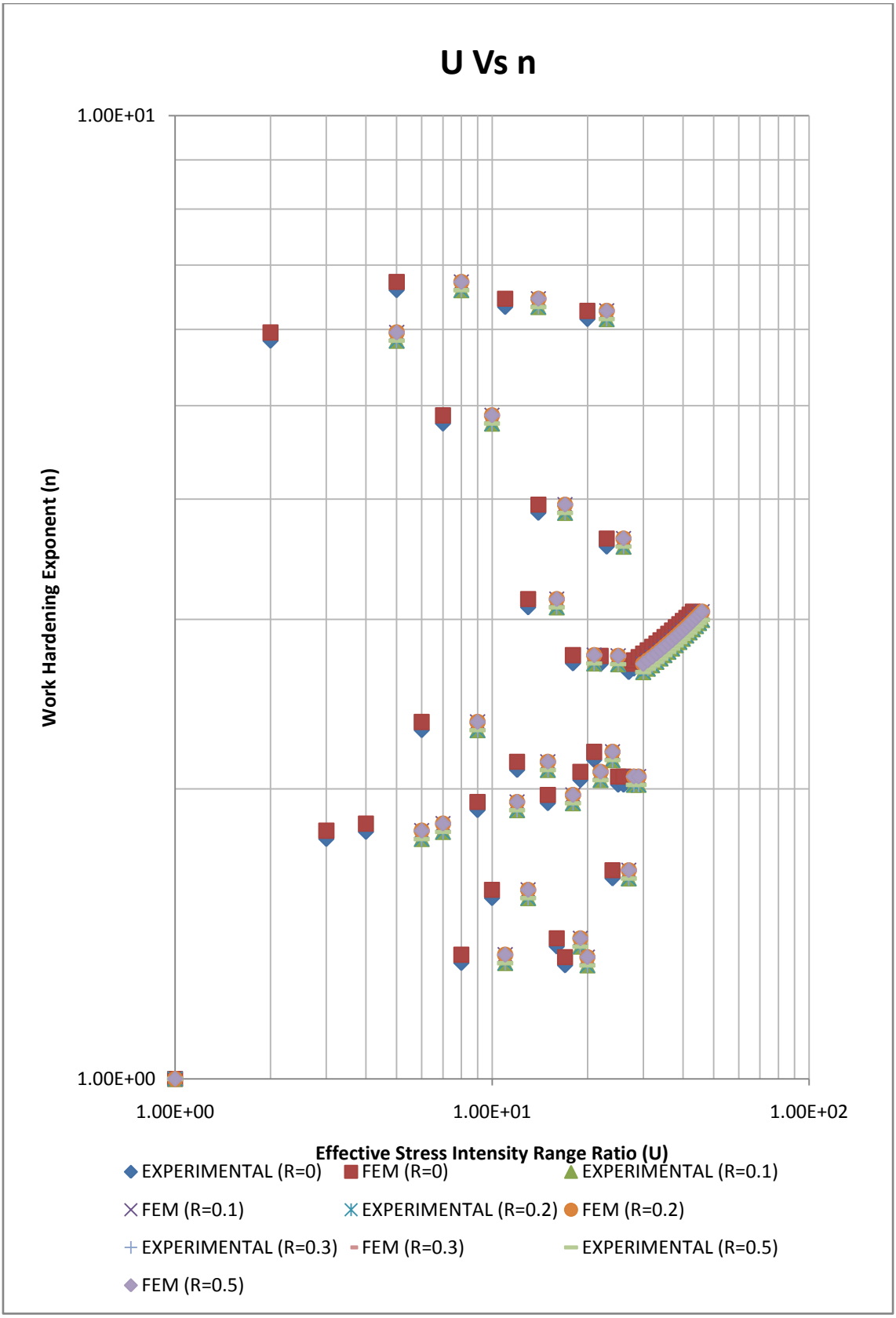

Fig 4.19 For ΔP= Constant (6061-T6 Al)

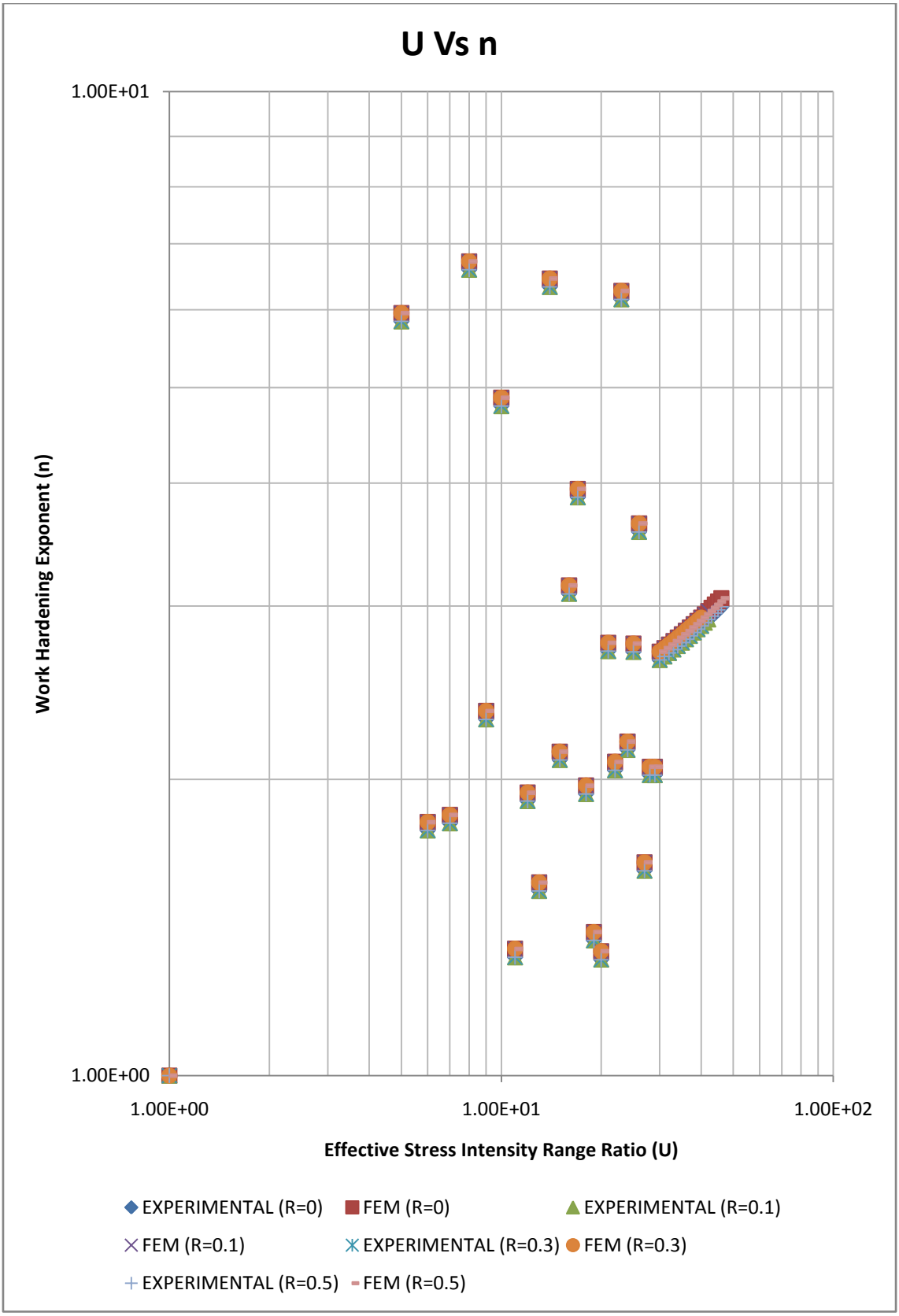

Fig 4.20 For Pmax=Constant (6061-T6 Al)

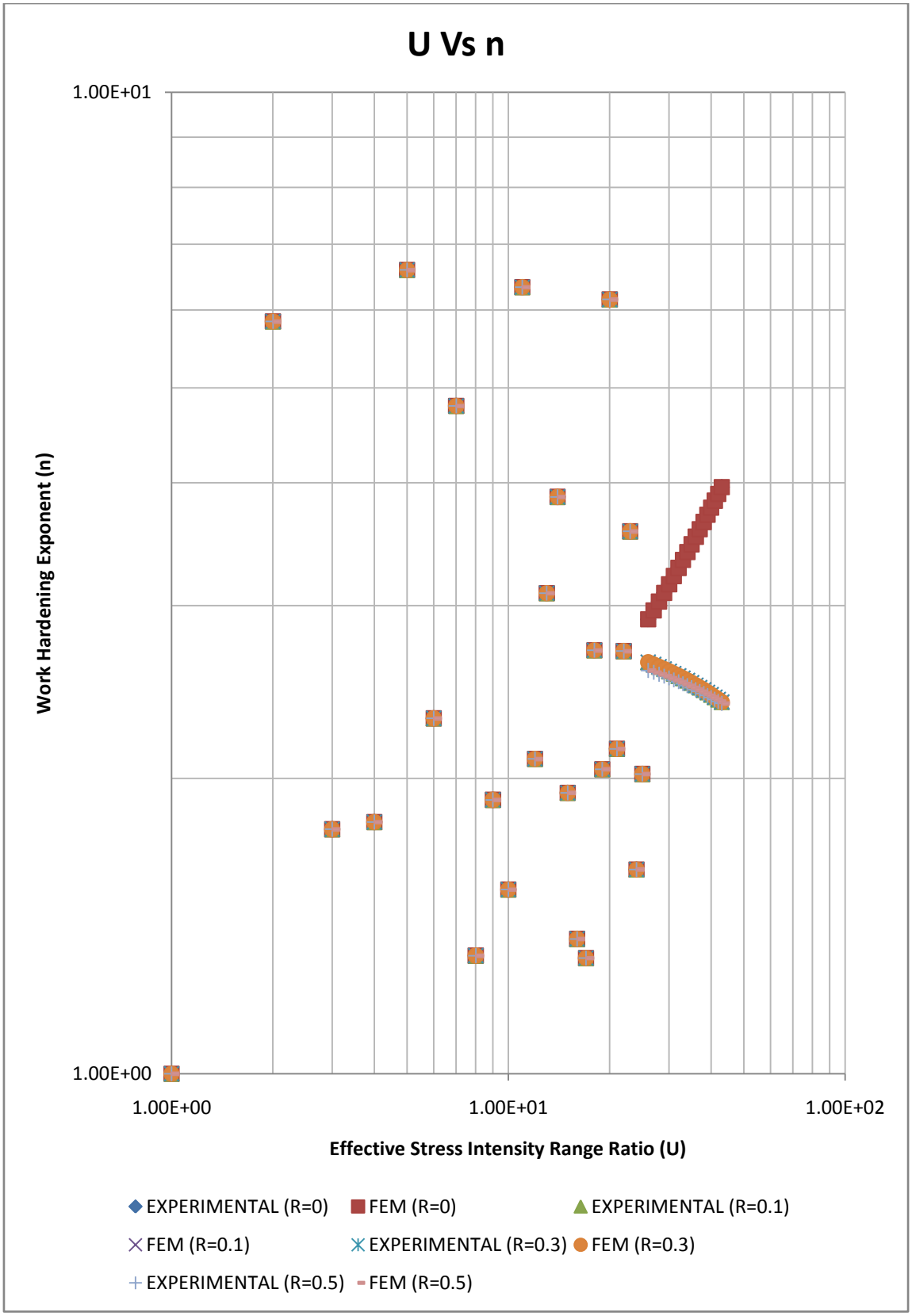

Fig 4.21 For Pmax= Constant (6063-T6 Al)

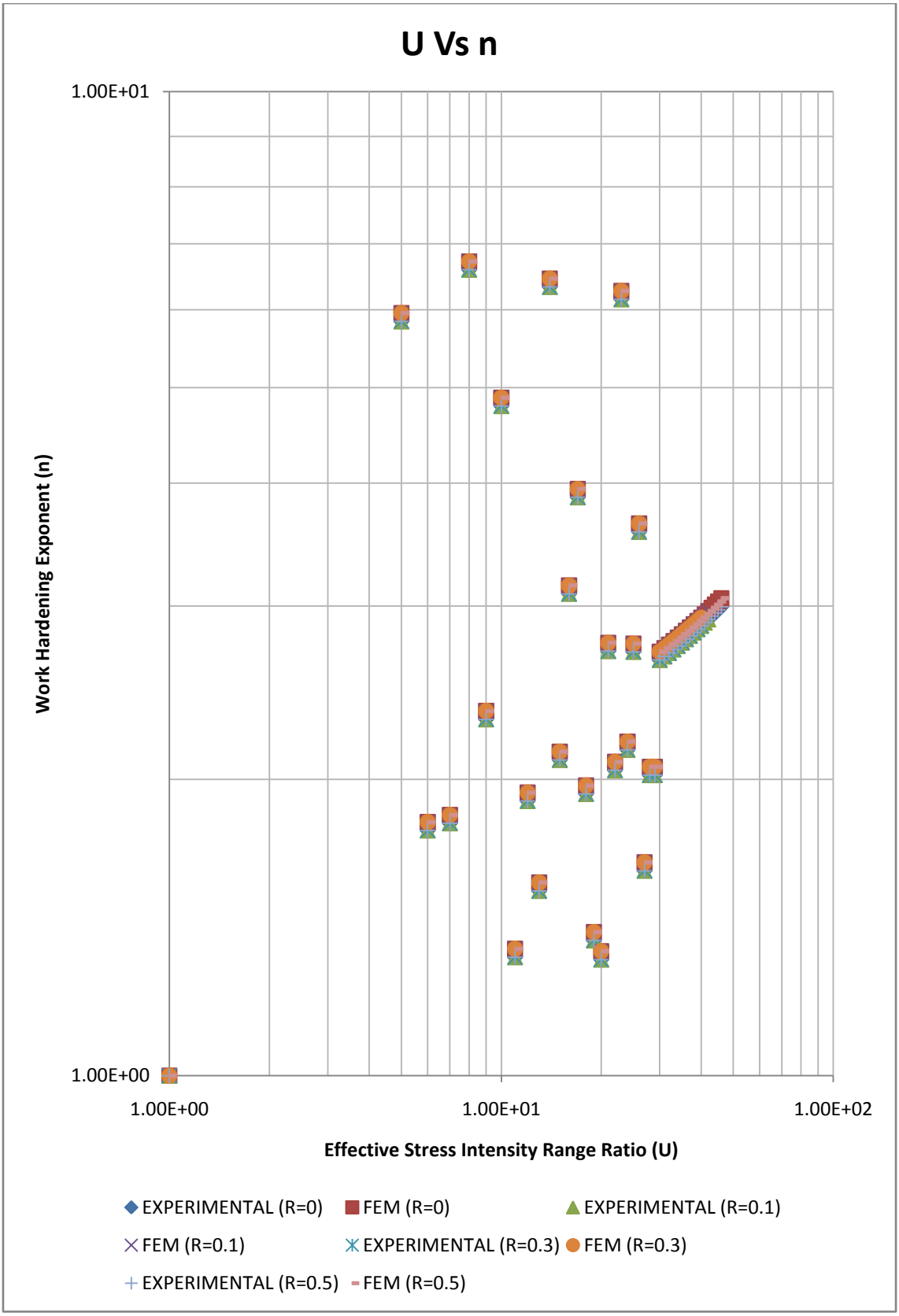

Fig 4.22 For ΔP=Constant (6063-T6 Al)

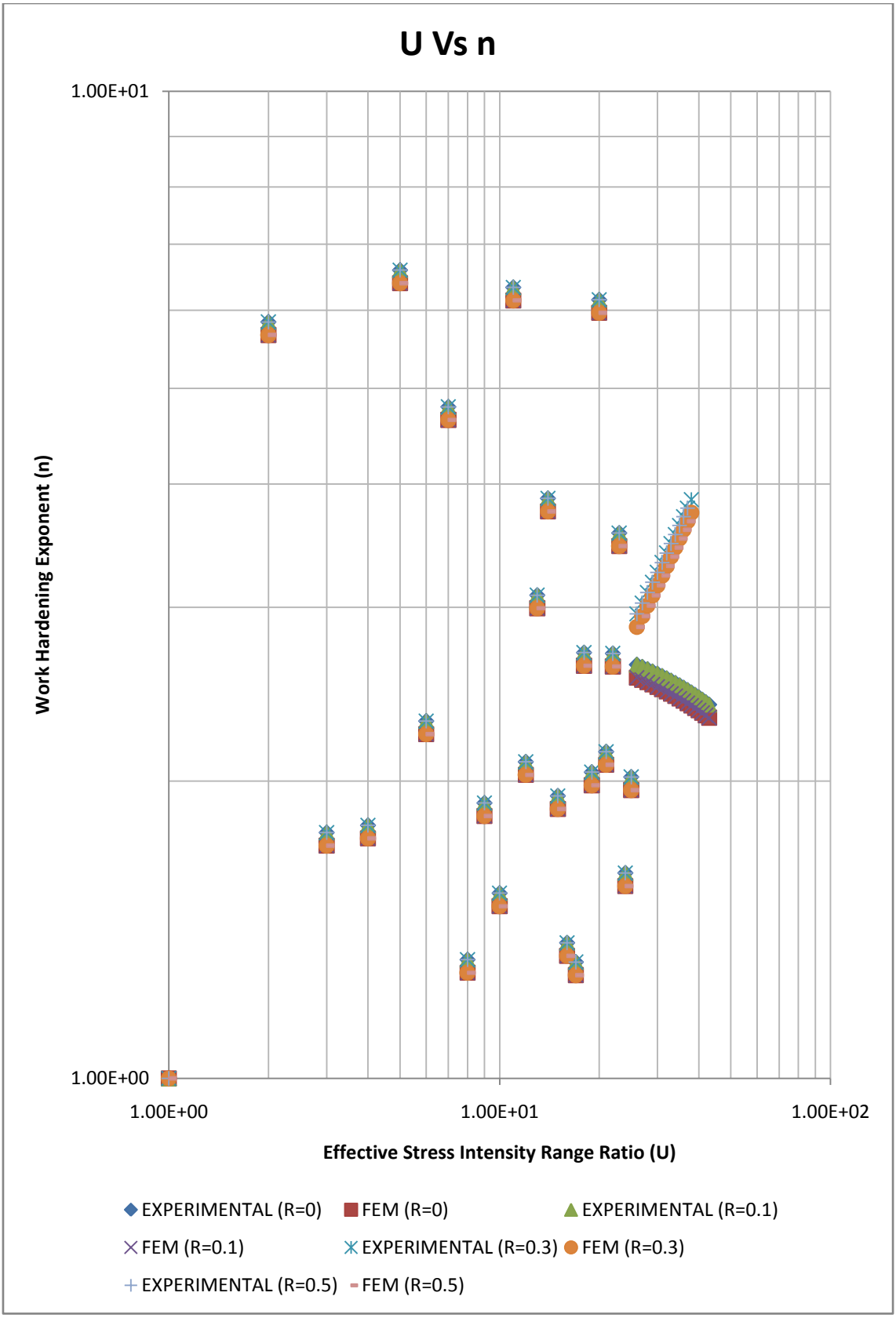

Fig 4.23 For ΔP=Constant (6351-T6 Al)

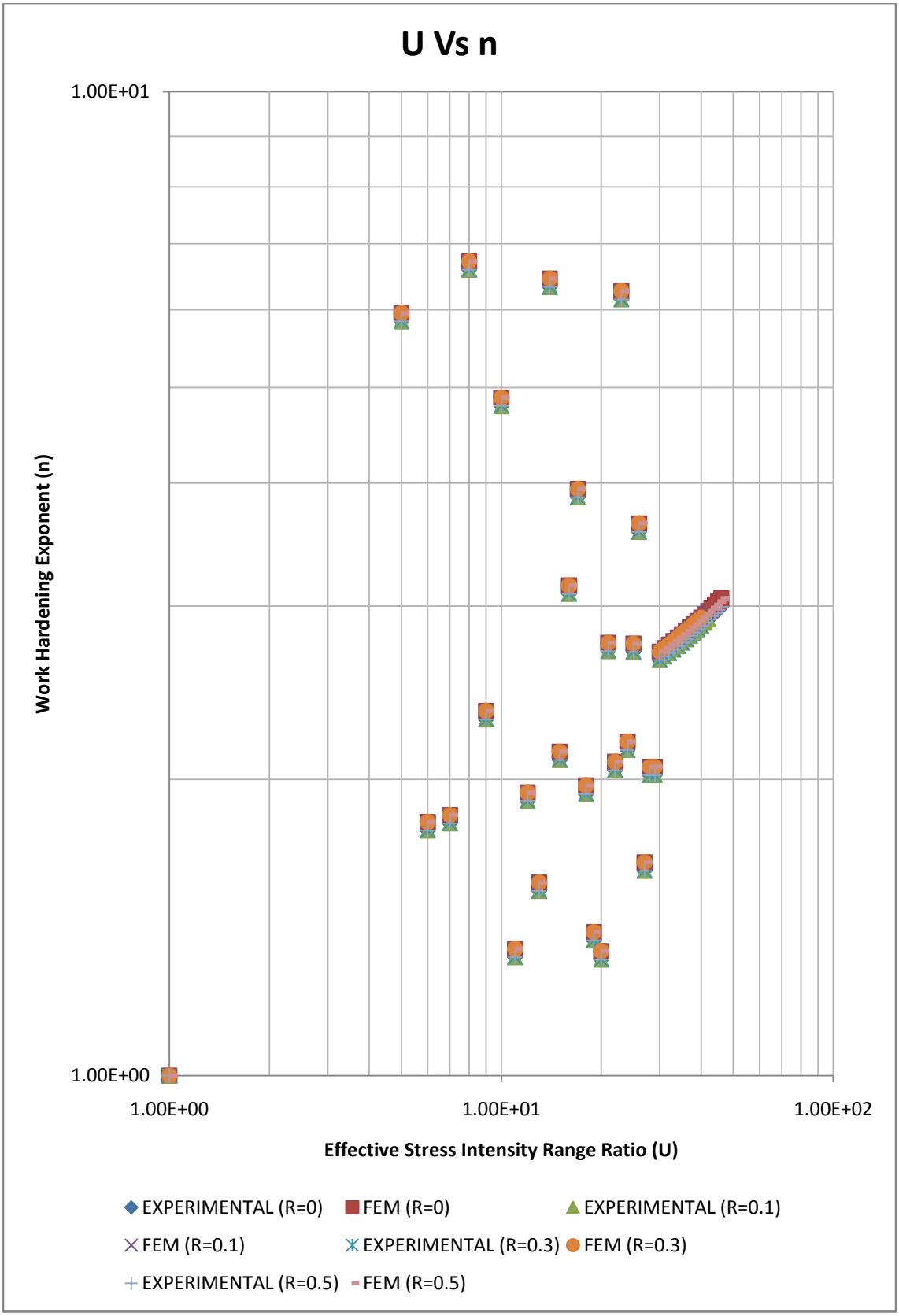

Fig 4.24 For Pmax= Constant (6351-T6 Al)

4.7 REGRESSION ANALYSIS

After FEM analysis, Regression analysis was done. From the output graph was plotted between U Vs n and drew a trend line in logarithmic mode. The details analysis and scheme of the curves are given below.

4.7.1 3003 Al Alloy for $\Delta P = Constant$

Table 4.8 Regression Analysis for 3003 Al Alloy for ΔP=Constant

Model Summary

R	R Square	Adjusted R Square	Std. Error of the Estimate
.182	.033	-.009	.001

The independent variable is n.

ANOVA

	Sum of Squares	Df	Mean Square	F	Sig.
Regression	.000	1	.000	.785	.385
Residual	.000	23	.000		
Total	.000	24			

The independent variable is n.

Coefficients

	Unstandardized Coefficients		Standardized Coefficients	t	Sig.
	B	Std. Error	Beta		
n	1.000	.000	1.199	7717.744	.000
(Constant)	1.478	.001		2316.565	.000

The dependent variable is ln(1 / U).

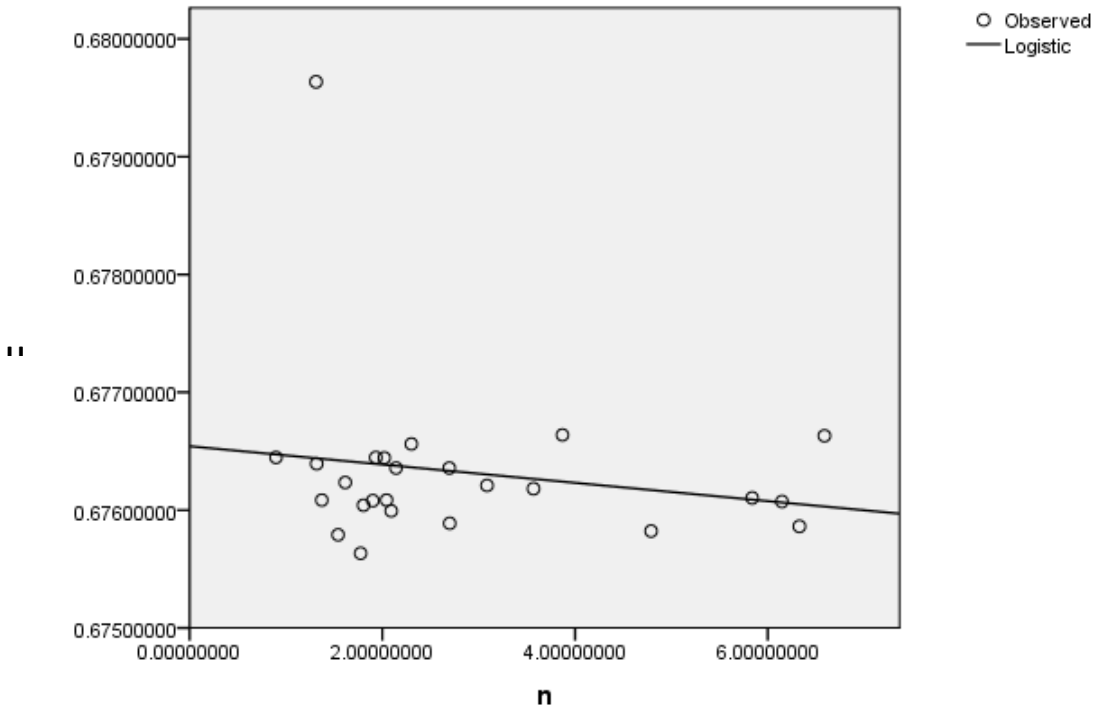

Fig 4.25 Regression Results for 3003 Al for ΔP=Constant

4.7.2 5052 Al Alloy for $\Delta P = Constant$

Table 4.9 Regression Analysis for 5052 Al Alloy for ΔP=Constant

Model Summary

R	R Square	Adjusted R Square	Std. Error of the Estimate
.485	.235	.203	.000

The independent variable is n.

ANOVA

	Sum of Squares	df	Mean Square	F	Sig.
Regression	.000	1	.000	7.382	.012

Residual	.000	24	.000		
Total	.000	25			

The independent variable is n.

Coefficients

	Unstandardized Coefficients		Standardized Coefficients		
	B	Std. Error	Beta	t	Sig.
n	1.000	.000	.616	3.381E7	.000
(Constant)	1.818	.000		1.023E7	.000

The dependent variable is ln(1 / U).

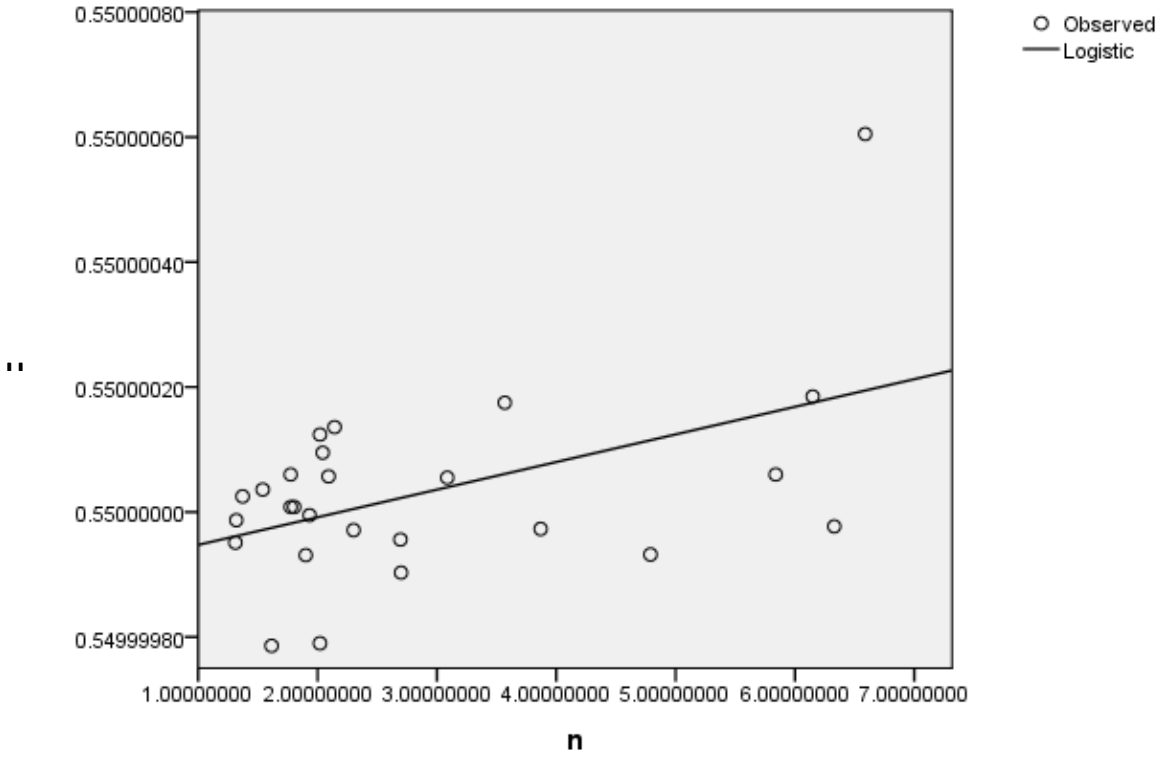

Fig 4.26 Regression Results for 5052 Al Alloy for ΔP=Constant

4.7.3 6061 Al Alloy for $\Delta P = Constant$

Table 4.10 Regression Analysis for 6061 Al Alloy for ΔP=Constant

Model Summary

R	R Square	Adjusted R Square	Std. Error of the Estimate
.057	.003	-.022	.008

The independent variable is n.

ANOVA

	Sum of Squares	Df	Mean Square	F	Sig.
Regression	.000	1	.000	.131	.719
Residual	.003	40	.000		
Total	.003	41			

The independent variable is n.

Coefficients

	Unstandardized Coefficients		Standardized Coefficients	t	Sig.
	B	Std. Error	Beta		
n	1.000	.001	.944	1006.474	.000
(Constant)	1.349	.004		319.758	.000

The dependent variable is ln(1 / U).

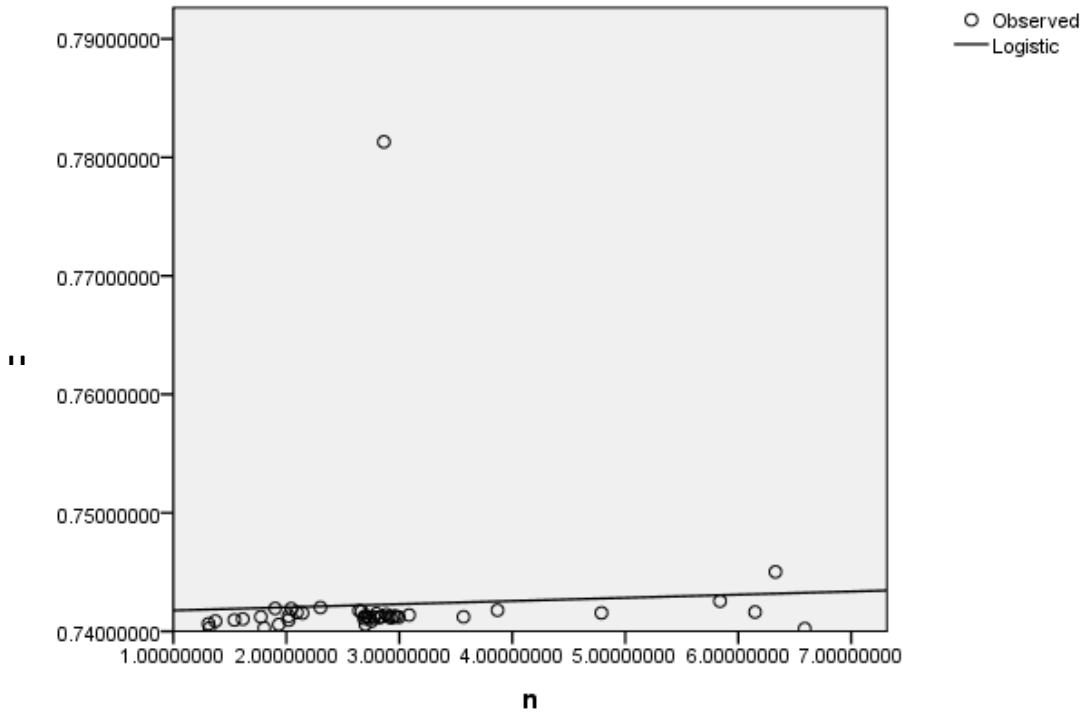

Fig 4.27 Regression Results for 6061 Al Alloy for ΔP=Constant

4.7.4 6063 Al Alloy for $\Delta P = Constant$

Table 4.11 Regression Analysis for 6063 Al Alloy for ΔP=Constant

Model Summary

R	R Square	Adjusted R Square	Std. Error of the Estimate
.096	.009	-.016	.020

The independent variable is n.

ANOVA

	Sum of Squares	Df	Mean Square	F	Sig.
Regression	.000	1	.000	.372	.545

Residual	.016	40	.000		
Total	.016	41			

The independent variable is n.

Coefficients

	Unstandardized Coefficients		Standardized Coefficients		
	B	Std. Error	Beta	t	Sig.
n	.999	.002	.908	424.519	.000
(Constant)	1.481	.012		124.232	.000

The dependent variable is ln(1 / U).

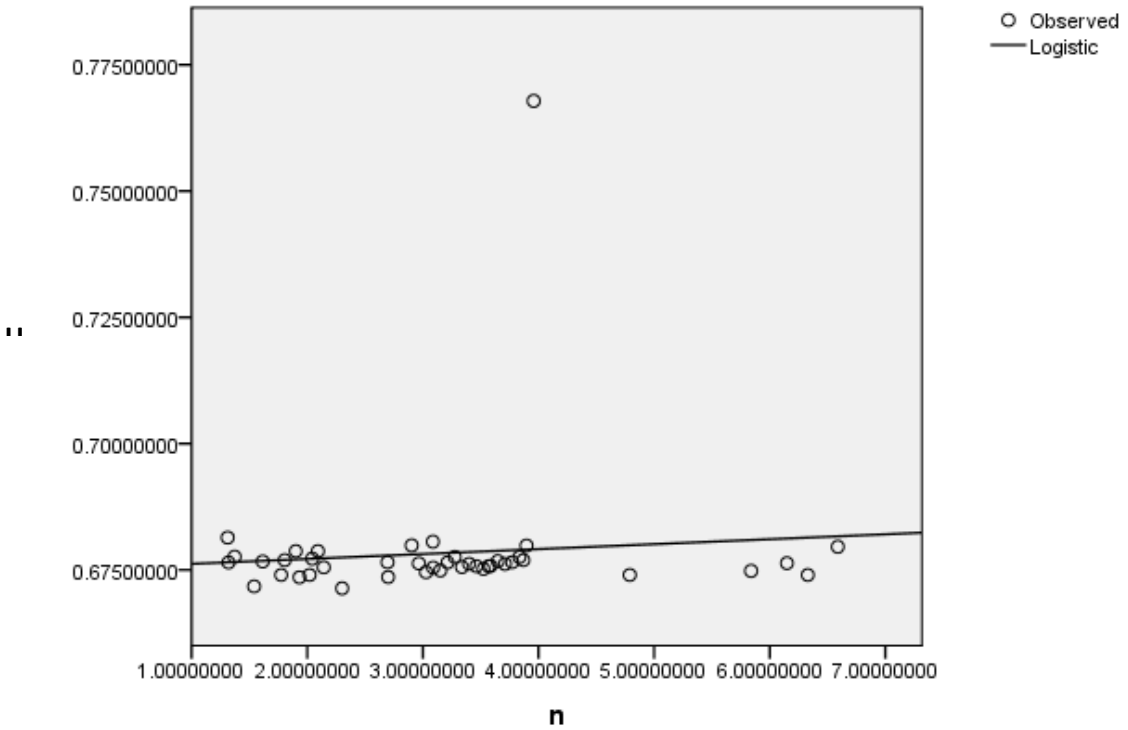

Fig 4.28 Regression Results for 6063 Al Alloy for ΔP=Constant

4.7.5 6351 Al Alloy for $\Delta P = Constant$

Table 4.12 Regression Analysis for 6351 Al Alloy for ΔP=Constant

Table 4.14 Model Summary

R	R Square	Adjusted R Square	Std. Error of the Estimate
.055	.003	-.022	.007

The independent variable is n.

Table 4.15 ANOVA

	Sum of Squares	df	Mean Square	F	Sig.
Regression	.000	1	.000	.122	.729
Residual	.002	40	.000		
Total	.002	41			

The independent variable is n.

Table 4.16 Coefficients

	Unstandardized Coefficients		Standardized Coefficients		
	B	Std. Error	Beta	T	Sig.
N	1.000	.001	1.057	1134.255	.000
(Constant)	1.346	.004		372.219	.000

The dependent variable is ln(1 / U).

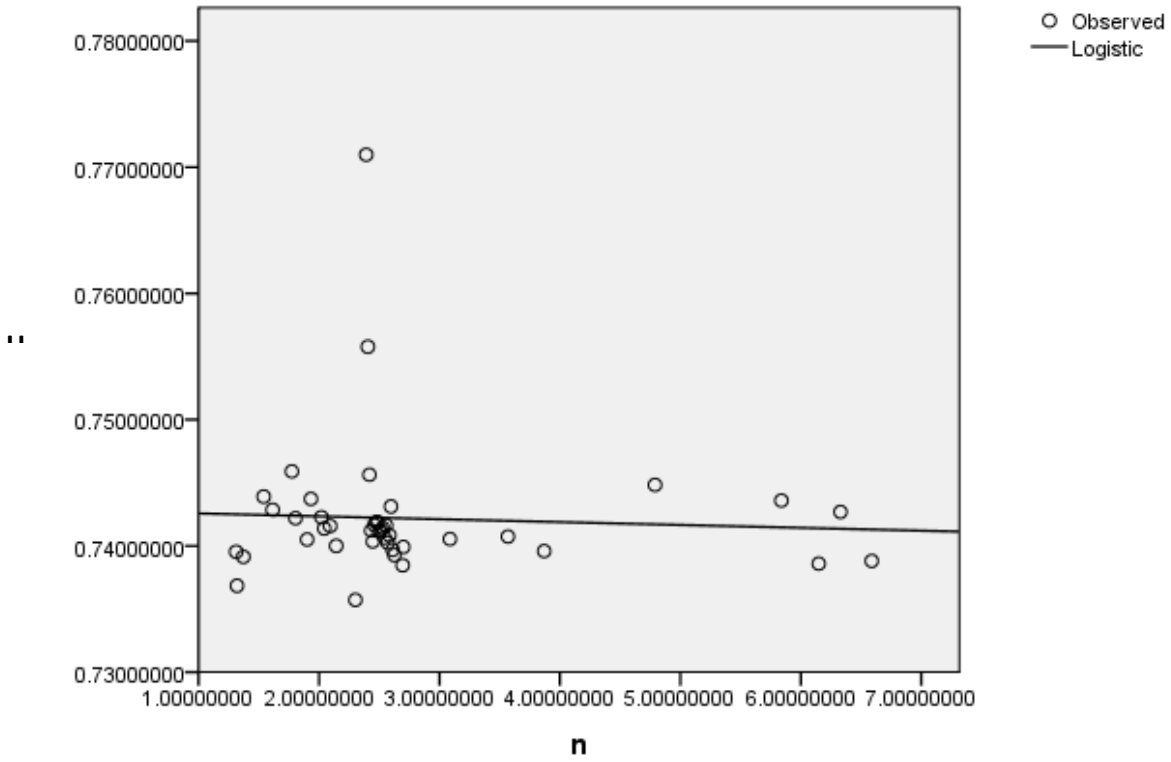

Fig 4.29 Regression Results for 6351 Al Alloy for ΔP=Constant

4.7.6 3003 Al Alloy for P_{max} = Constant

Table 4.13 Regression Analysis for 3003 Al Alloy for Pmax=Constant

Model Summary

R	R Square	Adjusted R Square	Std. Error of the Estimate
.270	.073	.033	.018

The independent variable is n.

ANOVA

	Sum of Squares	df	Mean Square	F	Sig.
Regression	.001	1	.001	1.806	.192

Residual	.007	23	.000		
Total	.008	24			

The independent variable is n.

Coefficients

	Unstandardized Coefficients		Standardized Coefficients		
	B	Std. Error	Beta	T	Sig.
n	.997	.002	.763	471.410	.000
(Constant)	1.365	.010		141.499	.000

The dependent variable is ln(1 / U).

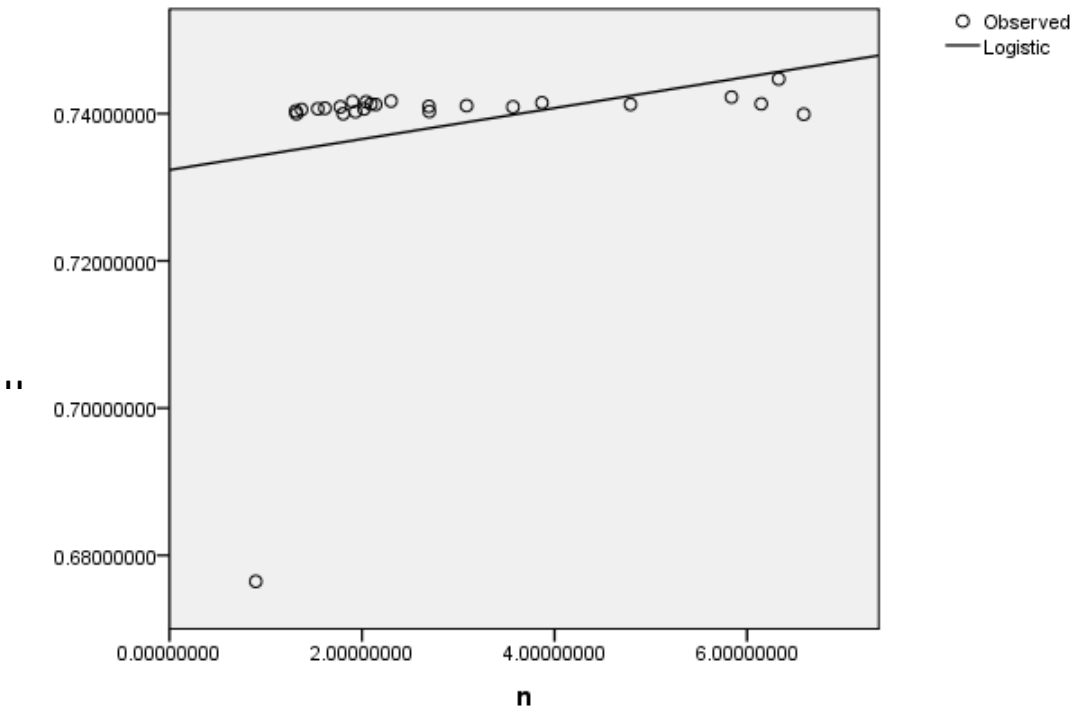

Fig 4.30 Regression Results for 3003 Al Alloy for Pmax=Constant

4.7.7 5052 Al Alloy for P_{max} = Constant

Table 4.14 Regression Analysis for 5052 Al Alloy for Pmax=Constant

Model Summary

R	R Square	Adjusted R Square	Std. Error of the Estimate
.222	.049	.006	.000

The independent variable is n.

ANOVA

	Sum of Squares	Df	Mean Square	F	Sig.
Regression	.000	1	.000	1.145	.296
Residual	.000	22	.000		
Total	.000	23			

The independent variable is n.

Coefficients

	Unstandardized Coefficients		Standardized Coefficients	T	Sig.
	B	Std. Error	Beta		
N	1.000	.000	1.249	2.875E7	.000
(Constant)	1.818	.000		8481198.639	.000

The dependent variable is ln(1 / U).

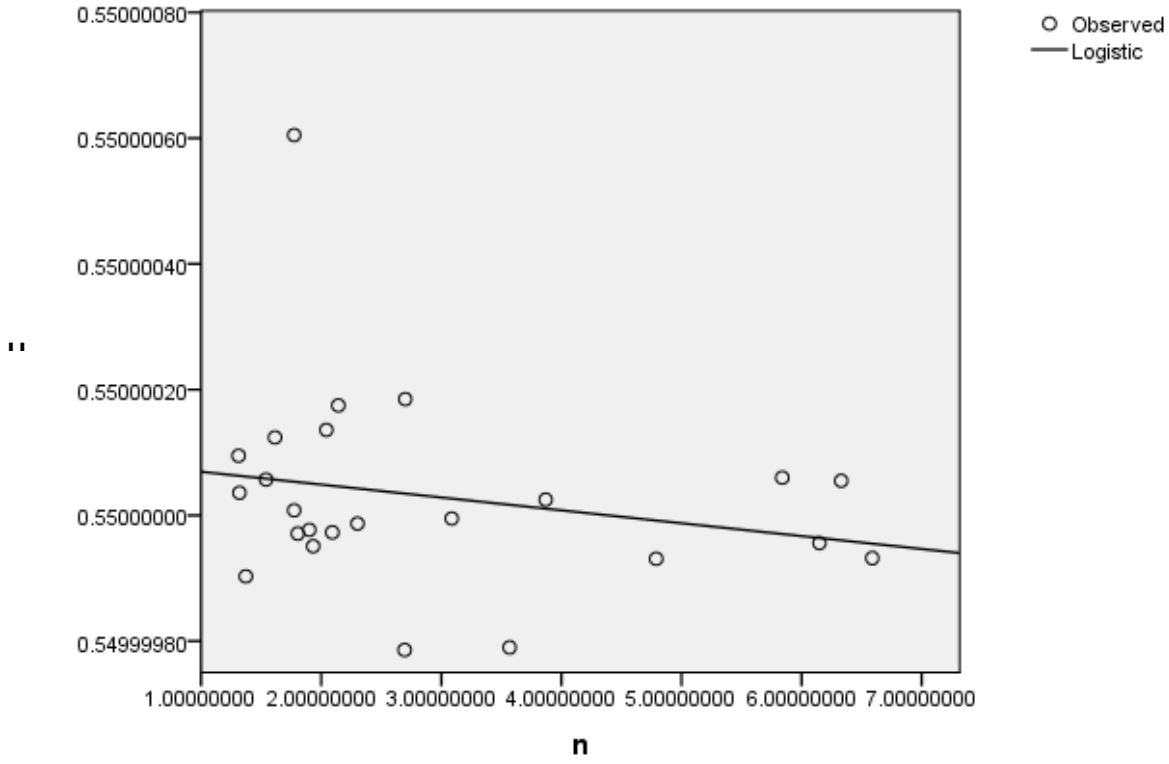

Fig 4.31 Regression Results for 5052 Al Alloy for Pmax=Constant

4.7.8 6061 Al Alloy for P_{max} = Constant

Table 4.15Regression Analysis for 6061 Al Alloy for Pmax=Constant

Model Summary

R	R Square	Adjusted R Square	Std. Error of the Estimate
.068	.005	-.020	.001

The independent variable is n.

ANOVA

	Sum of Squares	df	Mean Square	F	Sig.
Regression	.000	1	.000	.184	.670

Residual	.000	40	.000		
Total	.000	41			

The independent variable is n.

Coefficients

	Unstandardized Coefficients		Standardized Coefficients		
	B	Std. Error	Beta	T	Sig.
n	1.000	.000	1.070	6172.236	.000
(Constant)	1.449	.001		1960.927	.000

The dependent variable is ln(1 / U).

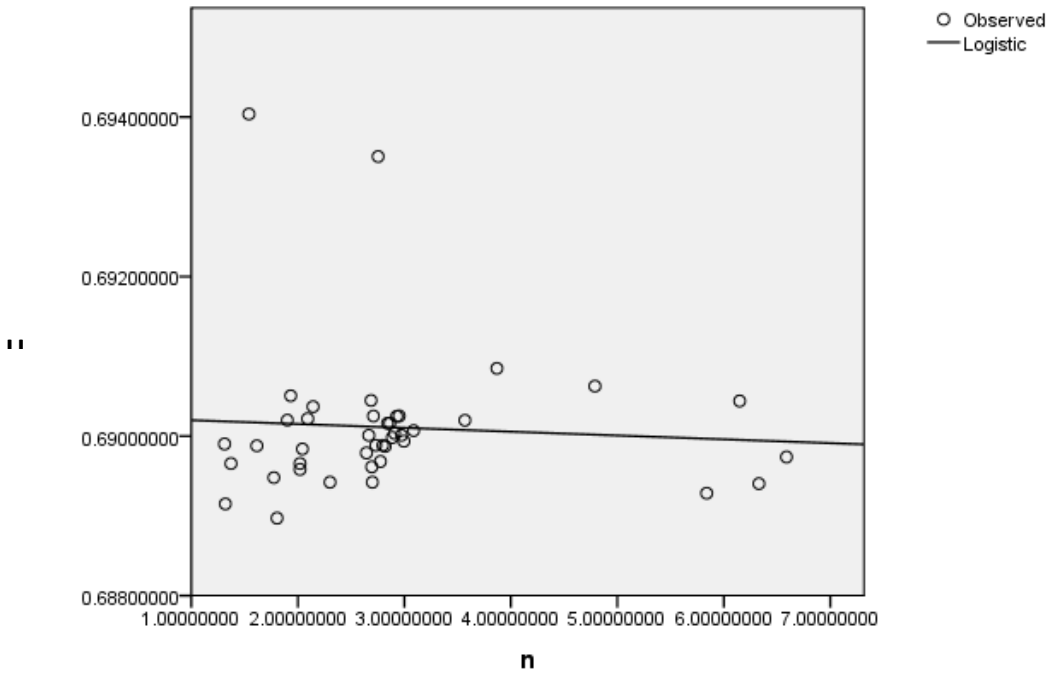

Fig 4.32 Regression Results for 6061 Al Alloy for Pmax=Constant

4.7.9 6063 Al Alloy for P_{max} = Constant

Table 4.16 Regression Analysis for 6063 Al Alloy for Pmax=Constant

Model Summary

R	R Square	Adjusted R Square	Std. Error of the Estimate
.144	.021	-.004	.003

The independent variable is n.

ANOVA

	Sum of Squares	df	Mean Square	F	Sig.
Regression	.000	1	.000	.827	.369
Residual	.000	39	.000		
Total	.000	40			

The independent variable is n.

Coefficients

	Unstandardized Coefficients		Standardized Coefficients	T	Sig.
	B	Std. Error	Beta		
n	1.000	.000	.866	2525.228	.000
(Constant)	1.481	.002		824.829	.000

The dependent variable is ln(1 / U).

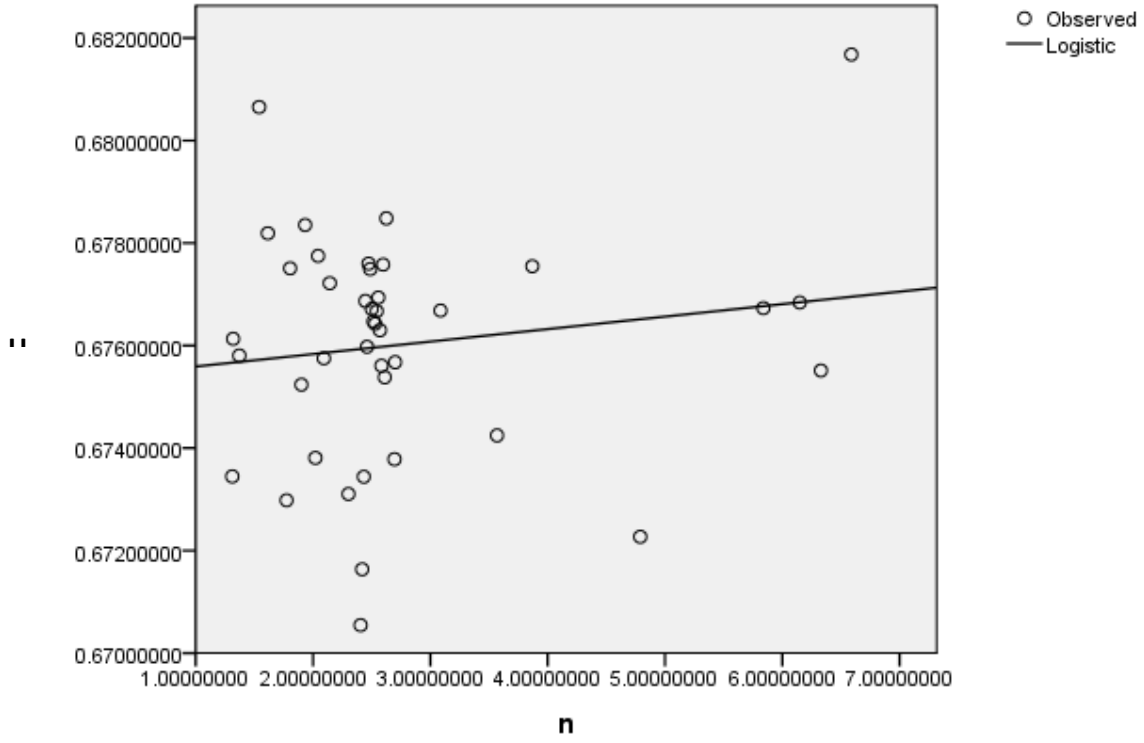

Fig 4.33 Regression Results for 6063 Al Alloy for Pmax=Constant

4.7.10 6351 Al Alloy for P_{max} = Constant

Table 4.17 Regression Analysis for 6351 Al Alloy for Pmax=Constant

Model Summary

R	R Square	Adjusted R Square	Std. Error of the Estimate
.121	.015	-.010	.002

The independent variable is n.

ANOVA

	Sum of Squares	df	Mean Square	F	Sig.
Regression	.000	1	.000	.595	.445

Residual	.000	40	.000		
Total	.000	41			

The independent variable is n.

Coefficients

	Unstandardized Coefficients		Standardized Coefficients		
	B	Std. Error	Beta	T	Sig.
n	1.000	.000	1.129	4016.002	.000
(Constant)	1.450	.001		1317.899	.000

The dependent variable is ln(1 / U).

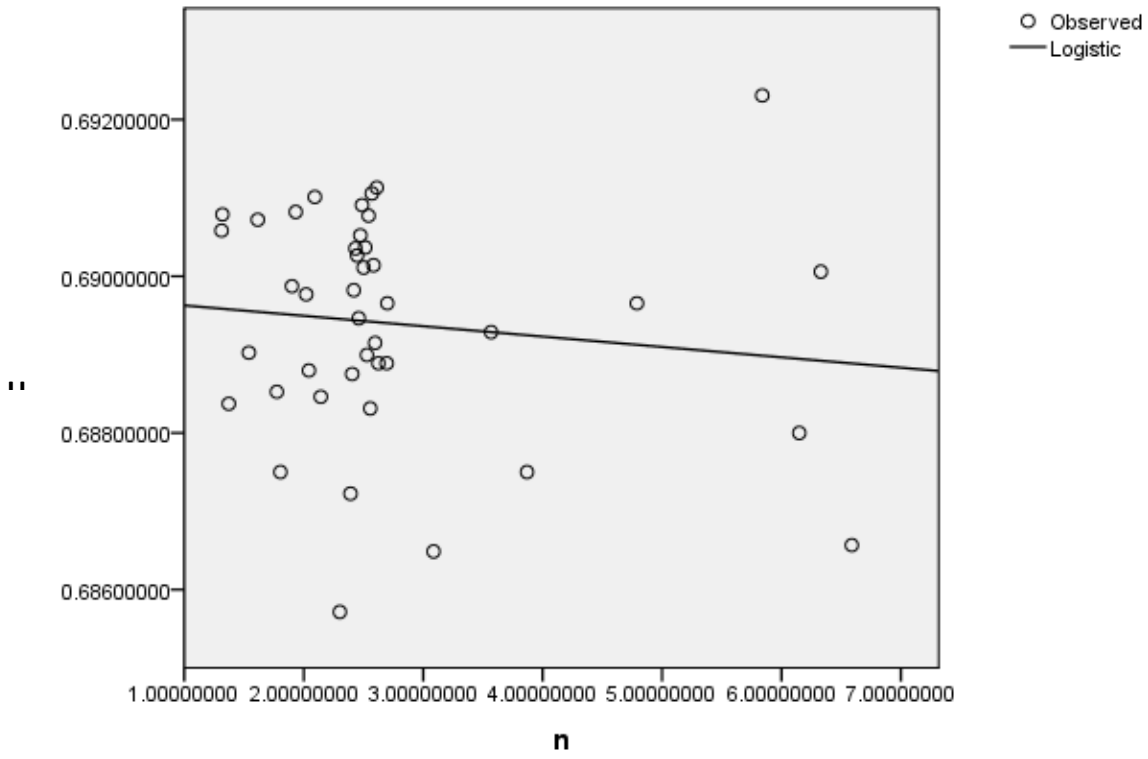

Fig 4.34 Regression Results for 6351 Al Alloy for Pmax=Constant

4.8 REGRESSION ANALYSIS FOR ΔP=CONSTANT

Table 4.18 Equations obtained after Regression Analysis for all materials when ΔP=Constant

Material (Aluminum Alloy)	Equations after Regression Analysis
3003 Al	$U=e^{(1.47-0.99n)}$
6061 T6 Al	$U=e^{(1.34-n)}$
5052 Al	$U=e^{(1.48-n)}$
6063 T6 Al	$U=e^{(1.48-n)}$
6351 Al	$U=e^{(1.34-n)}$

4.9 GENERALIZED EQUATIONFOR ΔP=CONSTANT

With the help of these equations we can form a generalized equation

i.e. $$\mathbf{U=e^{(1.48-n)}} \quad \textbf{(4.1)}$$

4.9.1 Validation of generalized equation

For the validation of the generalized equation obtained in Eq. (4.1) a graph was plotted initially between U & ΔK for material 6063 Al Alloy & 6061 Al Alloy shown in **Fig 4.35**&**Fig4.37** in which data was scattered and then graph was plotted between the UΔK and da/dN where the values of the U in generalized data was taken from data obtained from generalized equation. A very good agreement in pattern was found as shown in **Fig 4.36 & Fig 4.38** with the experimental results that validates the existence of generalized equation for Al Alloys. In Table 4.19 Values of U were verified.

Table 4.19 Validation of generalized equation

Material	U (by generalized Equation) For n=1.8	U(by individual equation) For n=1.8	Variation (%)
3003 Al	0.726149037	0.726149037	0
5052 Al	0.726149037	0.910050167	1.8
6061 T6 Al	0.726149037	0.631283646	1.5
6063 T6 Al	0.726149037	0.726149037	0
6351 Al	0.726149037	0.631283646	1.5

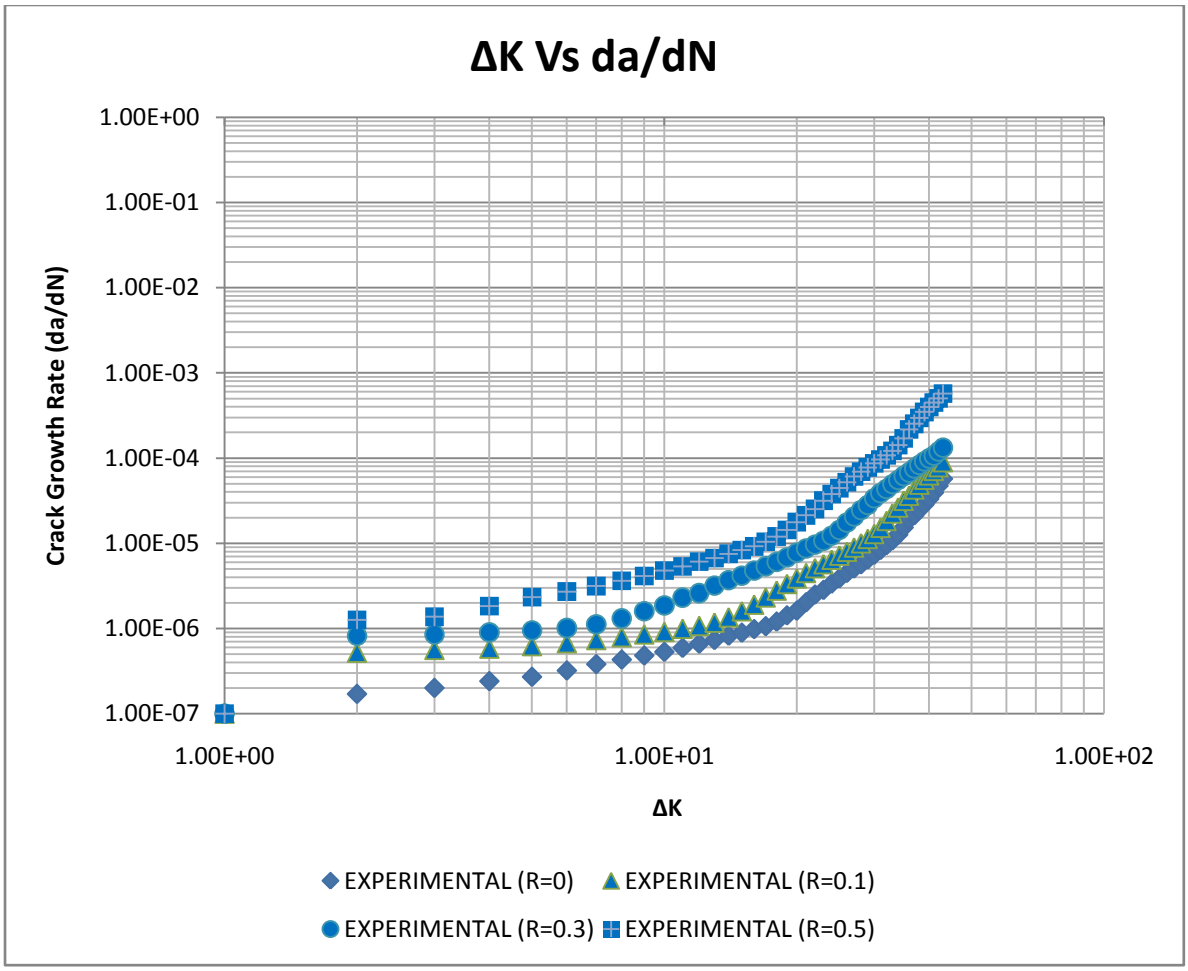

Fig 4.35 Before Application of Generalized Model on 6063 T6 Al Alloy

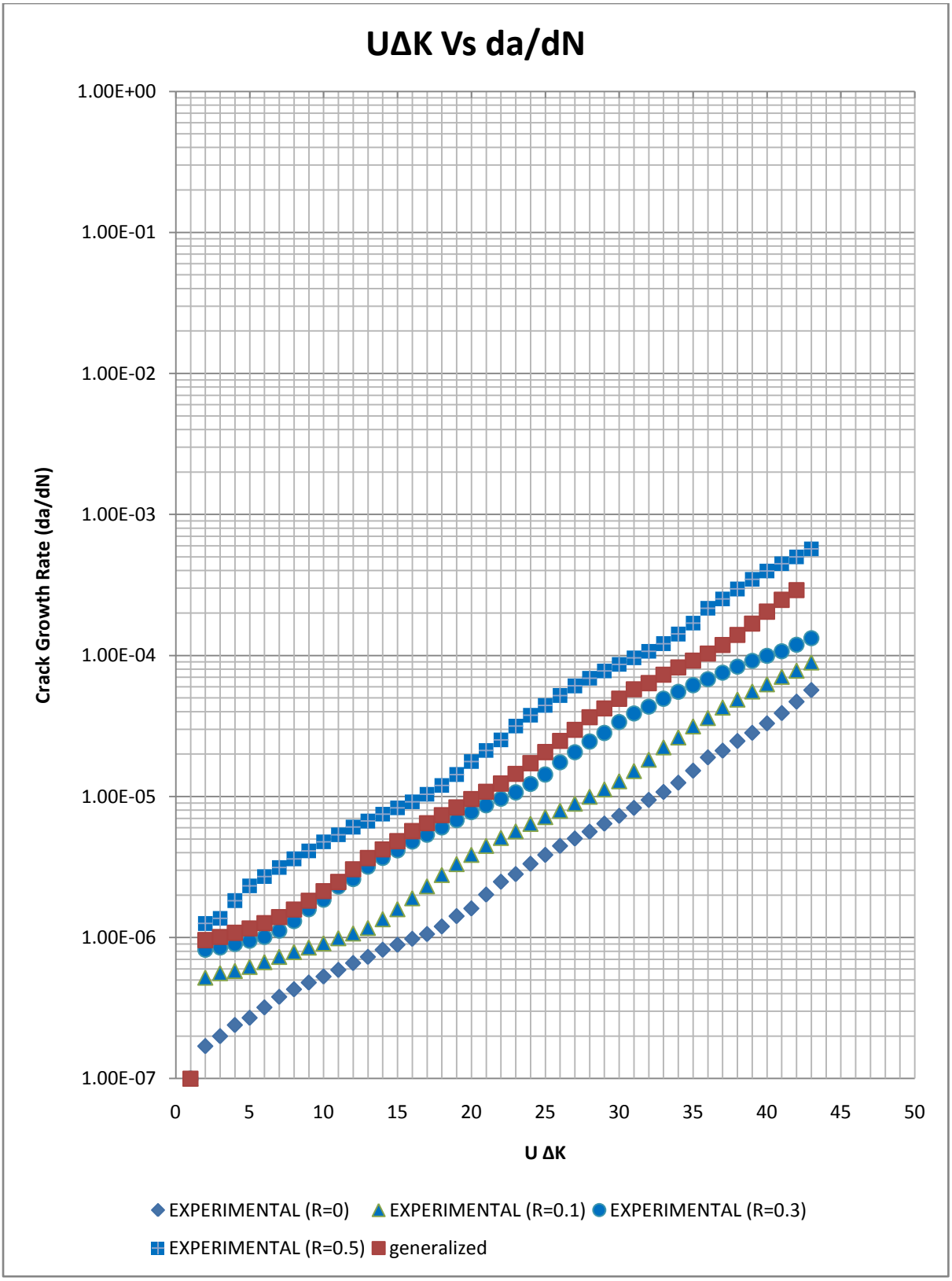

Fig 4.36 After Application of Generalized Model on 6063 T6 Al Alloy

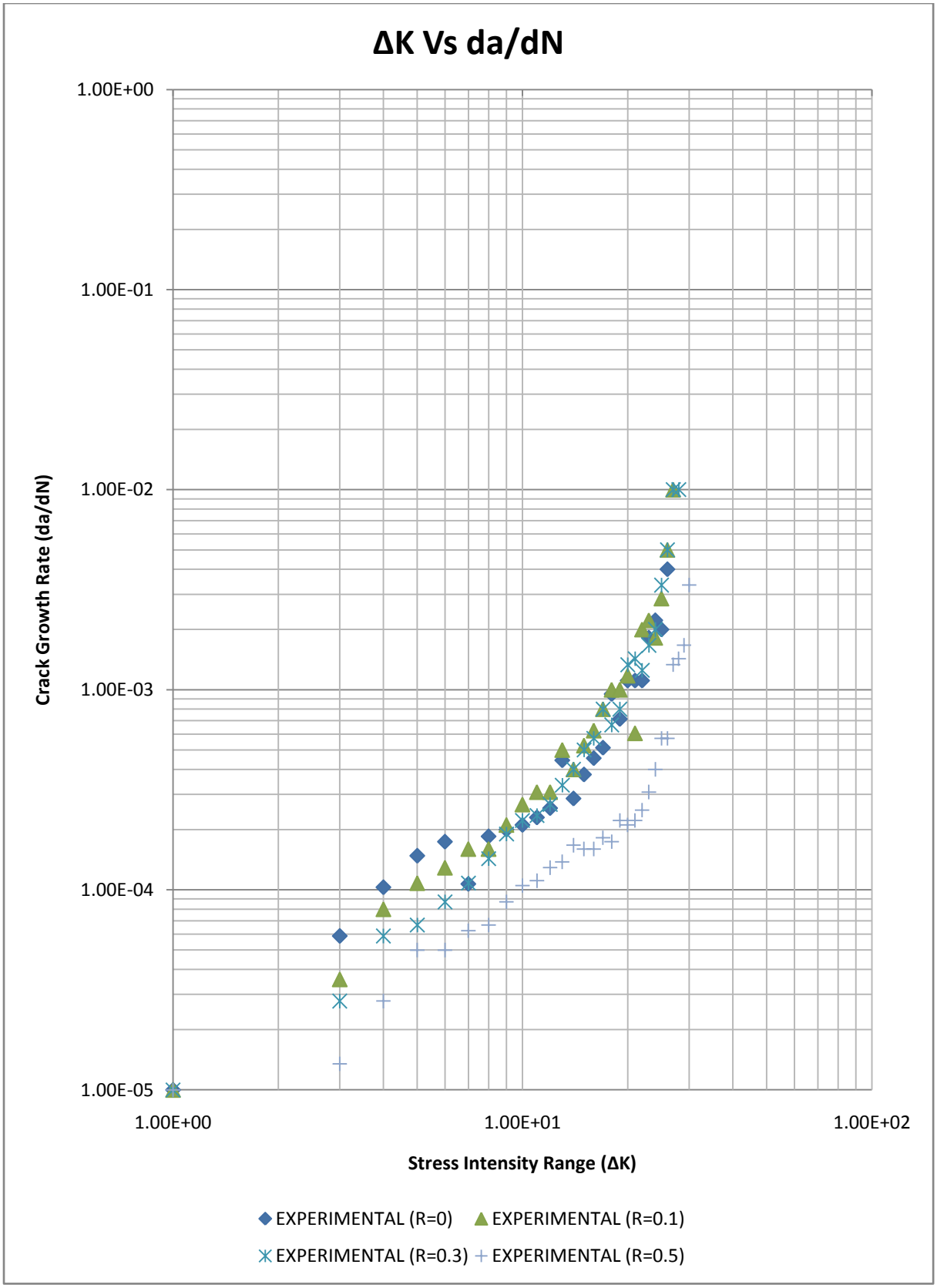

Fig 4.37 Before Application of Generalized Model on 6061 Al Alloy

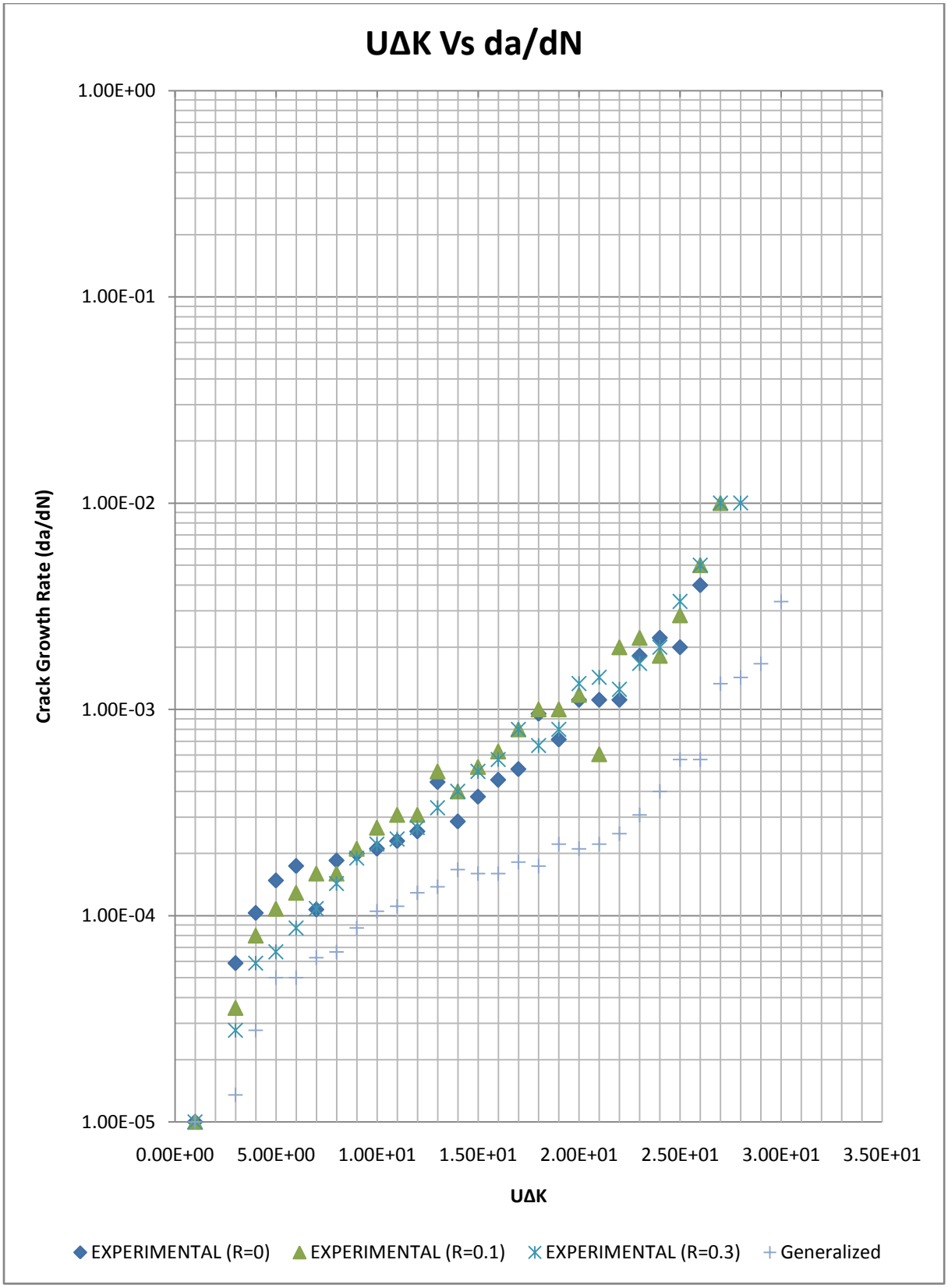

Fig 4.38 After Application of the Generalized Model on 6061 Al Alloy

4.9.2 Application of the Generalized Model

For application of the generalized model was tested on 6063 Al Alloy that gives very good agreement of the model proposed by Elber. We can see that in **Fig 4.35** all data points are scattered in nonlinear way and after application of the generalized Model that shows in the **Fig 4.36** all data points follow linearity that shows the dependency of K_{eff} (or UΔK)on Crack growth rate da/dN. Based on this a generalized Paris law was proposed.

4.10 MODIFIED PARIS LAW FOR ΔP=CONSTANT

Putting the above relationship between U and n we can easily modify Paris Relationship which is very well suitable for aluminum alloy

$$\mathbf{da/dN = C\left\{\left(e^{(1.48-n)}\right)\Delta K\right\}^{n}} \qquad \mathbf{(4.2)}$$

4.11 REGRESSION ANALYSIS FOR P_{max} = CONSTANT

Table 4.20Equations obtained after Regression Analysis for all materials when Pmax =Constant

Material (Aluminum Alloy)	Equations after Regression Analysis
3003 Al	$U=e^{(1.36-0.99n)}$
6061 T6 Al	$U=e^{(1.81-n)}$
5052 Al	$U=e^{(1.44-n)}$
6063 T6 Al	$U=e^{(1.48-n)}$
6351 Al	$U=e^{(1.45-n)}$

4.12 GENERALIZED EQUATION FOR P_{max} = CONSTANT

With the help of these equations we can form a generalized equation

i. e. $$U = e^{(1.45-n)} \quad (4.3)$$

4.12.1 Validation of the Generalized Equation

For the validation of the generalized equation obtained in Eq. (4.3) a graph was plotted initially between U & ΔK for material 6063 Al Alloy & 6061 Al Alloy shown in **Fig 4.39**&**Fig4.41** in which data was scattered in nonlinear manner and then graph was plotted between the UΔK and da/dN and the graph becomes linear where the values of the U in generalized data was taken from data obtained from generalized equation. A very good agreement in pattern was found as shown in **Fig 4.40& Fig 4.42**with the experimental results that validates the existence of generalized equation for Al Alloys. In Table 4.19 Values of U were verified.

Table 4.21Validation of generalized equation

Material	U (by generalized Equation) For n=1.8	U (by individual equation) For n=1.8	Variation (%)
3003 Al	0.704688	0.644036421	1.41
5052 Al	0.704688	0.810050167	1.89
6061 T6 Al	0.704688	0.697676326	1.00
6063 T6 Al	0.704688	0.726149037	1.95
6351 Al	0.704688	0.70468809	0

4.12.2 Application of the Generalized Model

For application of the generalized model was tested on 6061 Al Alloy &6063 Al Alloy that gives very good agreement of the model proposed by Elber. We can see that in **Fig 4.37** all data points are scattered in nonlinear way and after application of the generalized Model that shows in the **Fig 4.38** all data points follow linearity that shows the dependency of K_{eff} (or UΔK) on Crack growth rate da/dN. Based on this a generalized Paris law was proposed.

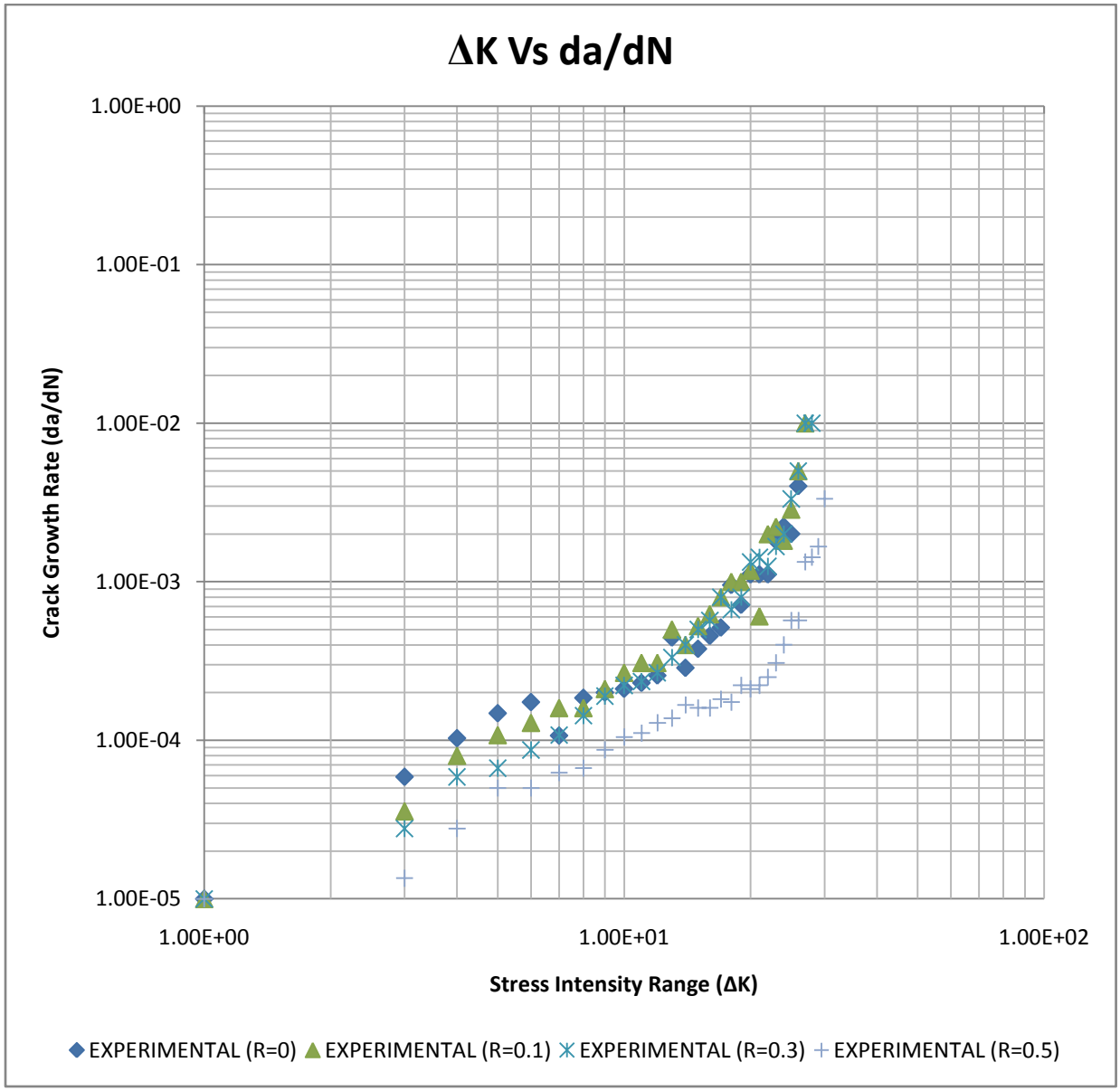

Fig 4.39 Before Application of Generalized Model on 6061 Al Alloy

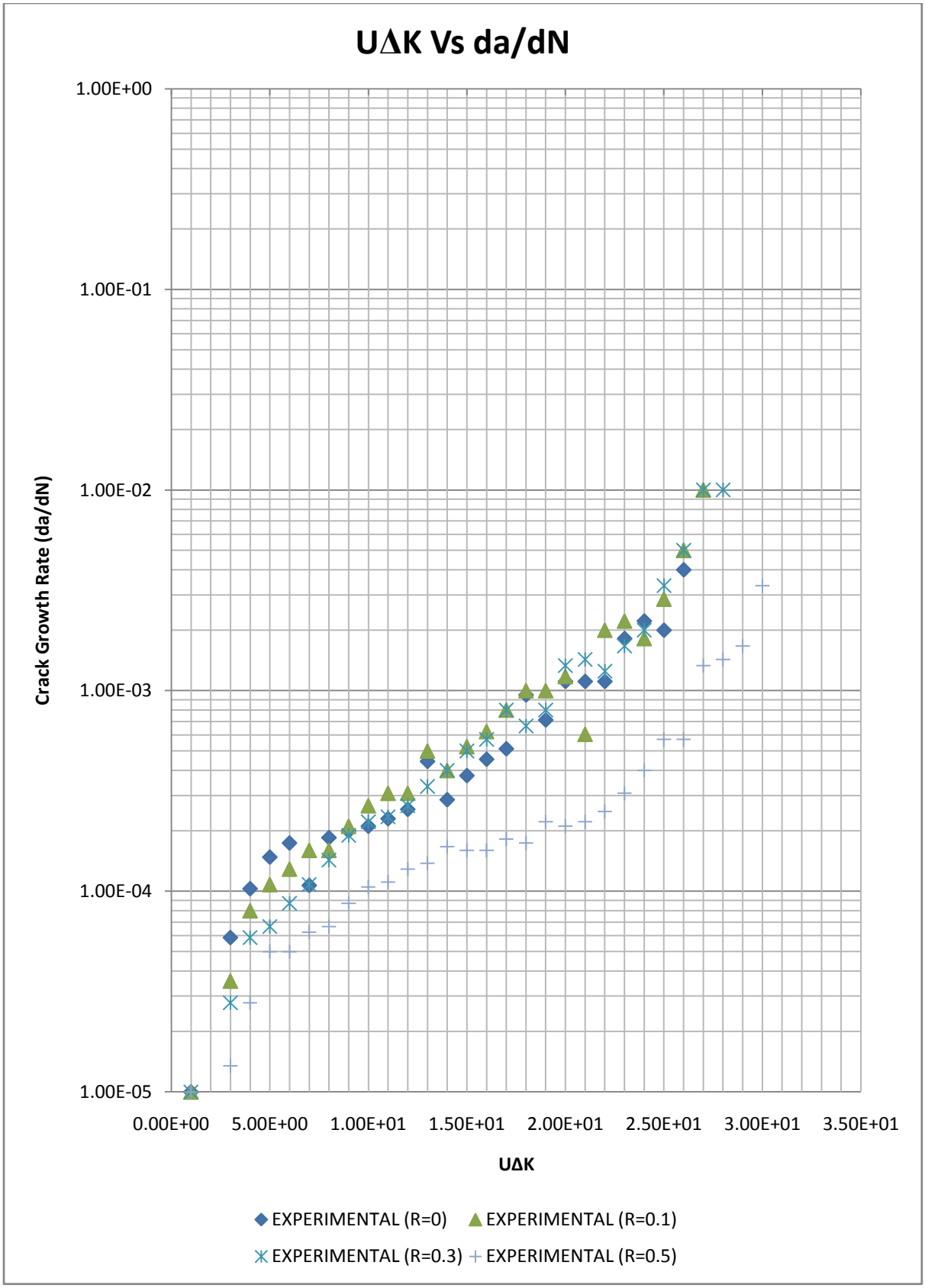

Fig 4.40 After Application of Generalized Model on 6061 Al Alloy

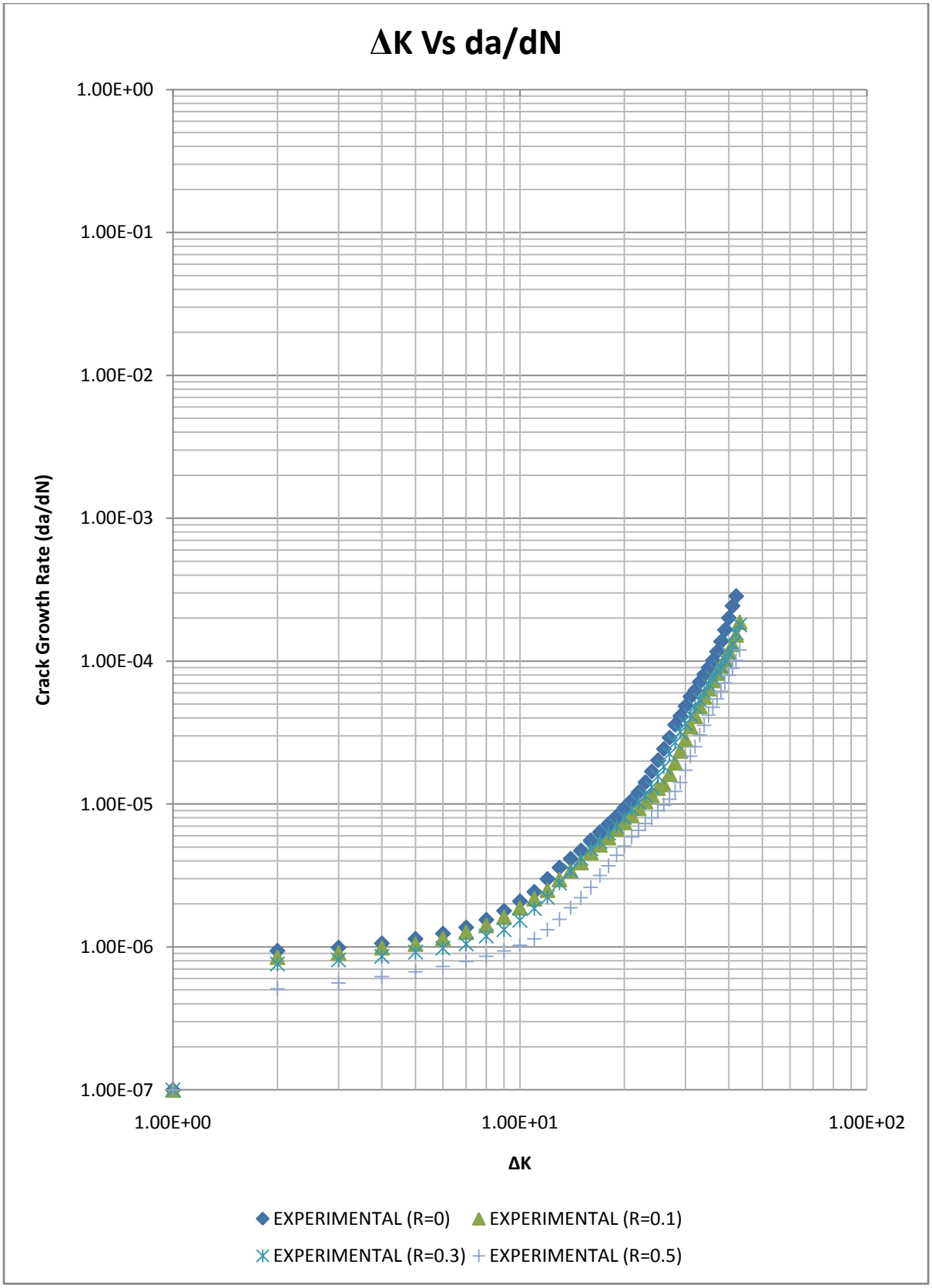

Fig 4.41 Before Application of the Generalized Model in 6063 T6 Al Alloy

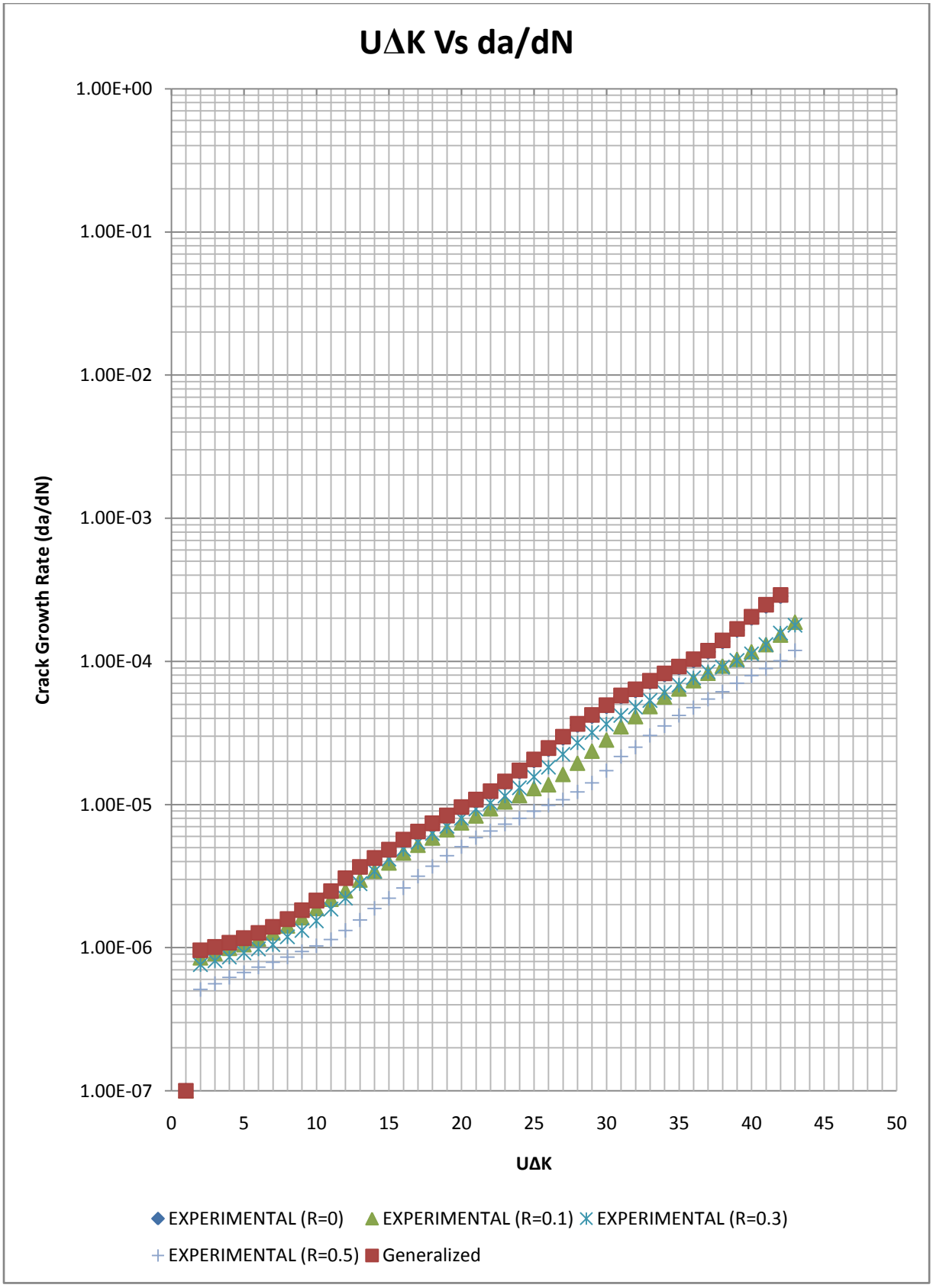

Fig 4.42 After Application of Generalized Model in 6063 T6 Al Alloy

4.13 MODIFIED PARIS LAW FOR P_{max} = CONSTANT

Putting the above relationship between U and n we can easily modify Paris Relationship which is very well suitable for aluminum alloys

$$da/dN = C\left\{\left(e^{(1.45-n)}\right)\Delta K\right\}^{n} \quad (4.4)$$

4.14 CONCLUSION

In constant amplitude loading Crack opening and closing loads are particularly equal. Effective stress intensity range ratio increases with increases work hardening exponent. U increases with crack length, yield strength and stress ratio also. The presented model equations are applicable for Al Alloy only and only SEN and Central Cracked Specimen.

Effect of strain hardening on crack growth were noticed as for lower R-ratios, i.e., R=0, R=0.1, R=0.3, crack growth rate decreases with the increasing work hardening effect and for R= 0.5, crack growth rate increases with the increasing strain hardening effect. The modified Paris Law has been proposed for Aluminum Alloys and SEN and Central Cracked Specimen.

CHAPTER: 05

5 EFFECT OF WORK HARDENING EXPONANT IN CONSTANT AMPLITUDE LOADING WITH SINGLE OVERLOAD

5.1 INTRODUCTION

In chapter 04 the work on effect of work hardening at the crack tip on crack growth and crack closure under constant (CA) loading was presented. In these studies empirical relationship describing U as a function of work hardening at the crack tip of the material was developed for five Al alloys. It was further shown that application of this model to CA loading gives a fairly good relationship between crack growth rate and work hardening exponent at the crack tip. In service, real structures are subjected to complex variable loads and any attempt to even partly predict their fatigue life requires consideration of these loads. A large number of attempts have been made in the past for studying the effect of variable amplitude loading on fatigue crack loading on fatigue crack growth.
The various causes of the retardation during crack propagation are as follows:[136]

- **i.** Fatigue crack closure
- **ii.** Residual Stresses
- **iii.** Crack tip blunting and sharpening
- **iv.** Cyclic strain hardening and softening

It is difficult proposition to separate the effect of all possible mechanism described above. Fortunately it is possible to measure crack closure though with same amount

of difficulty. It is therefore a factor, whose effect needs to be studied- particularly to justify and account for the correction offered by other factors.

The problem of variable amplitude loading has been attempted basically by offering modification in the stress intensity factor after overload.

The problem of fatigue retardation after overloads is a complex one and no satisfactory solution of the problems exists till date. Some factors involved in finding solution of the problem are:

a) The effect of work hardening at crack tip on crack growth rate
b) The effect of work hardening at crack tip on crack closure

The thesis is concerned with the effect of work hardening at the crack tip on crack opening and crack closing. We will therefore consider the effect by modifying the parameter U only.

As already described the work has been done on the five materials 3003, 5052, 6061, 6063, 6351 Al Alloys for changing the material properties of the material.

5.2 MATERIALS, SPECIMEN GEOMETRY & METHODOLOGY

As already mentioned the crack closure and crack propagation analysis were conducted on Abaqus®. The method of determining the crack closure load is the same as used in Chapter 04. The all test materials and specimen geometry are also same. The details of the load pattern are shown in Table 5.1 (a, b, c, d, e).

Some important points of the analysis are given below:

The single overload cycle at different overload ratios were given at the beginning, after exhausting 25% CA life and after 50% CA life.

The crack closure experiments were performed by loading and unloading the specimen at a frequency of 0.1 Hz.

Table 5.1Loading Conditions for 3003 Al Alloy

OLR	P_{min} (KN)	P_{max}(KN)	ΔP
1.0	0	6.2	6.2
1.5	0	6.2	6.2
2.0	0	6.2	6.2
2.5	0	6.2	6.2

Table 5.2 Loading Conditions for 5052 Al Alloy

OLR	P_{min}(KN)	P_{max}(KN)	ΔP
1.0	0	14	14
1.5	0	14	14
2.0	0	14	14
2.5	0	14	14

Table 5.3 Loading Conditions for 6061 Al Alloy

OLR	P_{min}(KN)	P_{max}(KN)	ΔP
1.0	0	14	14
1.5	0	14	14
2.0	0	14	14
2.5	0	14	14

Table 5.4 Loading Conditions for 6063 Al Alloy

OLR	P_{min}(KN)	P_{max}(KN)	ΔP
1.0	0	8.2	8.2
1.5	0	8.2	8.2
2.0	0	8.2	8.2
2.5	0	8.2	8.2

Table 5.5 Loading Conditions for 6351 Al Alloy

OLR	P_{min}(KN)	P_{max}(KN)	ΔP
1.0	0	8.2	8.2
1.5	0	8.2	8.2
2.0	0	8.2	8.2
2.5	0	8.2	8.2

5.3 FEM RESULTS& DISCUSSION

Results obtained from FEM analysis of fatigue crack in SEN specimen of five different Al Alloy under constant amplitude loading with single overload at different stress over load ratios, OLR=1.0, 1.5, 1.8 and 2 at every 2 mm crack length. These records are shown in **Fig 5.1** to **Fig 5.10.**

For various loading given in Table 5.1 to 5.5 the value of U and da/dN were determined. **Fig 5.1** to **Fig 5.5** show the graph between n Vs da/dN it was found that increase in Overload gives increase in the life of the specimen which is obtained as a result of retarded crack growth rate. The specimen life were increased from 50000 cycles to 132,000 in OLR=2.0. Similar results were obtained for all five materials. da/dN increases with increases of "n" and "n" increases with increasing of stress ratio for all the materials. The cyclic life is found to decrease with increase in strain hardening.

Fig5.6 to **Fig5.10**shows the graph between U Vs n. the following facts were recorded. Just after the overload the U decreases attains the minimum value and then increases slowly. Same trends were observed for all materials.

U decreases with increasing OLR. The amount of decrease of U with overload depends upon the amount of overload. It is found that for a given value of "n" the value of U increases in lower stress ratio up to 1mm fatigue length. In the end when the crack has become sufficiently large and crack propagation rate has increased to a fairly large value and the area available for tension has decreased to considerable extent effective stress intensity range ratio (U) increases. "U" increases with "n" at all stress ratio (R) for all the materials. The above results lead us to the conclusion that da/dN and U are dependent upon "n".

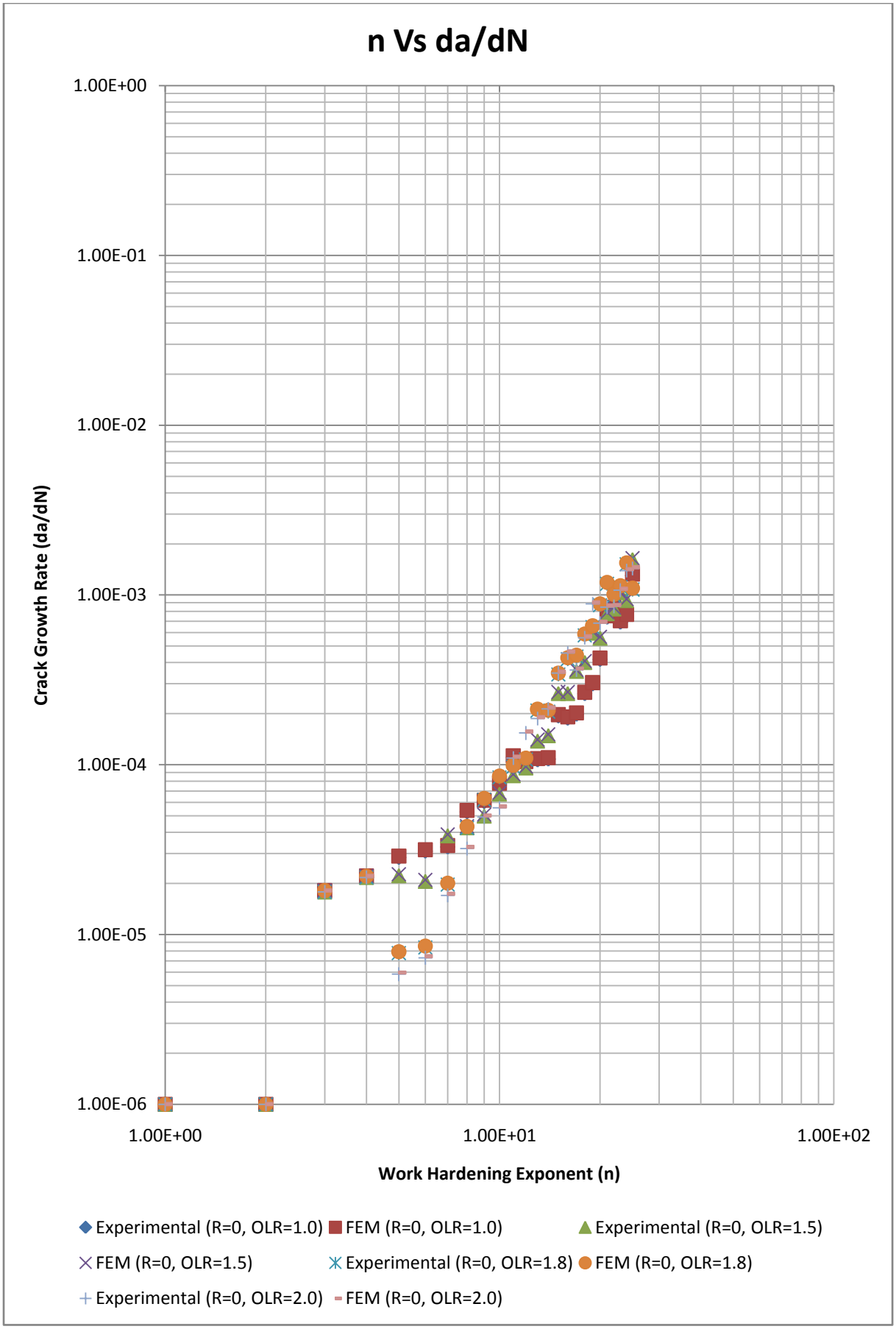

Fig 5.1 For R= Constant, OLR= Variable (3003 Al)

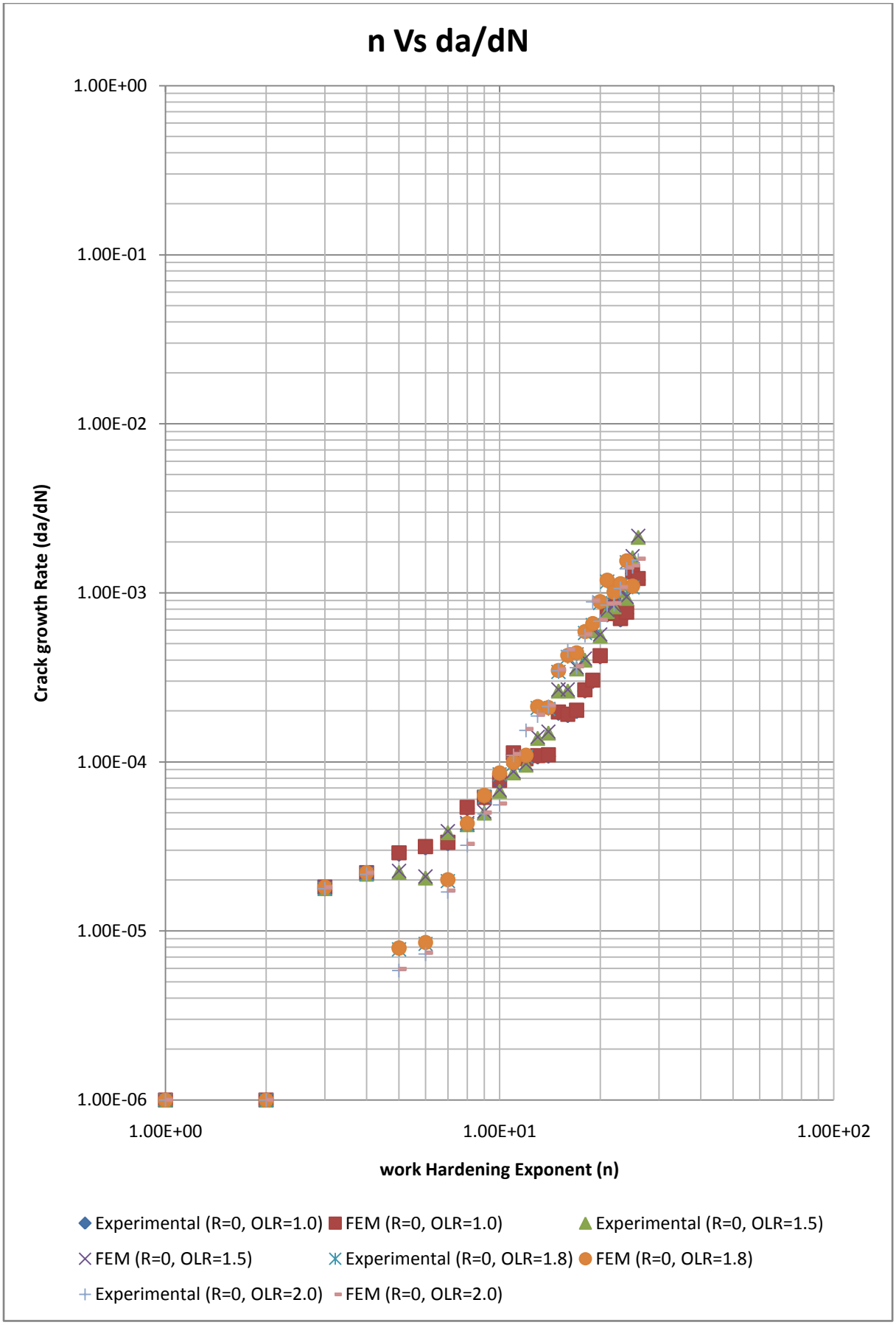

Fig 5.2 For R= Constant, OLR = Variable (5052Al)

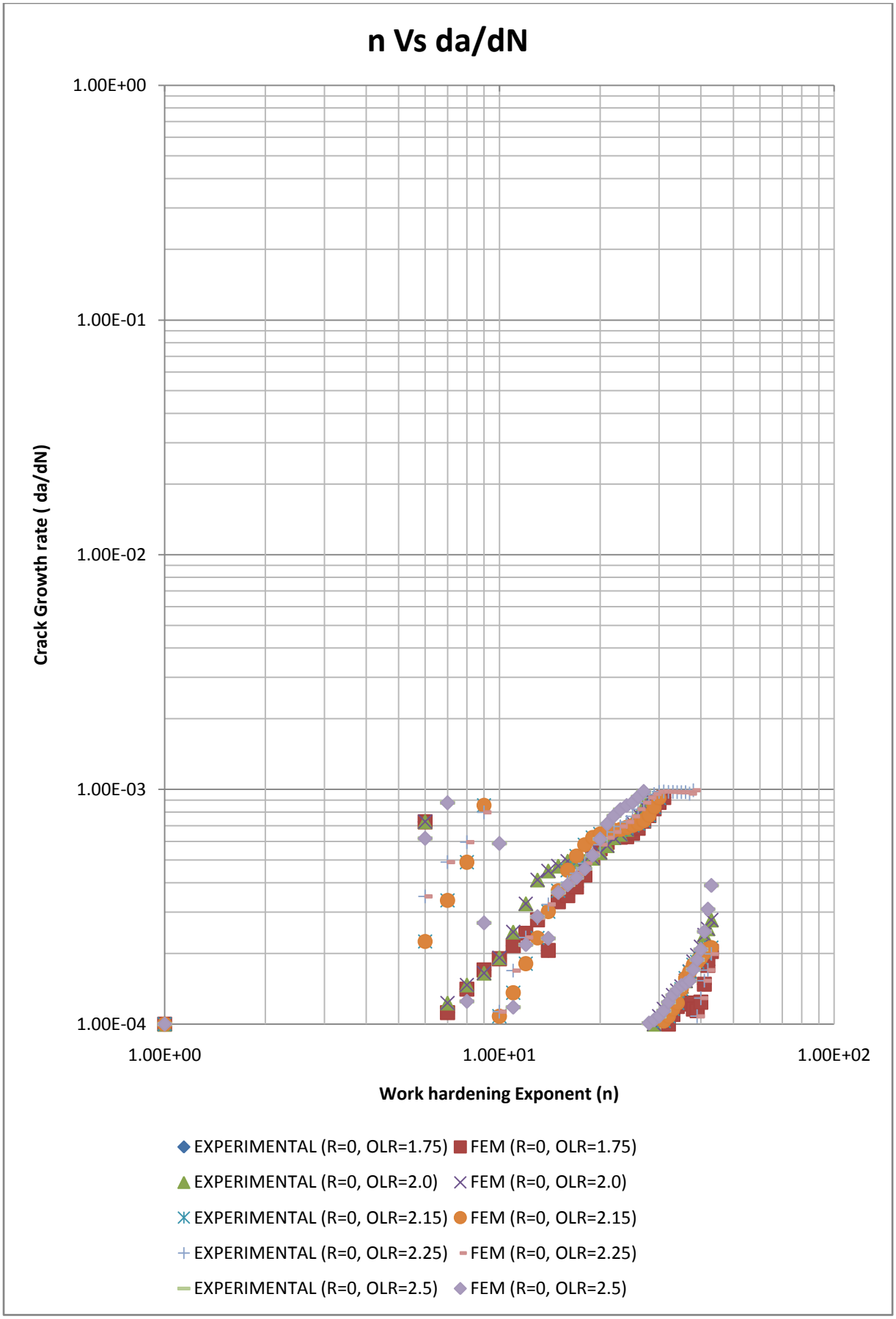

Fig 5.3 For R=Constant, OLR=Variable (6061 Al)

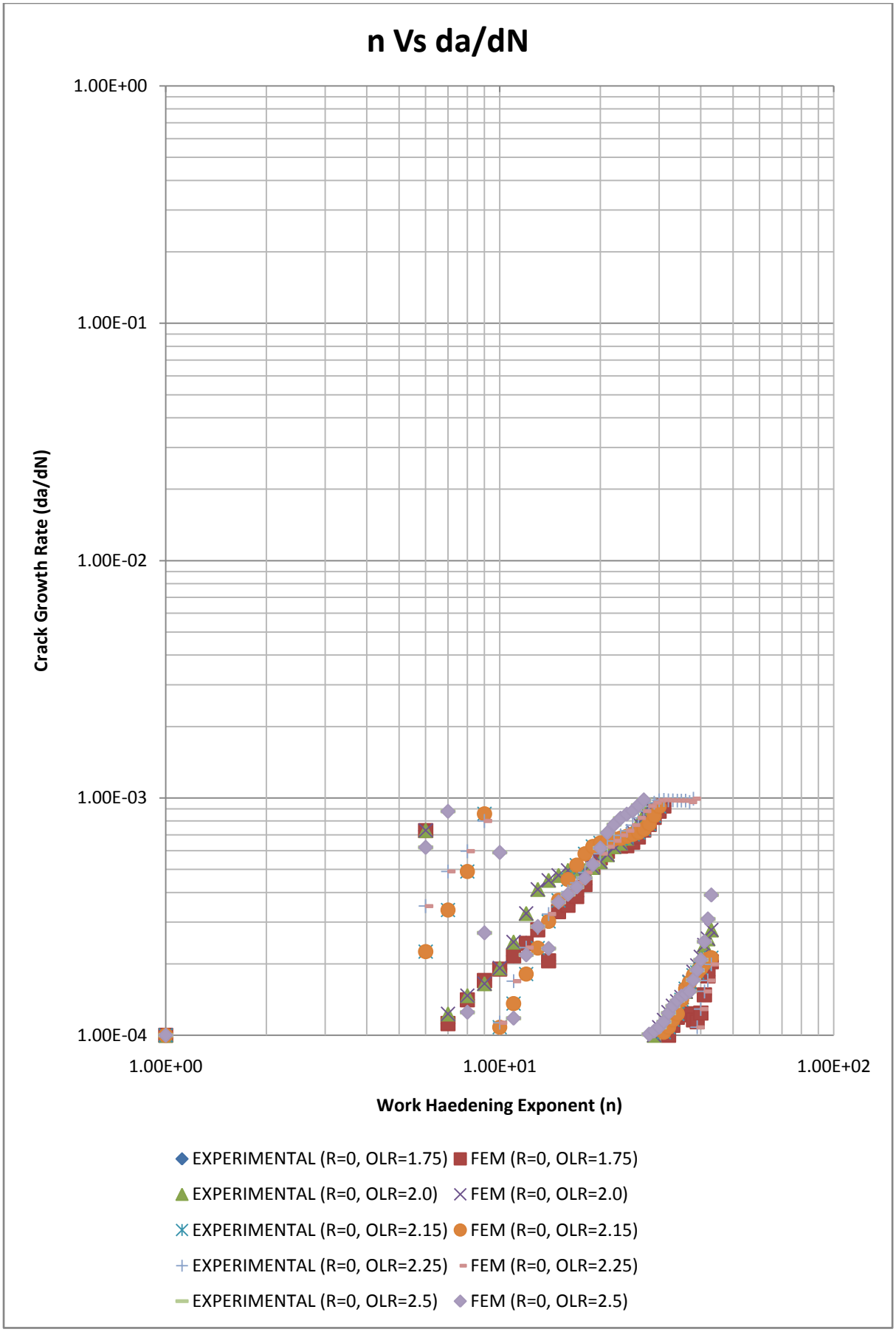

Fig 5.4 For R=Constant, OLR=Variable (6063 Al)

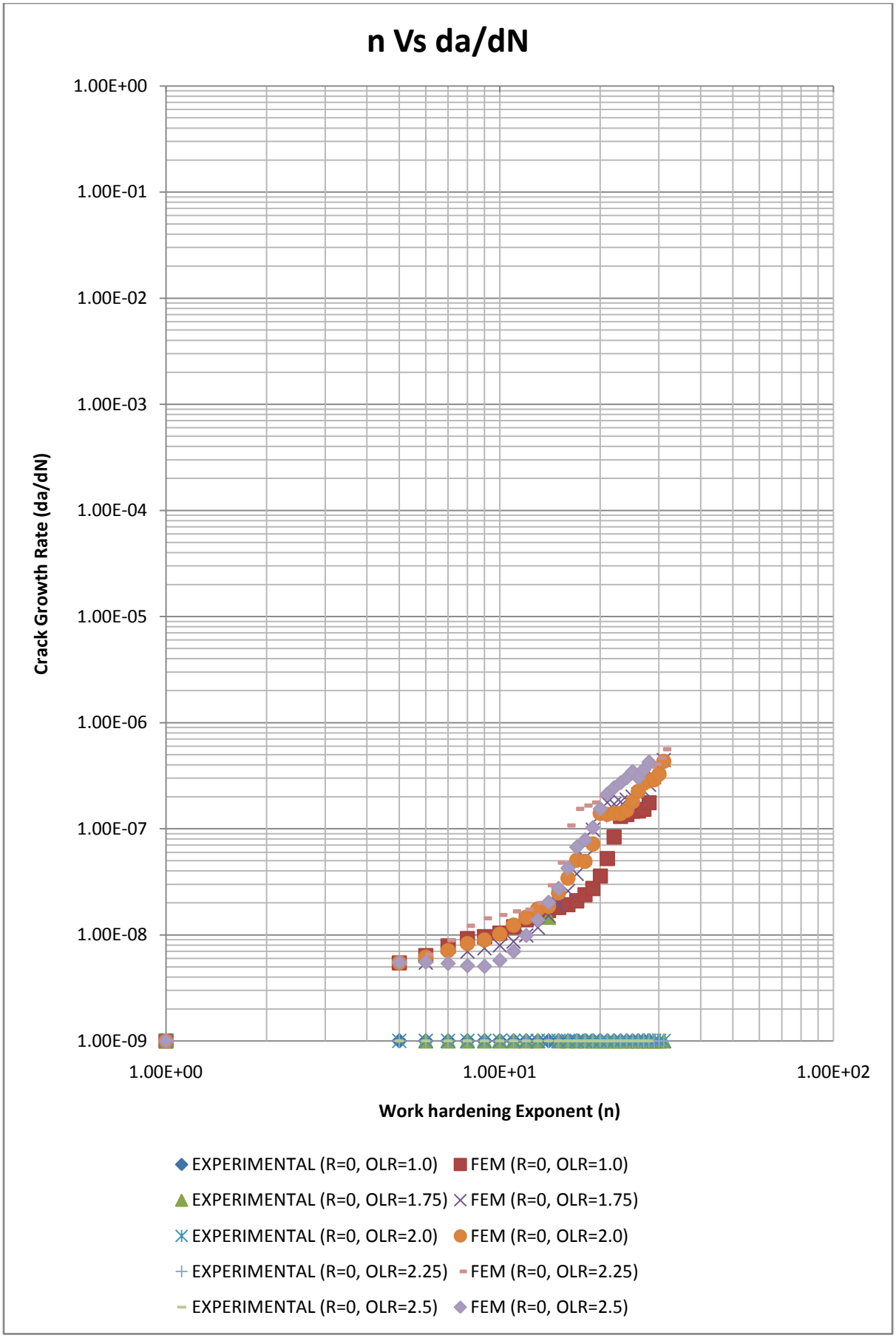

Fig 5.5 For R=Constant, OLR=Variable (6351 Al)

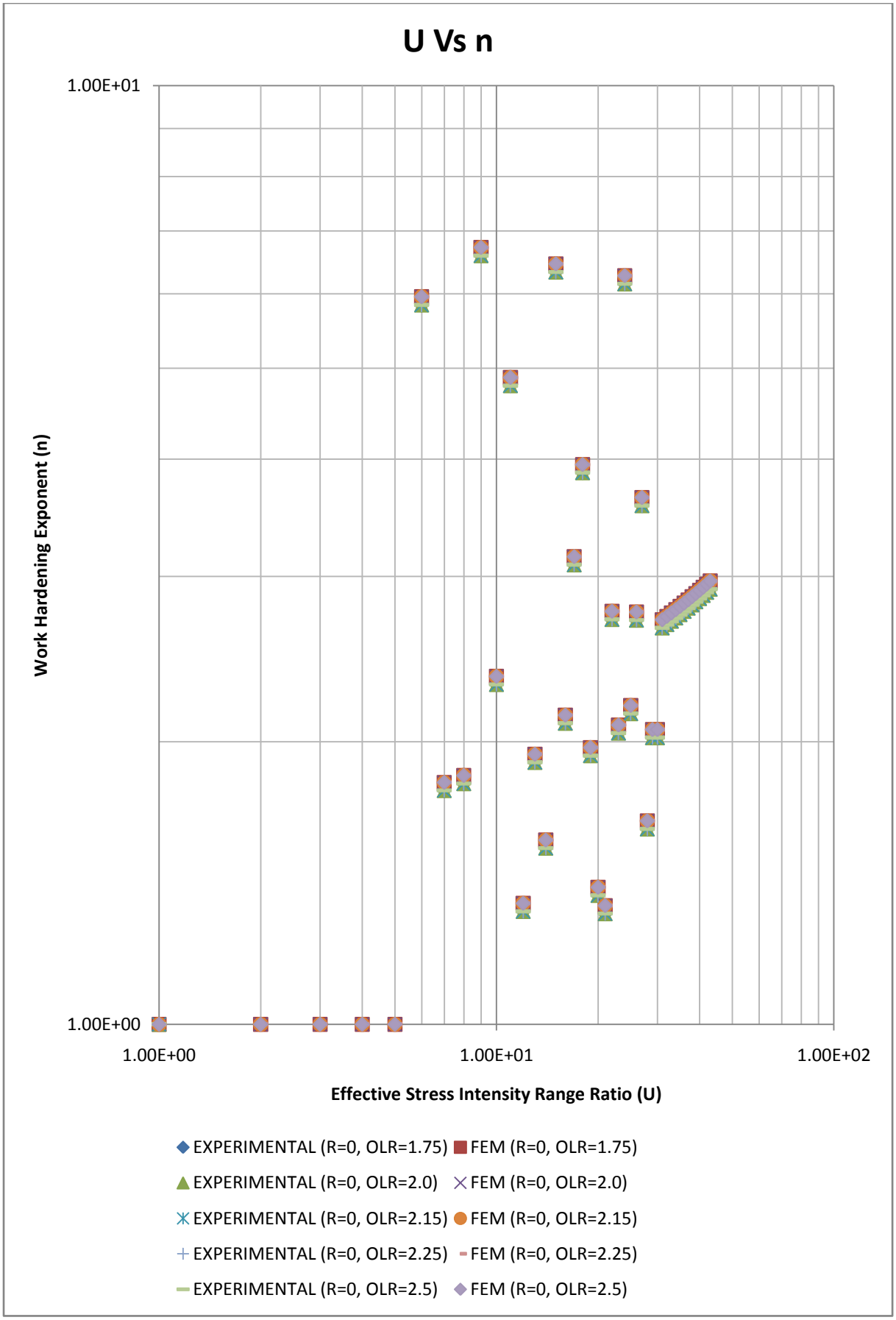

Fig 5.6 For R= Constant, OLR= Variable (3003 Al)

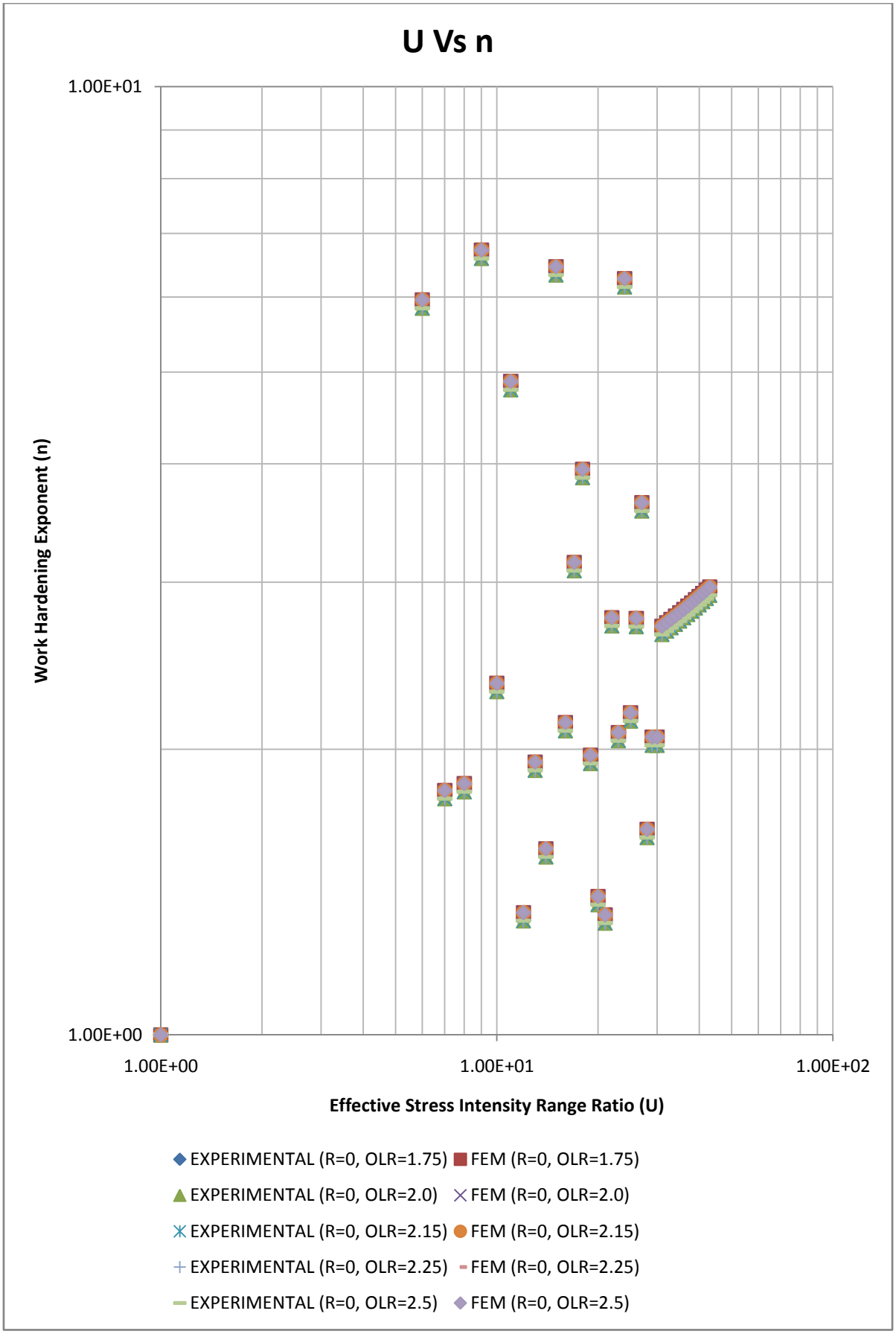

Fig 5.7 For R= Constant, OLR = Variable (5052Al)

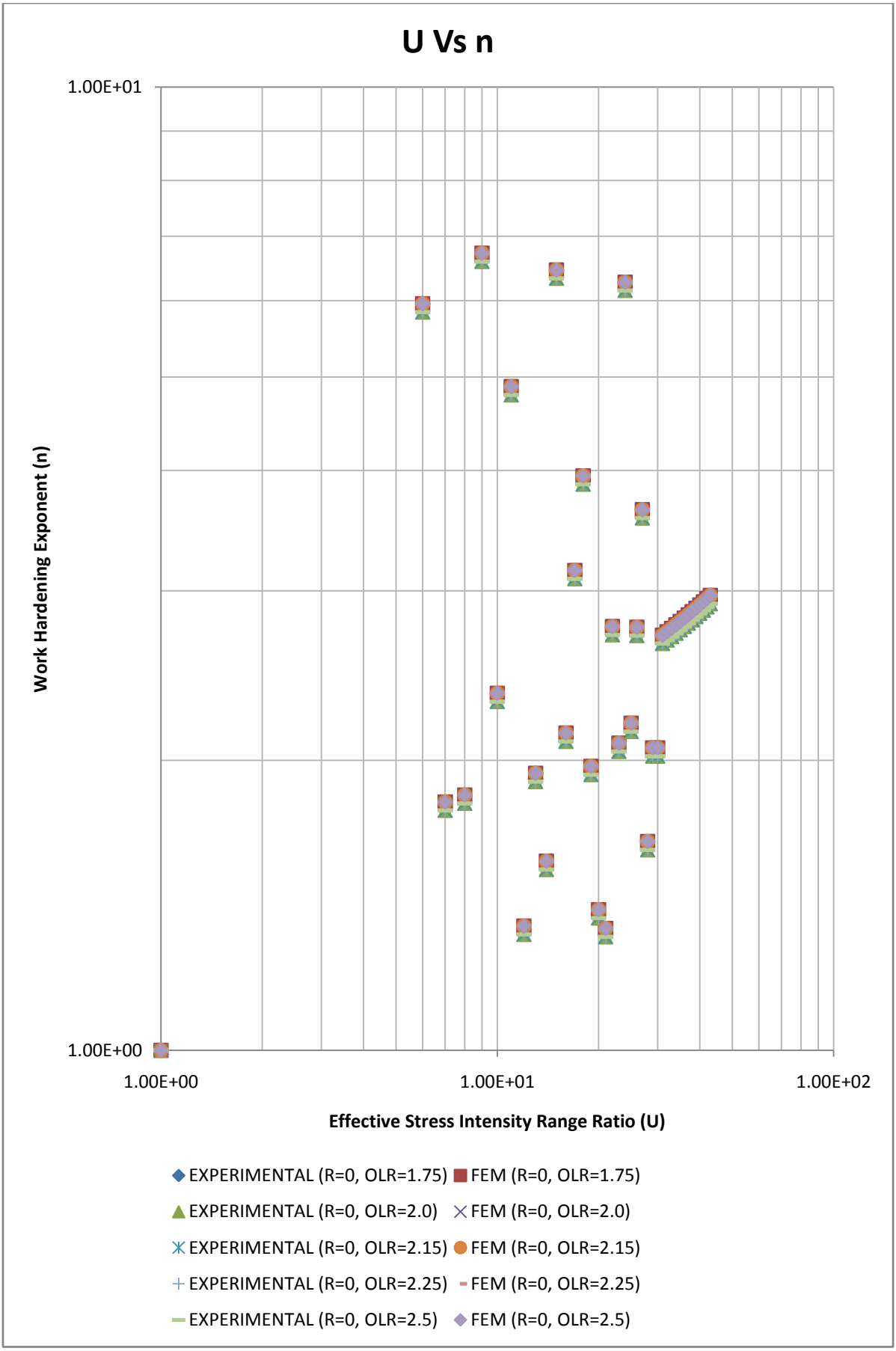

Fig 5.8 For R=Constant, OLR=Variable (6061 Al)

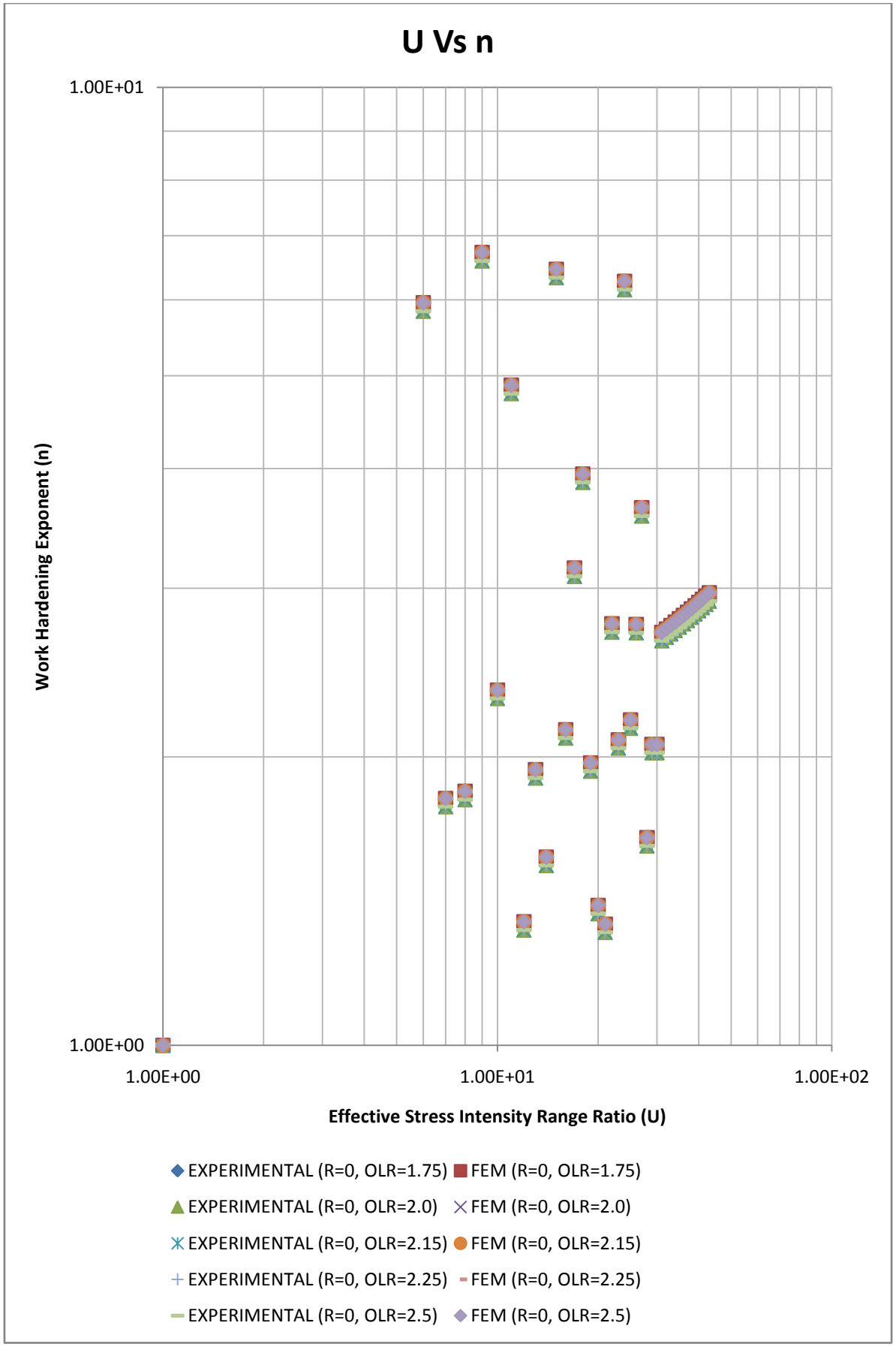

Fig 5.9 For R=Constant, OLR=Variable (6063 Al)

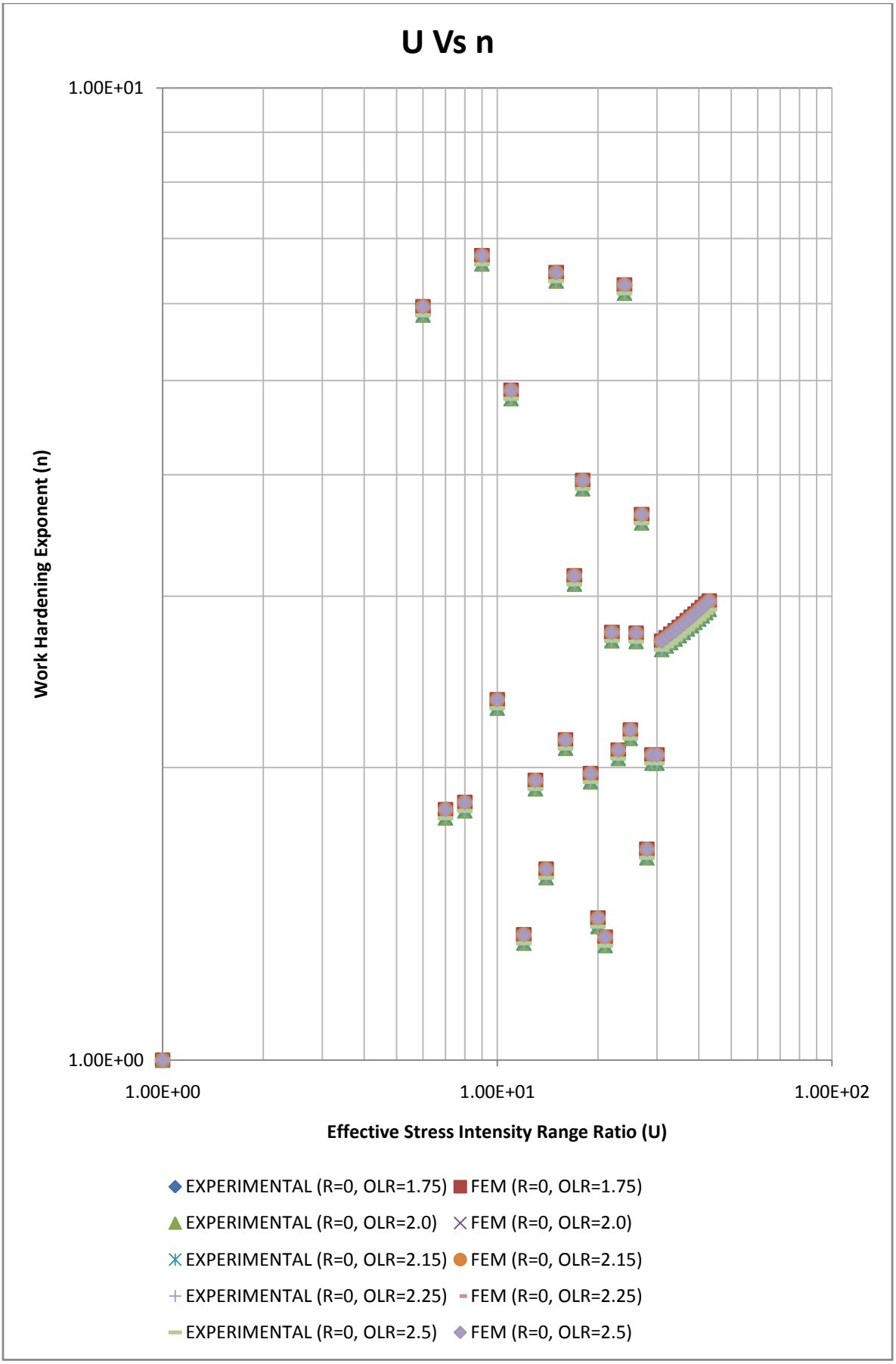

Fig 5.10 For R=Constant, OLR=Variable (6351 Al)

5.4 REGRESSION ANALYSIS

After FEM analysis, Regression analysis was done. From the output we have drawn the graphs between UVs n fitted the trend line and got coefficients value for trend line equation for each material. After getting equation for each material we formed a generalized equation that suits the result of all other materials and with the help of this we can predict the approximation for crack closure of other Aluminum alloys too. The scheme of the curves is given below.

5.4.1 3003 Al Alloy

Table 5.6 Regression Analysis for 3003 Al Alloy

Model Summary

R	R Square	Adjusted R Square	Std. Error of the Estimate
.197	.039	-.007	.020

The independent variable is n.

ANOVA

	Sum of Squares	Df	Mean Square	F	Sig.
Regression	.000	1	.000	.846	.368
Residual	.008	21	.000		
Total	.009	22			

The independent variable is n.

Coefficients

	Unstandardized Coefficients		Standardized Coefficients		
	B	Std. Error	Beta	t	Sig.
n	.998	.003	.821	384.269	.000
(Constant)	1.290	.011		118.322	.000

The dependent variable is ln(1 / U).

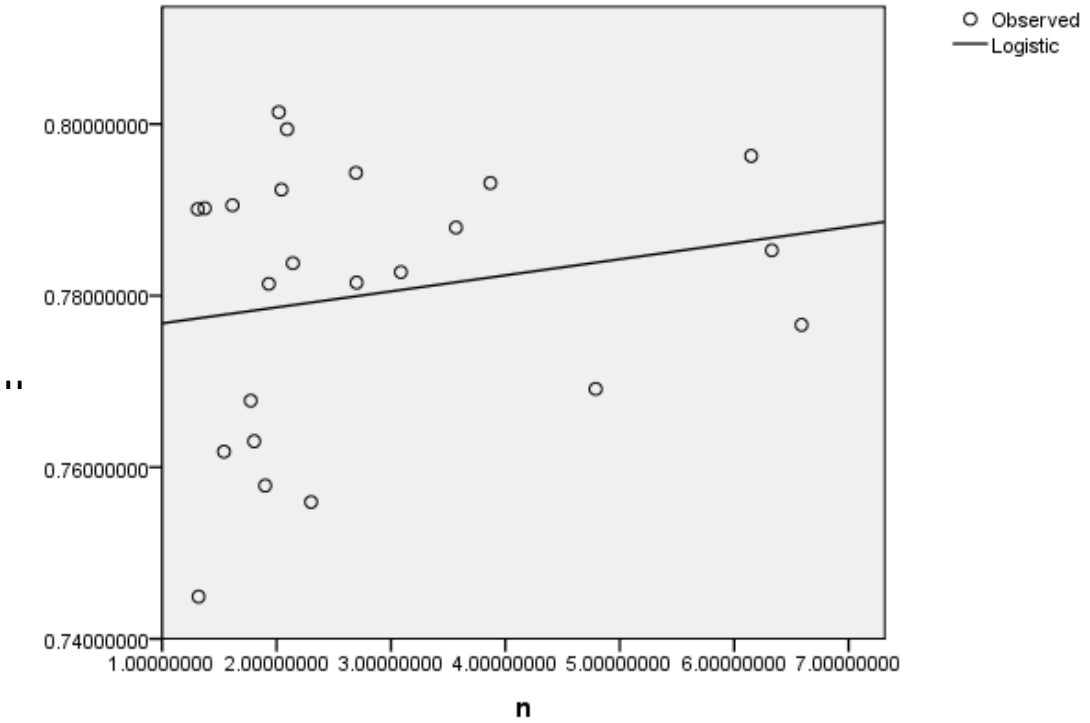

Fig 5.11 Regression Results for 3003 Al Alloy

5.4.2 5052 Al Alloy

Table 5.7 Regression Analysis for 5052 Al Alloy

Model Summary

R	R Square	Adjusted R Square	Std. Error of the Estimate
.028	.001	-.047	.001

The independent variable is n.

ANOVA

	Sum of Squares	df	Mean Square	F	Sig.
Regression	.000	1	.000	.016	.901
Residual	.000	21	.000		
Total	.000	22			

The independent variable is n.

Coefficients

	Unstandardized Coefficients		Standardized Coefficients		
	B	Std. Error	Beta	t	Sig.
n	1.000	.000	1.028	5240.774	.000
(Constant)	1.479	.001		1613.713	.000

The dependent variable is ln(1 / U).

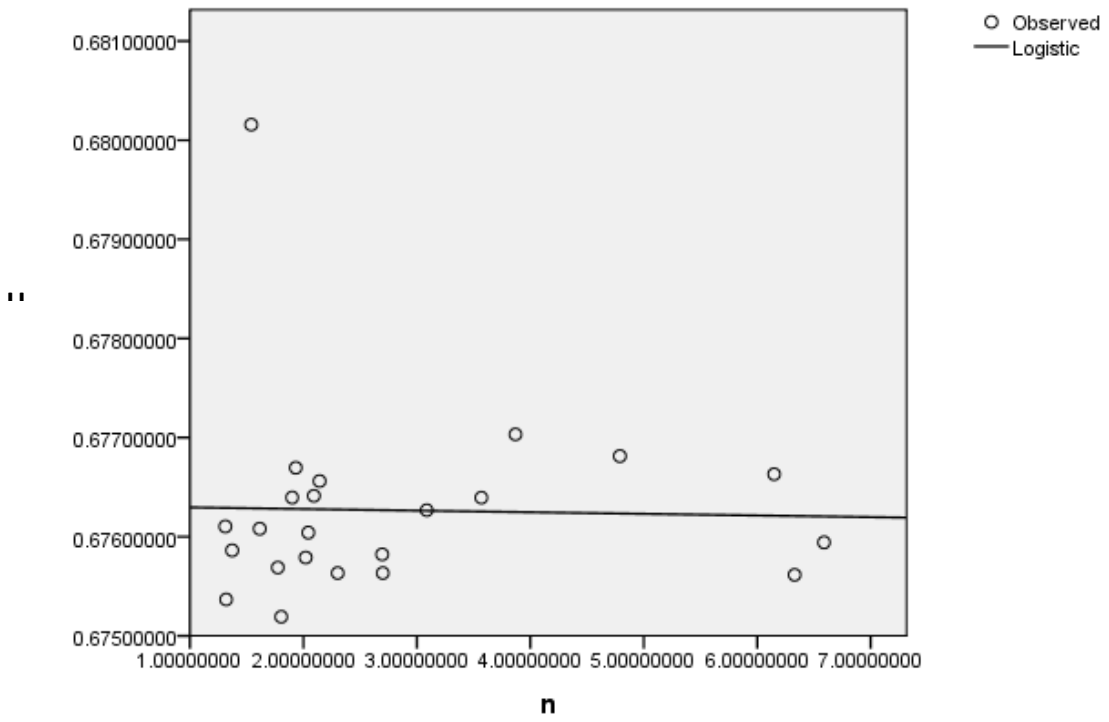

Fig 5.12 Regression Results for 5052 Al Alloy

5.4.3 6061 Al Alloy

Table 5.8 Regression Analysis for 6061 Al Alloy

Model Summary

R	R Square	Adjusted R Square	Std. Error of the Estimate
.101	.010	-.018	.036

The independent variable is n.

ANOVA

	Sum of Squares	df	Mean Square	F	Sig.
Regression	.000	1	.000	.362	.551

Residual	.045	35	.001		
Total	.046	36			

The independent variable is n.

Coefficients

	Unstandardized Coefficients		Standardized Coefficients		
	B	Std. Error	Beta	t	Sig.
n	.997	.005	.904	219.594	.000
(Constant)	1.221	.017		70.309	.000

The dependent variable is ln(1 / U).

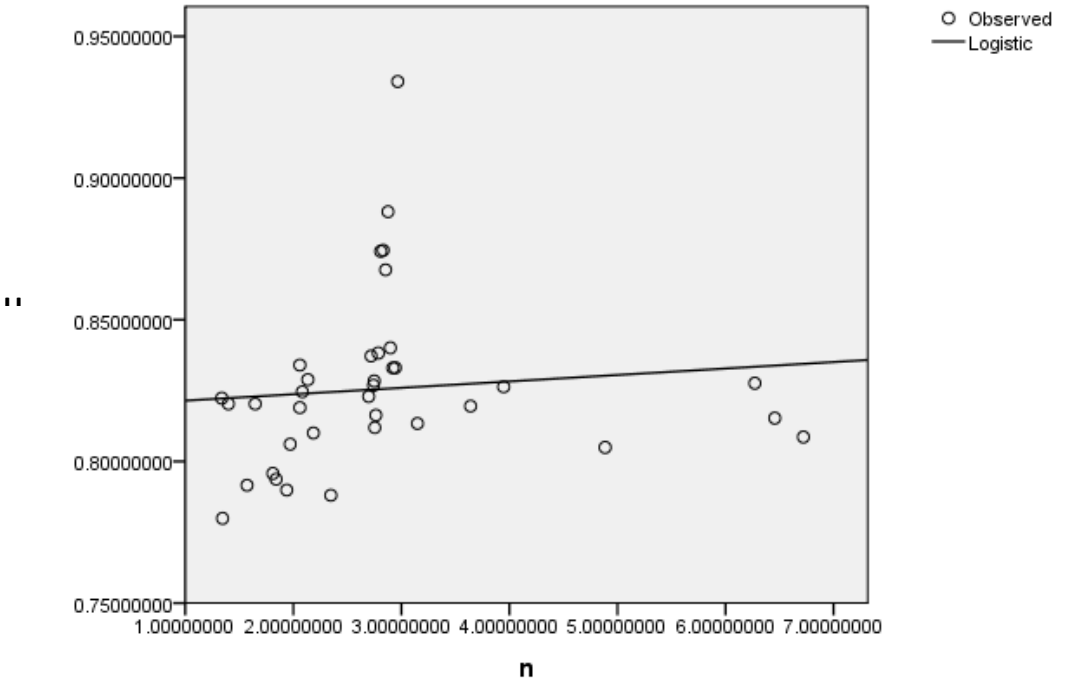

Fig 5.13 Regression Results for 6061 Al Alloy

5.4.4 6063 Al Alloy

Table 5.9 Regression Analysis for 6063 Al Alloy

Model Summary

R	R Square	Adjusted R Square	Std. Error of the Estimate
.101	.010	-.018	.036

The independent variable is n.

ANOVA

	Sum of Squares	df	Mean Square	F	Sig.
Regression	.000	1	.000	.362	.551
Residual	.045	35	.001		
Total	.046	36			

The independent variable is n.

Coefficients

	Unstandardized Coefficients		Standardized Coefficients	t	Sig.
	B	Std. Error	Beta		
n	.997	.005	.904	219.594	.000
(Constant)	1.221	.017		70.309	.000

The dependent variable is ln(1 / U).

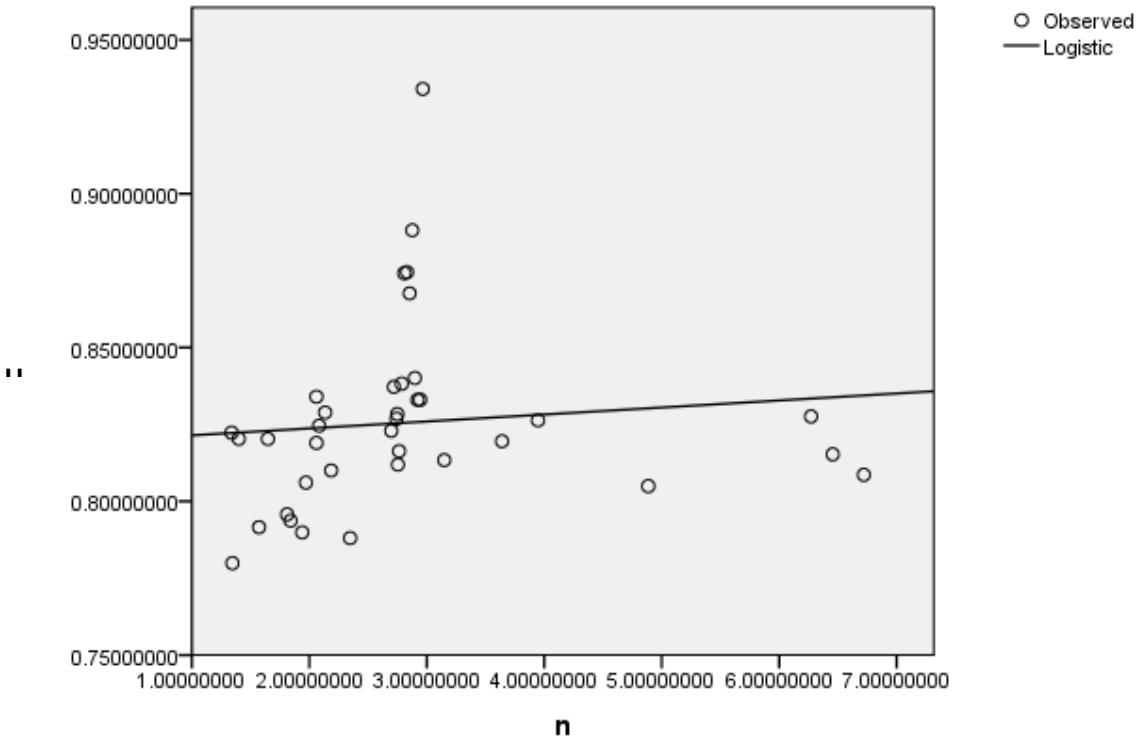

Fig 5.14 Regression Results for 6063 Al Alloy

5.4.5 6351 Al Alloy

Table 5.10 Regression Analysis for 6351 Al Alloy

Model Summary

R	R Square	Adjusted R Square	Std. Error of the Estimate
.370	.137	.098	.002

The independent variable is n.

ANOVA

	Sum of Squares	df	Mean Square	F	Sig.
Regression	.000	1	.000	3.500	.075

Residual	.000	22	.000		
Total	.000	23			

The independent variable is n.

Coefficients

	Unstandardized Coefficients		Standardized Coefficients		
	B	Std. Error	Beta	t	Sig.
n	1.001	.000	1.448	3739.940	.000
(Constant)	1.407	.001		1211.191	.000

The dependent variable is ln(1 / U).

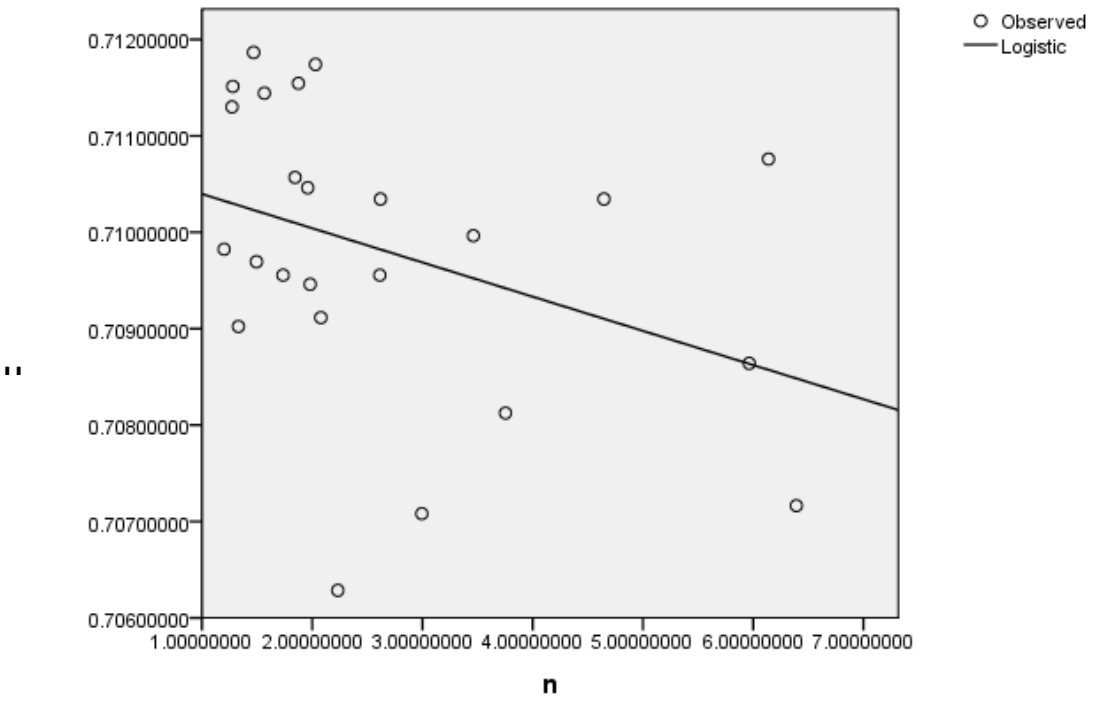

Fig 5.15 Regression Results for 6351 Al Alloy

5.5 RESULTS OBTAINED AFTER REGRESSION ANALYSIS FOR SINGLE OVERLOAD

Table 5.11Equations obtained for all materials after regression analysis for single overload

Material (Aluminum Alloy)	Equations after Regression Analysis
3003 Al	$\mathbf{U = e^{(1.29-0.99n)}}$
6061 T6 Al	$\mathbf{U = e^{(1.49-n)}}$
5052 Al	$\mathbf{U = e^{(1.22-0.99n)}}$
6063 T6 Al	$\mathbf{U = e^{(1.23-0.99n)}}$
6351 Al	$\mathbf{U = e^{(1.40-n)}}$

5.6 GENERALIZED EQUATION FOR SINGLE OVERLOAD

With the help of these equations we can form a generalized equation

i.e. $\mathbf{U=e^{(1.29-n)}}$ **(5.1)**

5.6.1 Validation of the Generalized Equation

For the validation of the generalized equation obtained in Eq. (5.1) a graph was plot between the UΔK and da/dN where the values of the U in generalized data was taken from data obtained from generalized equation for material 6063 Al Alloy. A very good agreement in pattern was found as shown in Fig 5.16 with the experimental results that validates the existence of generalized equation for Al Alloys. In Table 5.12 Value of U was verified.

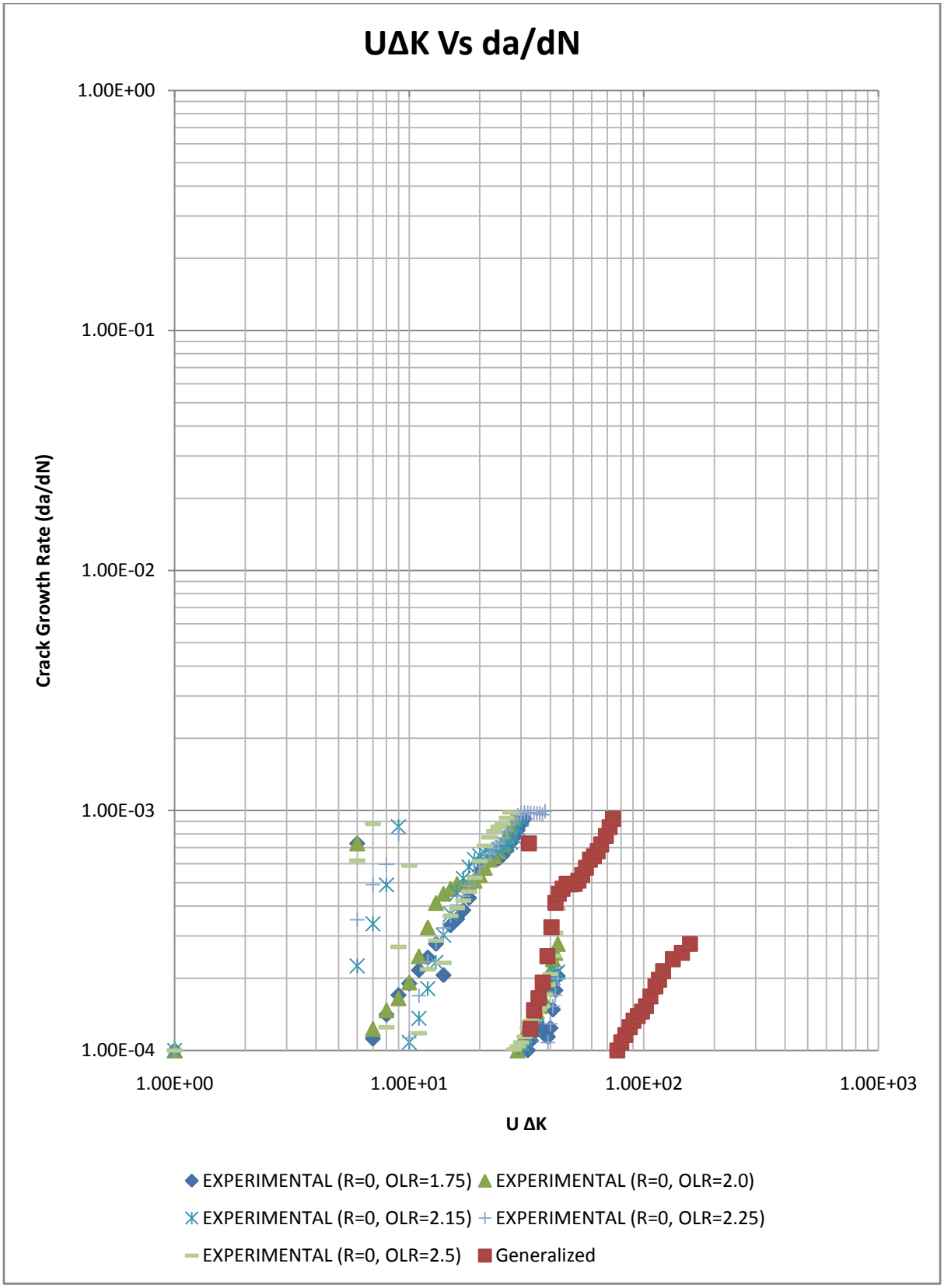

Fig 5.16 Validation of Generalized Equation

5.6.2 Application of the Generalized Model

For application was tested as shown in **Fig 5.16** of the generalized model on 6063 Al Alloy that gives very good agreement of the model proposed by Elber that shows the linear dependency of K_{eff} (or UΔK) Based on this a generalized Paris law was proposed.

Table 5.12Validation of the generalized equation

Material	**U (by generalized Equation) For n=1.8**	**U(by individual equation) For n=1.8**	**Variation (%)**
3003 Al	0.600496	0.600495579	0
5052 Al	0.600496	0.618923733	1.64
6061 T6 Al	0.600496	0.559898367	1.72
6063 T6 Al	0.600496	0.559898367	1.73
6351 Al	0.600496	0.670320046	1.41

5.7 MODIFIED PARIS LAW FOR SINGLE OVERLOAD

Putting the above relationship between U and n we can easily modify Paris Relationship which is very well suitable for aluminum alloy

$$da/dN = C\left\{\left(e^{(1.29-n)}\right)\Delta K\right\}^{n} \quad (5.2)$$

5.8 CONCLUSION

Increasing overload ratio decreases the effective stress range ratio U. The decrease is related to overload ratio. Change in U is related to overload ratio by power law. For all overload ratios, the cyclic life is found to decrease with increase in strain hardening-the effect is more on larger stress ratios. The effect of strain hardening is realized on yield strength of the material. The increase in strain hardening gives larger yield strength. A generalized relationship was formed for evaluation of U accordingly and modified Paris Law were obtained having limitation to Al Alloy only.

CHAPTER: 06

6 EFFECT OF WORK HARDENING EXPONANT IN BLOCK LOADING

6.1 INTRODUCTION

Since one part of the research is connected with the effect of loading and its frequency on the crack closing loads, loading cycles having simple loading programs were used to study crack closing loads and crack propagation rates. Experiments with programmed loads were performed to know the effect of load changes in crack opening /closing stresses. The details of the load are given in the figure given below. All the experiments were carried out on 6061-T6 Al Alloy except one which was conducted on 6063-T6 Al Alloy.
The details of experiments planned are given as follows:

i) Single cycle of peak load in each band is given after an interval 10% CAL life (Material 6061-T6 Al Alloy)

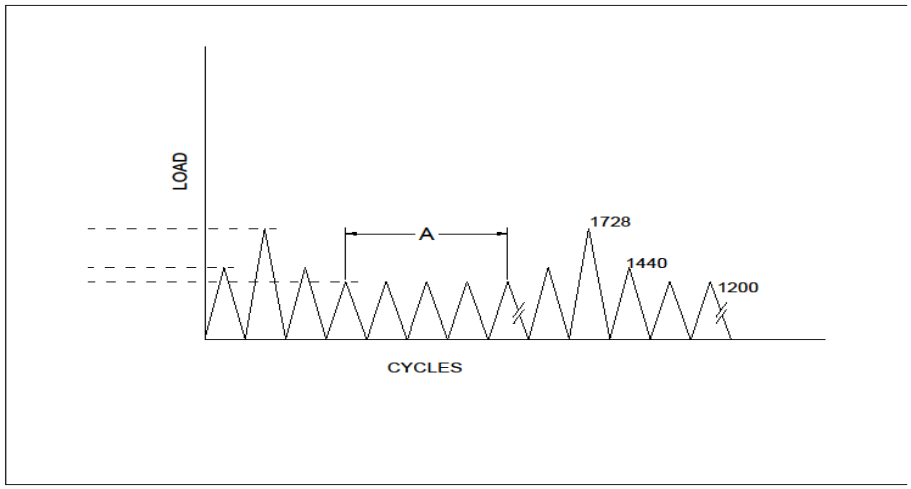

Fig 6.1Single cycle of peak load in each band

ii) 10 cycles of peak load in each band is given after an interval of 10% CAL life (Material 6061-T6 Al Alloy)

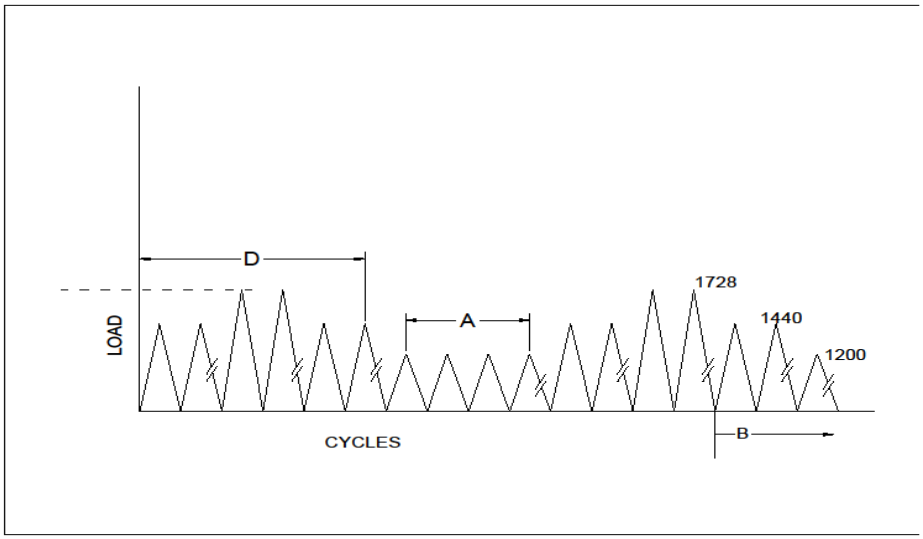

Fig 6.210 cycles of peak load in each band

iii) Single cycle of peak load in each band is given after exhausting 50% CAL life at interval of 10% CAL life (Material 6061-T6 Al Alloy)

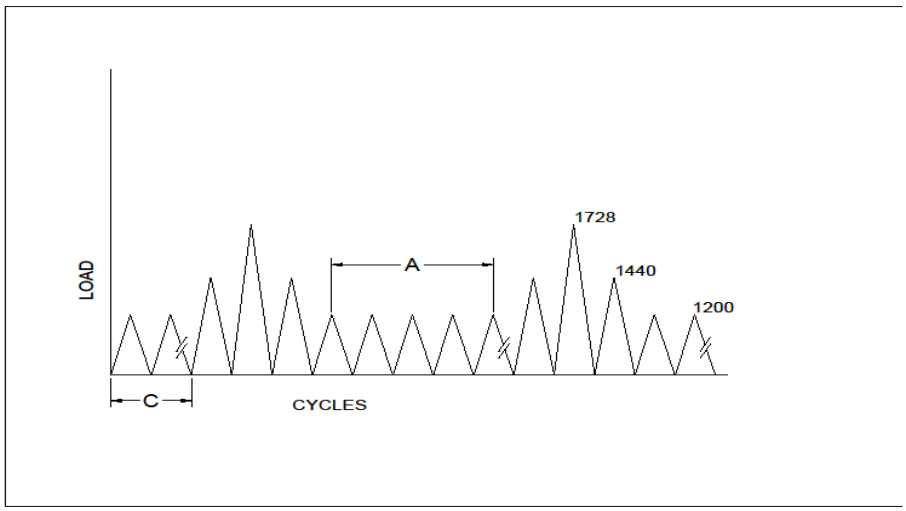

Fig 6.3Single cycle of peak load in each band after exhausting 50% CAL life

iv) Sequence of overloads containing 2mm crack length in each band (for Low-High & High to Low Sequences)

(a) For 6061-T6 Al-Alloy

(b) For 6063-T6 Al Alloy

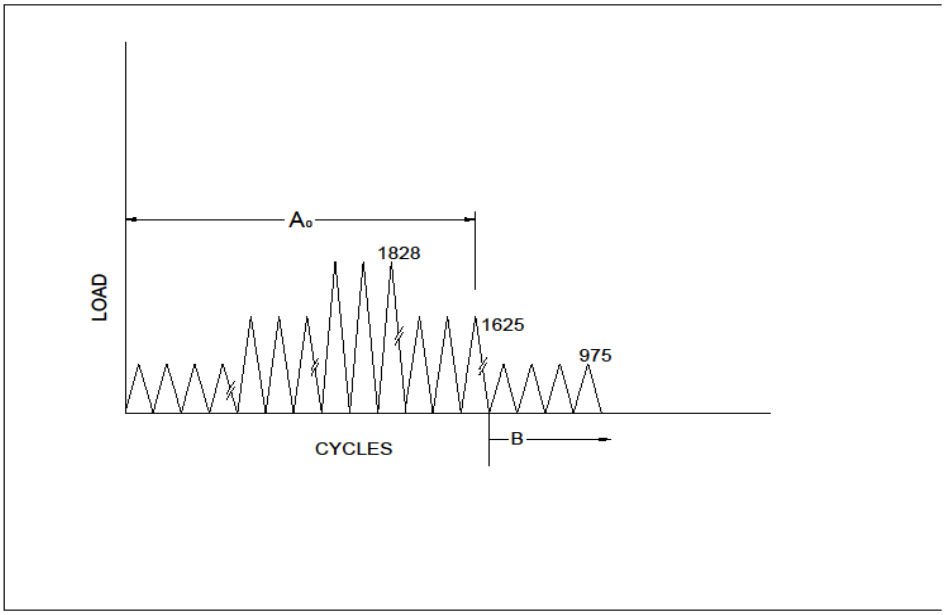

(a)

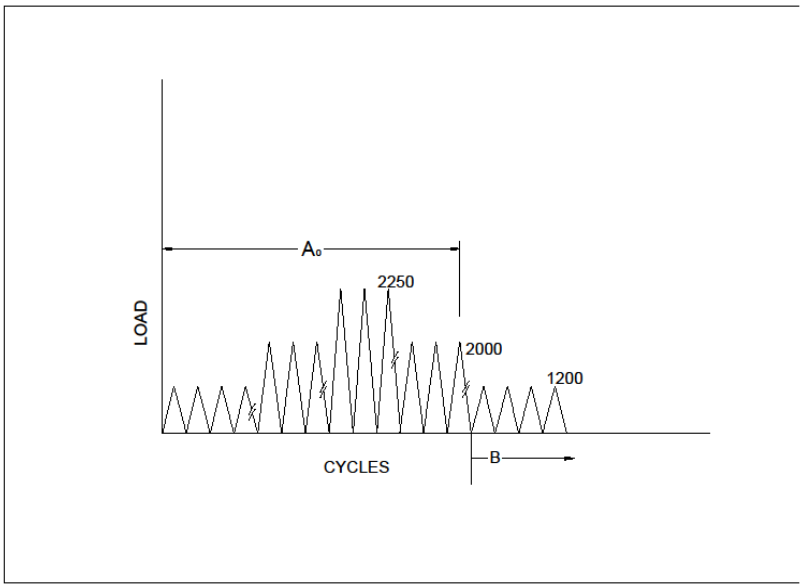

(b)

Fig 6.4Sequence of overloads for (a) 6061 T6 Al Alloy, (b) 6063 T6 Al Alloy

A = 10 % of CAL Life

A_0 = Each Block is given for 2 mm crack length

B = After A_0 crack length steady load continue up to failure

C= 50% of CAL Life

D= Each Block Contains 10 Cycles

The details of the load pattern are given in Table no 6.1. for different programmed loading the a Vs N curves are shown in **Fig6.1, Fig 6.2** for finding crack closure loads, displacement records were taken. The crack closure loads found from these records were used to find the effective stress intensity range ratio, U.

Since side edge notched specimen were used for all these Tests. Some important details of each of these Tests are given below.

The base load range for 6061-T6 was 0-1200 Kg and for 6063-T6 it was 0-975 kg

i) **Test 01 (For 6061-T6)-** Frequent overload bands having consecutive peaks of 1440, 1728, and 1440 kg were applied after exhausting 50% CAL life of the specimen at the periodic interval of 10% CAL life.

ii) **Test 02 (For 6061-T6) -** In this Test peaks of same magnitude were applied in each overload band as in Test 01. These loads were applied from the beginning of loading at an interval of 10 % CAL life.

iii) **Test03 (For 6061-T6) -** It is a Test similar to Test 02 except that each overload peak in an overload band contain 10overload cycles. The overload bands were given from the beginning. The peak had the overload ratios of 1.2 and 1.4.

iv) **Test 04 (For 6061-T6)-**This was a stepped loading program and each load block was continued up to 2 mm crack length. This Test was performed with load blocks having overload ratios of 1.66 and 1.87

v) **Test 04 (For 6063-T6)-**This stepped loading Test was conducted with same overload ratio as given for Test04. Each load block was continued up to 2mm crack length.

6.2 FEM RESULTS & DISCUSSION

The a Vs N curves for 6061 T-6 Al Alloy and 6063 T-6 Al Alloy are shown in **Fig6.1, Fig 6.2** respectively. In each case life is found to increase as compared to CAL life of the specimen. The increase in life was largest in the case of Test 02 in which each peak in an overload band contains one cycle and overload bands are given from the beginning.

For Test 03 in which each peak in an overload band contains 10 cycles, the life is found to be lesser than that obtained for Test 02.

The life for Test 01 is smallest. In this case overload bands were given after exhausting 50% CAL life. The full effect of overloads is therefore not realized.

6.2.1 Crack Growth Rate Curve for Stepped Loading

For these Tests, a Vs N curves were shown in **Fig 6.2, Fig 6.3**. In these experiments each block was continued up to 2 mm crack length. It is clear from these figures that crack length increases rapidly with increase in load. As magnitude decreased the crack growth rate gets retarded the curve.

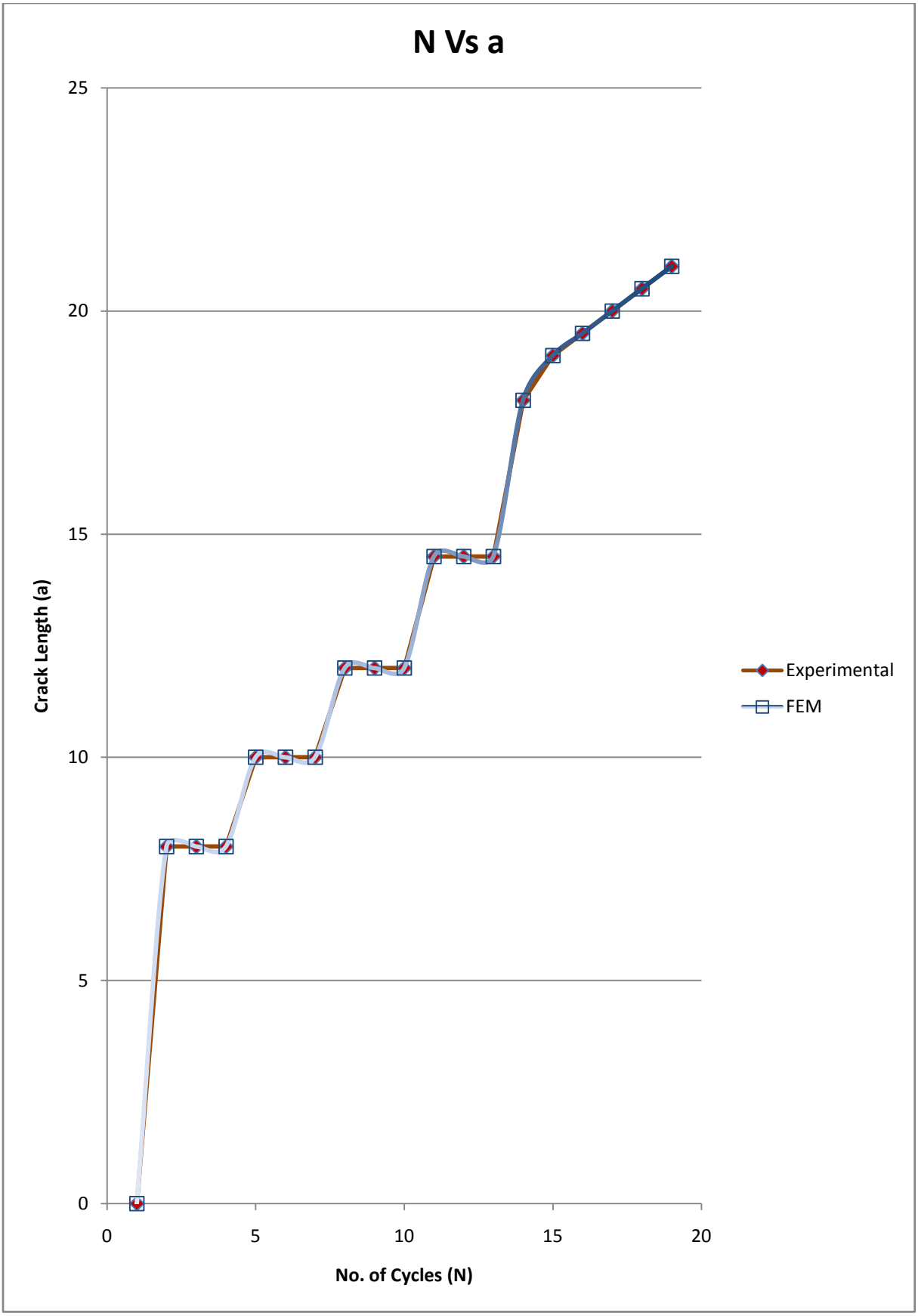

Fig 6.5 N Vs a for 6061-T6 Al Alloy

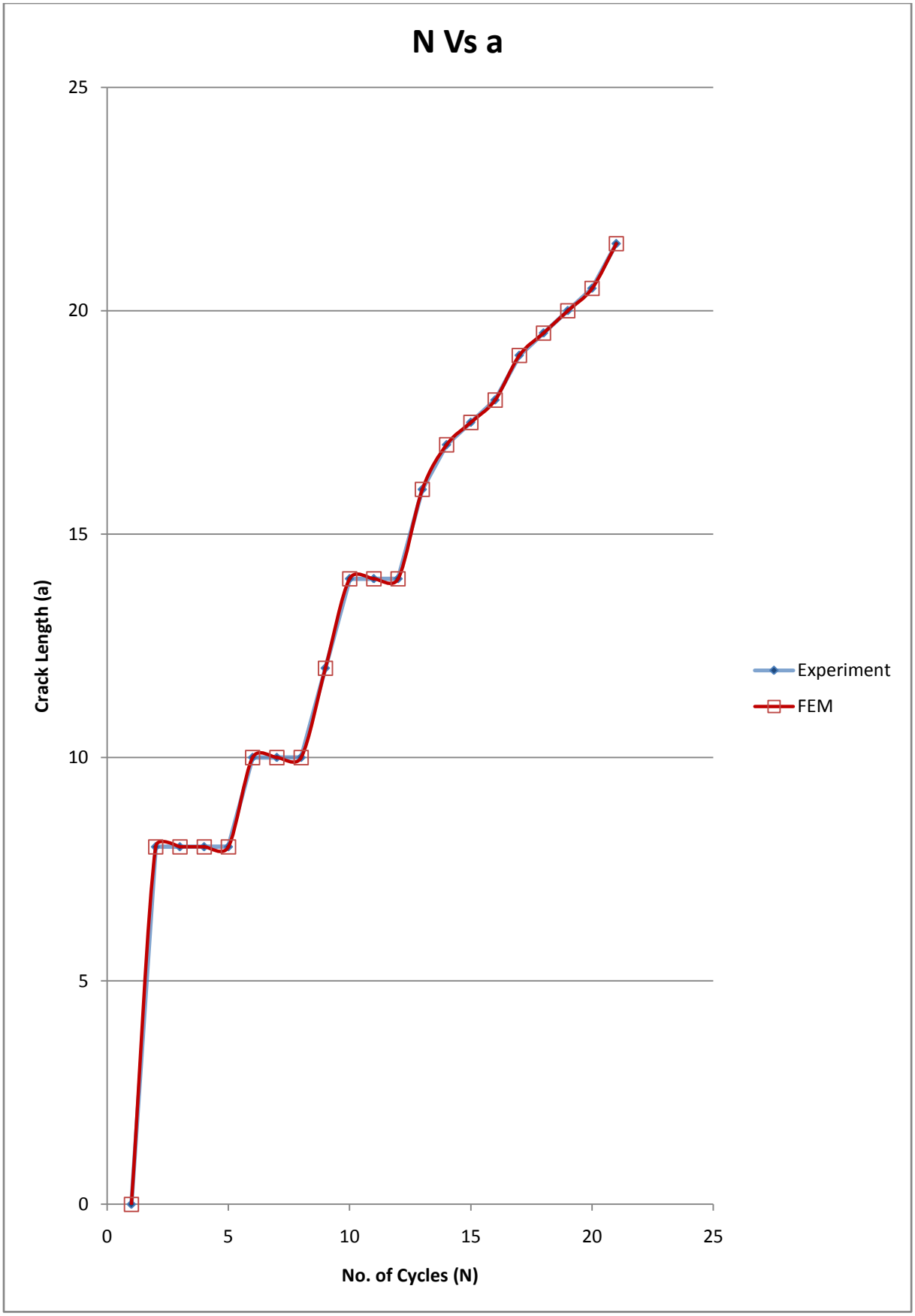

Fig 6.6 N Vs a for 6063-T6 Al Alloy

6.2.2 Crack Growth Rate Vs n for Stepped Loading

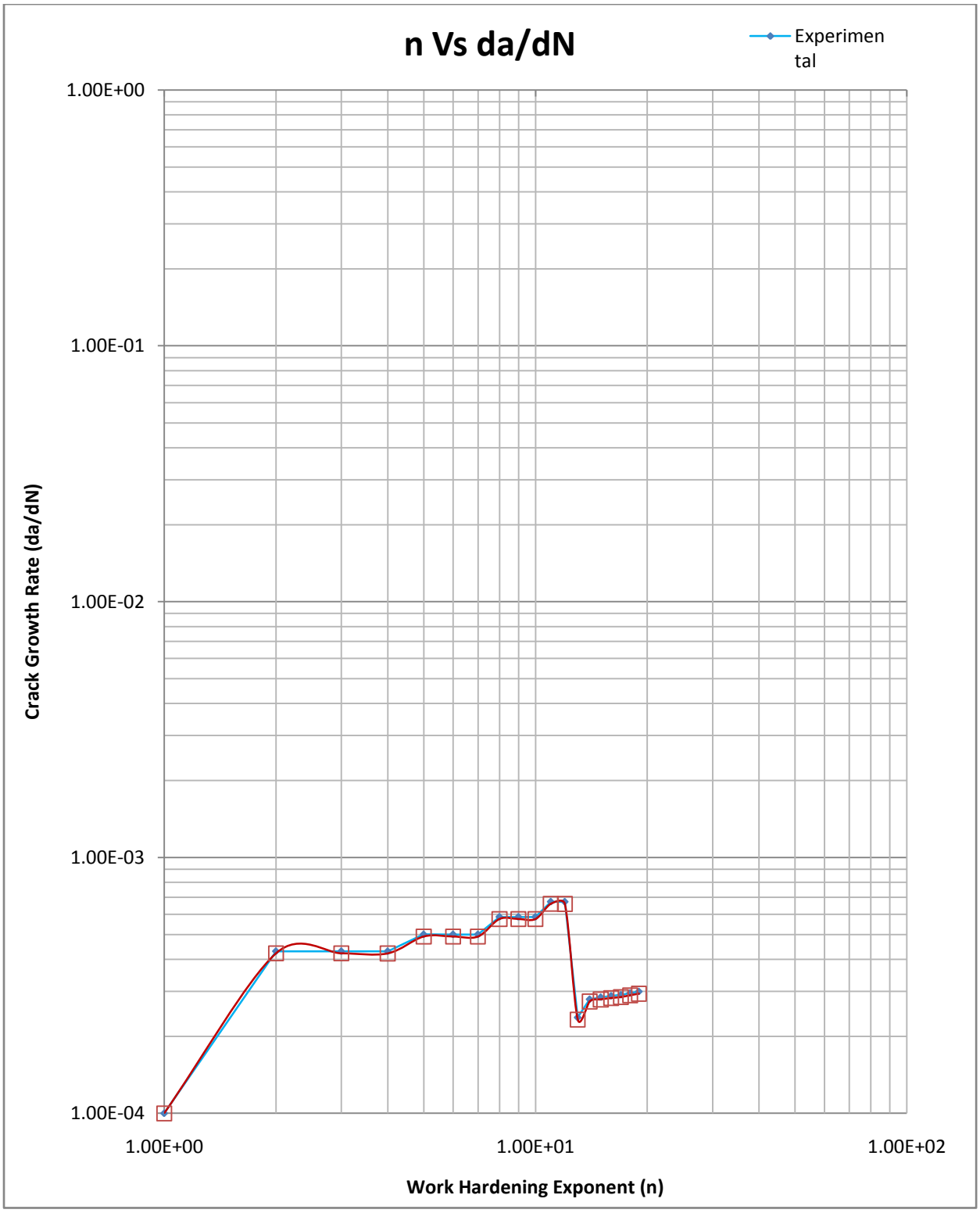

Fig 6.7n Vs da/dN for 6061-T6 Al Alloy

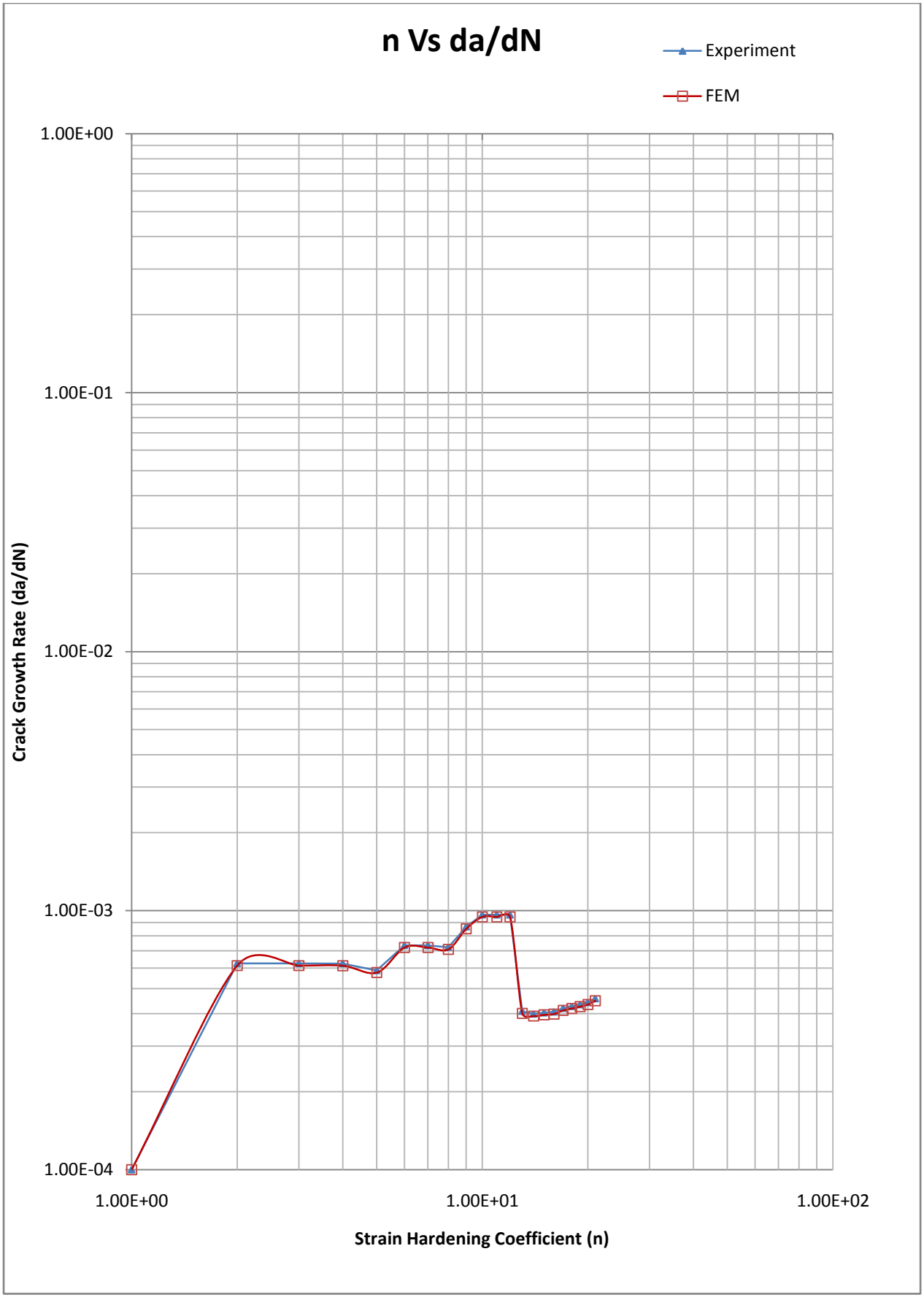

Fig 6.8n Vs da/dN for 6063-T6 Al Alloy

6.3 STUDY OF EFFECTIVE STRESS INTENSITY RANGE RATIO (U) DURING PROGRAMMED LOADING

Finite element analysis was done to find the effective stress intensity range ratio with loading condition s as minimum load was kept zero. Overload bands were applied at different intervals and the crack closing loads for different peaks are determined. The values of U found from these Tests and plotted.

In Test 01, U for CAL was found to be 0.69 which remained same up to 15000 cycles. After application of overload cycle band U was found to increase to 0.75. When load was decreased in the same overload sequence U decreased to 0.48 which remained constant till CAL cycles were applied. When next load band was applied, U increased. The value of U in Tests 02 and 03 are also found to follow the same trend.

6.3.1 U Vs n Curve for Stepped Loading

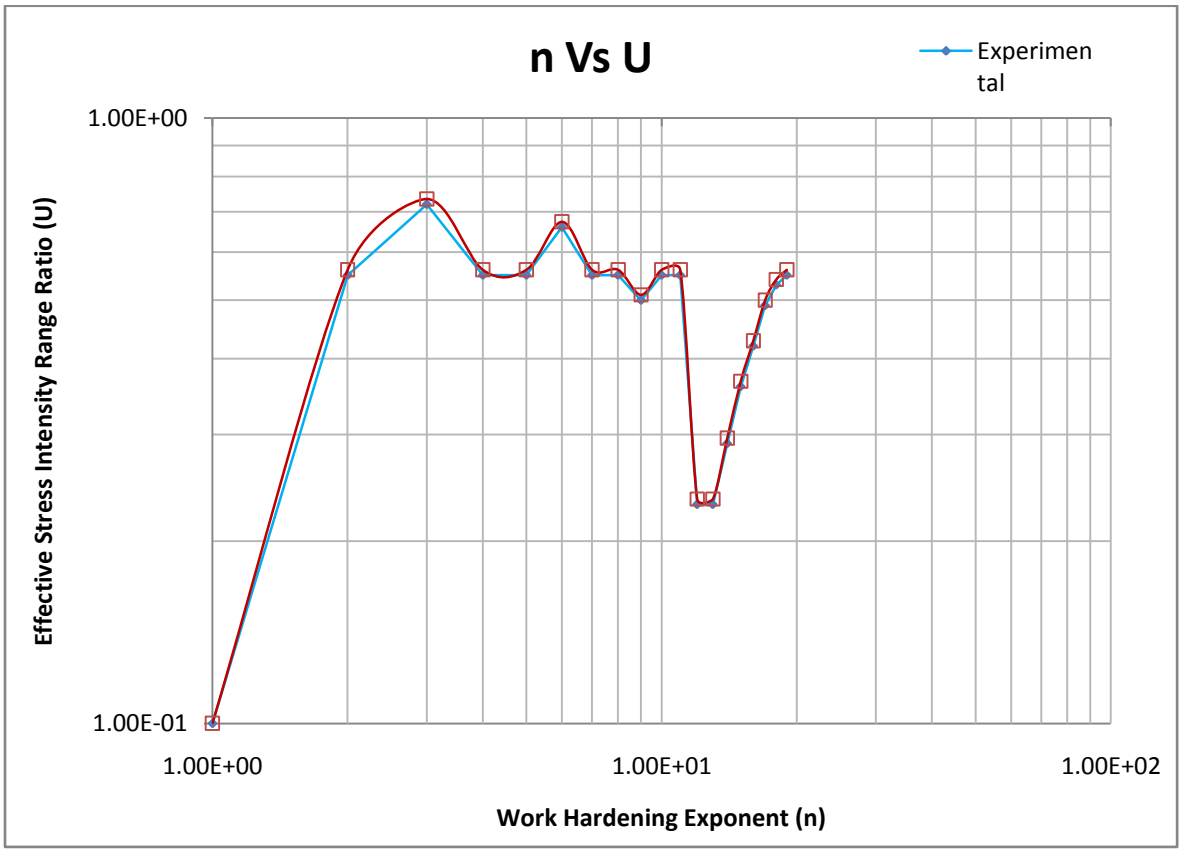

Fig 6.9nVs U for 6061-T6 Al Alloy

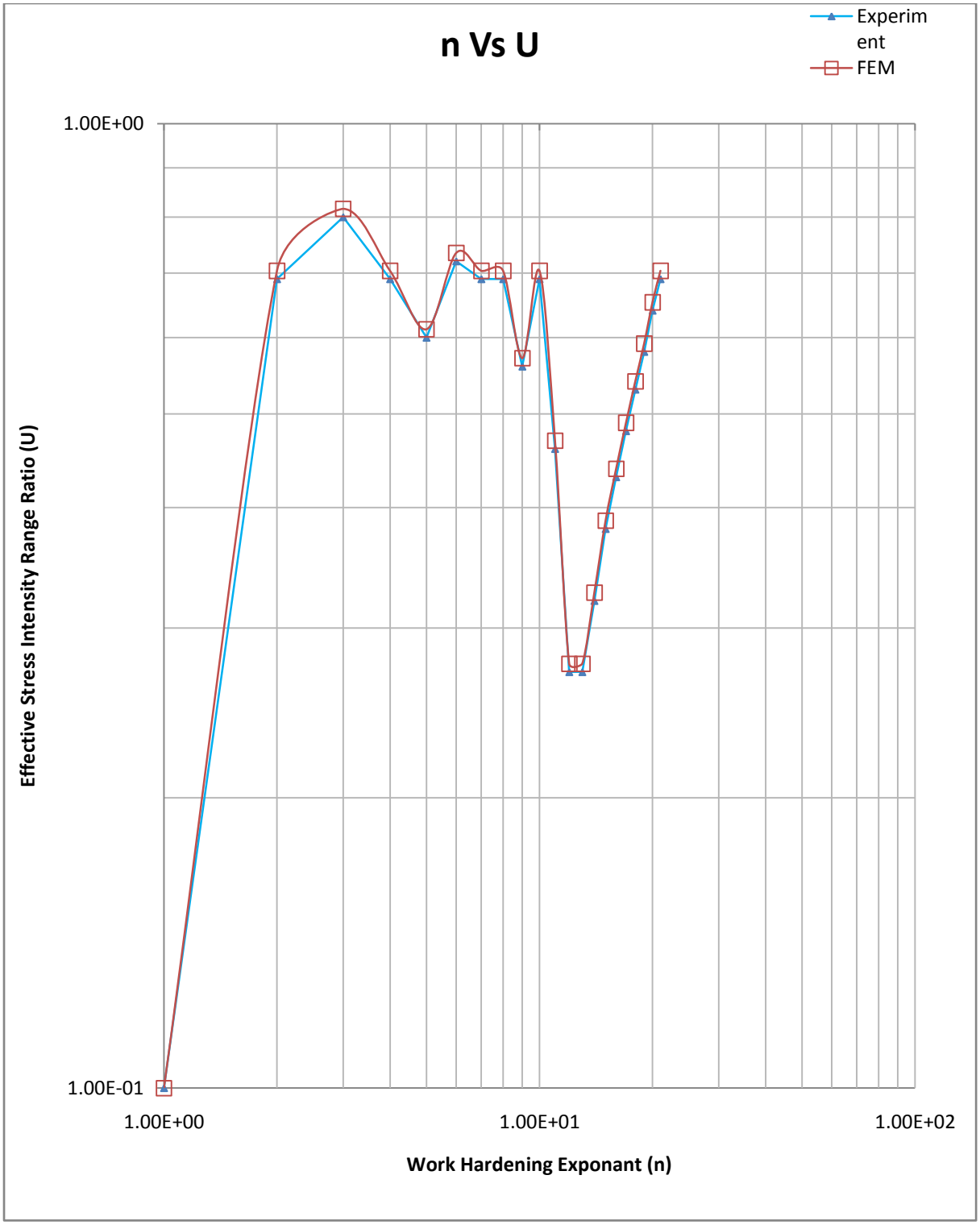

Fig 6.10n Vs U for 6063-T6 Al Alloy

For this case in U Vs n curve; it is found that value of U is 0.69 for value of n 3.3 for 6061-T6 Al Alloy. As the value of n is increased the value of U is also increased. After stabilization the curve shows a linear relationship between the U and n for both the materials.

6.4 REGRESSION ANALYSIS FOR BLOCK LOADING

Regression analysis was done on the data collected after FEM analysis for getting an empirical relationship between U & n and to get the modified Paris Law.

6.4.1 For 6061T-6 Al Alloy

Table 6.1 Regression Analysis for 6061Al Alloy under block loading

Model Summary

	R Square	Adjusted R Square	Std. Error of the Estimate
.166	.027	-.033	.336

The independent variable is n.

ANOVA

	Sum of Squares	df	Mean Square	F	Sig.
Regression	.051	1	.051	.451	.511
Residual	1.802	16	.113		
Total	1.853	17			

The independent variable is n.

Coefficients

	Unstandardized Coefficients		Standardized Coefficients	T	Sig.
	B	Std. Error	Beta		
N	1.133	.210	1.180	5.398	.000
(Constant)	1.535	.716		2.143	.048

The denpendent variable is ln(1 / U).

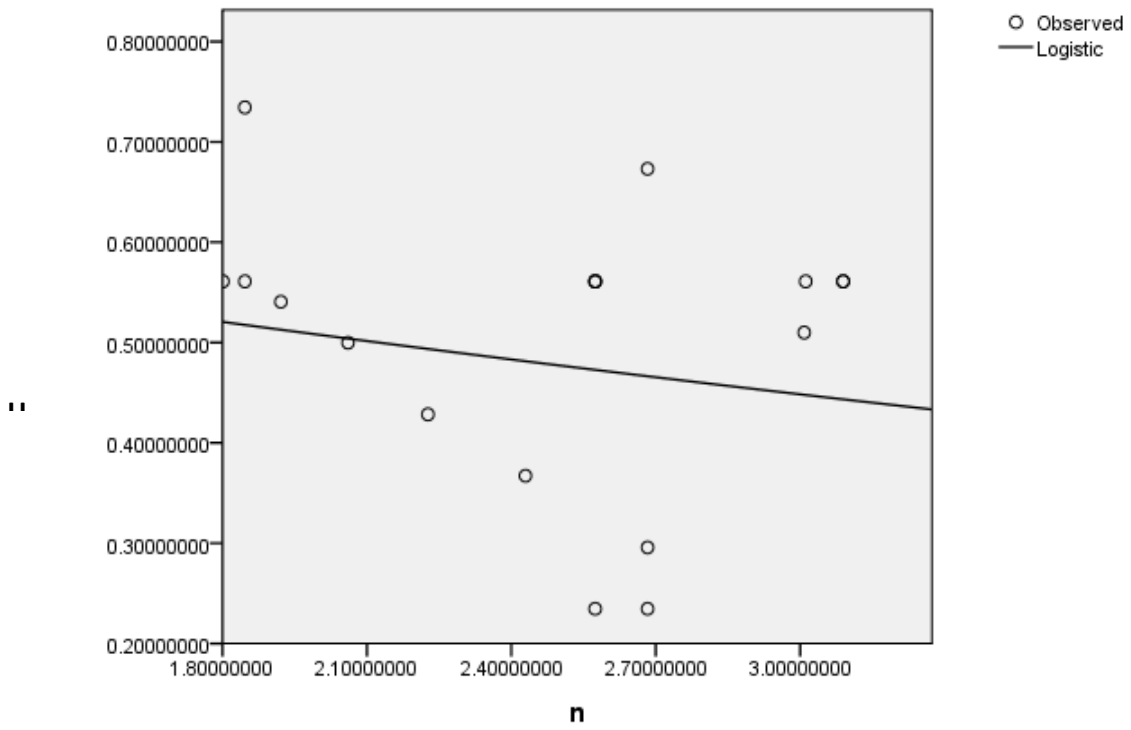

Fig 6.11Curve Fitting between U and n for 6061-T6 Al Alloy

6.4.2 For 6063T-6 Al Alloy

Table 6.2 Regression Analysis for 6063Al Alloy under block loading

Model Summary

R	R Square	Adjusted R Square	Std. Error of the Estimate
.745	.555	.530	.227

The independent variable is n.

ANOVA

	Sum of Squares	df	Mean Square	F	Sig.
Regression	1.160	1	1.160	22.418	.000

Residual	.931	18	.052		
Total	2.091	19			

The independent variable is n.

Coefficients

	Unstandardized Coefficients		Standardized Coefficients		
	B	Std. Error	Beta	t	Sig.
N	1.548	.143	2.106	10.840	.000
(Constant)	.647	.146		4.417	.000

The dependent variable is ln(1 / U).

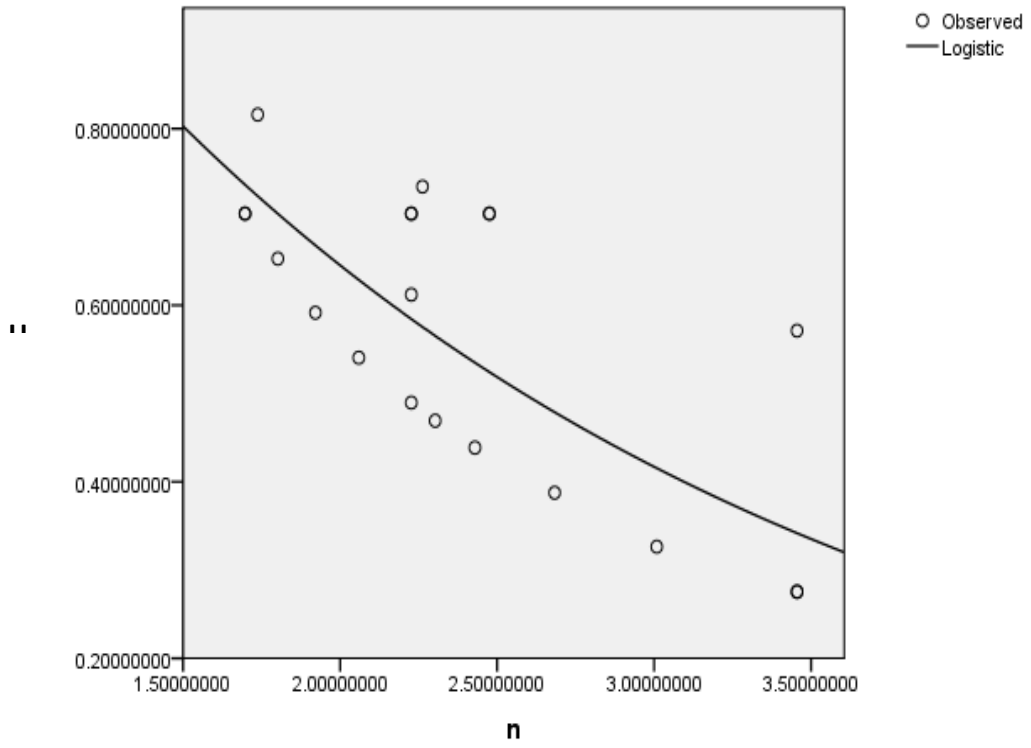

Fig 6.12Curve Fitting between U and n for 6063-T6 Al Alloy

6.4.3 Relationship obtained After Regression Analysis

Table 6.3 Equations obtained After Regression Analysis

S.No.	Materials	Equations Obtained
1	6061-T6 A Alloy	$U = e^{(1.535-1.133n)}$
2	6063-T6 A Alloy	$U = e^{(0.647-1.548n)}$

6.5 GENERALIZED EQUATION FOR BLOCK LOADING

$$U = e^{(1.091-1.340n)} \quad (6.1)$$

6.5.1 Validation of the generalized Equation

Table 6.4Validation of the generalized Equation

Materials	U (from Generalized Equation)	U (from individual Equation)	% Variation
6061-T6 Al Alloy	0.7038	0.708	1.87
6063-T6 Al Alloy	0.612	0.617	1.38

6.6 MODIFIED PARIS LAWFOR BLOCK LOADING

Putting the above relationship between U and n we can easily modify Paris Relationship which is very well suitable for aluminum alloy

$$da/dN = C\left\{\left(e^{(1.091-1.340n)}\right)\Delta K\right\}^n \quad (6.2)$$

6.7 CONCLUSION

After an overload band, the value of U decreases as was found for the case of single overload. At constant amplitude loading, this value of crack closure remains almost constant till the load again increases. During subsequent cycles after an overload band, U reaches a minimum value. This shows that crack propagation during a number of cycles takes place at minimum U, resulting in considerable increase in life. In the Lo-Hi load sequence the crack closure load increases but the value of U remains same. The crack growth rate however increases due to larger value of ΔK. These values of U are found to stabilize in about 10 cycles. Acceleration takes place in crack growth rate during Lo-Hi load sequences.

CHAPTER: 07

7 CONCLUSION AND SUGGESTION FOR FUTURE WORK

The phenomenon of crack closure in side edged notch specimen (SEN) has been studied both experimentally and FEM. While the significant contribution of the present study is the comparison between the finite element based computer results and the experimental results on crack closure loads under constant amplitude loading, constant amplitude loading with single over load and block loading, the contributions are:

Development of an efficient FEM based computer program which is for elastic plastic non – linearly strain hardening material. It is necessary that such a program is developed exclusively for crack propagation studies.

1) Obtaining extensive results for trends in crack closure behavior under the same loading conditions taken up for experimental study.

2) Development and validation of a generalized relationship between crack growth rate and work hardening exponent for Aluminum Alloys.

3) Development and Validation of a generalized relationship between effective stress intensity range ratio and work hardening exponent for Aluminum Alloys.

4) Development of modified Paris Law for Aluminum Alloys.

These are discussed below:

It has been found to be possible to measure accurately the crack closure loads using the Finite Element Method. The FEM investigation on side edge notched specimens show a monotonic increase of crack closure loads up to a/b ratio of approximately which crack closure loads stabilize for constant amplitude loading. This is probably due to mode transition. The effect of work hardening on crack closure under various loading shows the

following trends:

7.1 UNDER CONSTANT AMPLITUDE LOADING

In constant amplitude loading Crack opening and closing loads are particularly equal. Effective stress intensity range ratio increases with increases work hardening exponent. U increases with crack length, yield strength and stress ratio also. A generalized empirical formula has been developed and validated for Aluminum Alloy which gives very good agreement with the experimental results. The presented model equations are applicable for Al Alloy and SEN only. Effect of strain hardening on crack growth were noticed as for lower R-ratios, i.e., R=0, R=0.1, R=0.3, crack growth rate decreases with the increasing work hardening effect and for R= 0.5, crack growth rate increases with the increasing strain hardening effect. The modified Paris Law has been proposed for Aluminum Alloys and SEN.

For P_{max}= Constant

Generalized Equation: $\mathbf{U=e^{(1.45-n)}}$

Modified Paris Law: $\mathbf{da/dN = C\left\{(e^{(1.45-n)})\Delta K\right\}^{n}}$

For ΔP=Constant

Generalized Equation: $\mathbf{U=e^{(1.48-n)}}$

Modified Paris Law: $\mathbf{da/dN =C\left\{(e^{(1.48-n)})\Delta K\right\}^{n}}$

7.2 UNDER CONSTANT AMPLITUDE LOADING WITH SINGLE OVERLOAD

Increasing overload ratio decreases the effective stress range ratio U. The decrease is related to overload ratio. Change in U is related to overload ratio by power law. For all overload ratios, the cyclic life is found to decrease with increase in strain hardening- the effect is more on larger stress ratios. The effect of strain hardening is realized on yield strength of the material. The increase in strain hardening gives larger yield strength. A generalized relationship was formed for evaluation of U accordingly and modified Paris Law was obtained having limitation to Al Alloy only.

Generalized Equation: $\mathbf{U=e^{(1.29-n)}}$

Modified Paris Law: $\mathbf{da/dN=C\left\{(e^{(1.29-n)})\Delta K\right\}^{n}}$

7.3 UNDER BLOCK LOADING

After an overload band, the value of U decreases as was found for the case of single overload. At constant amplitude loading, this value of crack closure remains almost constant till the load again increases. During subsequent cycles after an overload band, U reaches a minimum value. This shows that crack propagation during a number of cycles takes place at minimum U, resulting in considerable increase in life. A generalized equation has been developed that gives very good agreement with the values obtained from experiments. Below 2% error was recorded in values obtained by generalized equation obtained after regression analysis on the data obtained by FEM analysis

Generalized Equation: $\mathbf{U = e^{(1.091-1.340n)}}$

Modified Paris Law: $\mathbf{da/dN = C\left\{(e^{(1.091-1.340n)})\Delta K\right\}^{n}}$

In order to study the crack closure behavior at a distance sufficiently far from the crack tip an approximate procedure has been proposed. This has been found to be very useful. Detailed quantitative results have been obtained on crack closure loads all loading conditions chosen for experimental & analytical study. It is significant that there is good agreement between the analytical and experimental results for stress distribution at the wake of crack tip under all loading conditions. It is significant that there is good agreement between the analytical and experimental results from the point of view of crack closure loads. However, since only a quasi-static approach has been used in crack propagation without incorporating the dynamic crack growth criterion, only the general trends of crack closure behavior can be compared with experimental study. These are found to be in good agreement.

The present study has ensured beyond doubt the utility of finite element method for accurate simulation of crack growth behavior in practical applications with reasonable computing cost and the proposed empirical relationships can be used for selecting an Al Alloy majorly in aerospace industries.. The following problems can be taken up for immediate study:

1) Development of a suitable automated mesh generation procedure which

positions the fine mesh region in the neighborhood of the crack tip as the crack advances;

2) Application to practical problems under general conditions.

3) More Materials can be taken to get more generalized relationship that will be applicable for all materials.

8 REFERENCES

[1] B. Li, L. Reis, M. de Freitas, " Simulation of cyclic stress/strain evolutions for multiaxial fatigue life prediction" International Journal of Fatigue, 28, pp 451–458,(2006)

[2] Bailon, J.P., Masourave, J. & Bathias, C., "On the Relationship Between Parameters of Paris Law for Fatigue Crack Growth Rate in Aluminium Alloys", Scripta Metall 11, pp 1101-1106, (1977)

[3] Barsom, J.M. and McNicol, R.C. "Effect of stress concentration on fatigue crack initiation in HY-130 Steel, ASTM STP 559, American Society for Testing and Materials, Philadelphia, pp. 183-204, (1974)

[4] Barsoum, R.S. "On the use of isoparametric elements in linear fracture mechanics,"International journal for numeric methods in engineering, 10, pp. 25-38.(1976)

[5] Basquin, O.H., "The Exponential Law of Endurance Tests", Proc. Annual Meeting ASTM, 10, 625, (1919)

[6] Belytschko, Gracie, Ventura, "A Review of Extended/Generalized Finite Element Methods for Material Modeling"International journal for numeric methods in engineering, 18, pp. 55-68 (2009)

[7] Braithwaite, F. "On the Fatigue and Consequent Fracture of Metals", Minutes of Proc. ICE, 463,(1854)

[8] Branco R, Antunes FV, Martins RF "Modeling fatigue crack propagation in CT specimen", Fatigue and Fracture of Engineering Materials and Structures, 31, pp. 452-465,(2008)

[9] Branco R, Antunes FV. "Finite element modeling and analysis of crack shape evolution in mode-I fatigue Middle Cracked Tension specimens", Engineering Fracture Mechanics, 75, pp. 3020-303(2008).

[10] Branco R., "Numerical study of fatigue crack growth in MT specimens". MSc Thesis, Department of Mechanical Engineering, University of Coimbra, (2006).

[11] Broek, D., "Elementary Engg. Fracture Mechanics", Martinus Nijhoff Publishers, London, (1982)

[12] Burdekin, F.M.; Stone, D.E.W.: The Crack Opening Displacement Approach to Fracture Mechanics in Yielding Materials, Journal of Stress Analysis, Vol.1, 145,pp. 143-150(1966)

[13] C.K.Clark and G.C. Cassat, "A study of fatigue crack closure using electric potential and compliance techniques." Engineering fracture mechanics. Vol. 9, pp. 675-688, (1977)

[14] Chan, S.K., Tuba, I.S. and Wilson, W.K., "On the finite element method in linear fracture mechanics, Vol. 2, pp. 1-17, (1970)

[15] Chand, S. &Garg. S.B.L. , "Crack Propagation Under constant Amplitude Loading", Engineering Fracture Mechanics, Vol. 21, No. 1, pp 1-30, (1985).

[16] Chien-Yuan Hou, "Three-dimensional finite element analysis of fatigue crack closure behavior in surface flaws", International Journal of Fatigue Vol.26 pp.1225–1239,(2004)

[17] Coffin, Manson, "Introduction to high-temperature low-cycle fatigue." Experimental Mechanics, Vol.8, p218-224 (1955)

[18] Couroneau N, Royer J. "Simplified model for the fatigue crack growth analysis of surface cracks in round bars under mode I." International Journal of Fatigue Vol.20 pp.711–719 (1998)

[19] Elber, W., "Fatigue Crack Closure-Under Cyclic Tension" Engg. Fracture Mechanics Vol. 2, pp 37-45, (1970)

[20] Elber, W., "The significance of fatigue crack closure ASTM 486, pp 230-242, (1971)

[21] Elber, W.: Fatigue Crack Propagation: Some Effects of Crack Closure on the Mechanism of Fatigue Crack Propagation under Cyclic Tension Loading, PhD Thesis, University of New South Wales (1968)

[22] Ewing, J.A.; Humfrey, J.C.W. "The Fracture of Metals under Repeated Alternations of Stress", Philosophical Transactions, Royal Society London, pp. 241-249,(1903)

[23] F. Romeiro, M. de Freitas, M. da Fonte, "Fatigue crack growth with overloads/underloads: Interaction effects and surface roughness" International Journal of Fatigue Vol. 31 pp. 1889–1894(2009)

[24] F. Taheria, D. Traskb, N. Pegg. "Experimental and analytical investigation of fatigue characteristics of 350WT steel under constant and variable amplitude loadings" Marine Structures Vol.16, 69–91,(2003)

[25] F.K. Ibrahim, T.H. Topper, "A Study of effect of mechanical variables on fatigue crack closure and propagation". International Journal of Fatigue Vol. 85, pp. 139–142,(2009)

[26] Fatigue Failures, Failure Analysis andPrevention, Vol 11, ASM Handbook, ASM International, (2002)

[27] Foreman, R.G., Mearney, V.E. & Engle, R.M., 'Numerical Analysis of Crack Propagation in Cyclic Loaded Structures", J.I. Basic Engg., Trans. ASME, Sr. D. 89, pp 454, (1967)

[28] G. Jovicic, M. Zivkovic, N. Jovicic, "Extended Finite Element Method for Two-dimensional Crack Modeling" Journal of the Serbian Society for Computational Mechanics Vol. 1, pp. 184-196,(2007)

[29] Gifford, Jr. L.N. and Hilton, P.D. "Stress intensity factors by enriched finite elements "Engineering Fracture Mechanics, Vol. 10, pp.507-496,(1978)

[30] Griffith, A.A. "The Phenomena of Rupture and Flow in Solids." Philosophical Transactions A, Vol. 05, pp. 221-235,(1920)

[31] H. Alizadeh , D.A. Hills , P.F.P. de Matos, D. Nowell , M.J. Pavier ,R.J. Paynter, D.J. Smith, S. Simandjuntak. "A comparison of two and three-dimensional analyses of fatigue crack closure" International Journal of Fatigue Vol. 29,pp.222–231,(2007)

[32] Hertzberg, Richard W., "Deformation and Fracture Mechanics of Engineering Materials, John Wiley & Sons, New York.International Journal of Fatigue Vol. 19,pp.22–31 (1989)

[33] I.V. Singh, B.K. Mishra, S. Bhattacharya, R.U. Patil. " The numerical simulation of fatigue crack growth using extended finite element method." International Journal of Fatigue Vol.36,pp.109–119,(2012)

[34] Inglis, C.E. "Stresses in a Plate due to the Presence of Cracks and Sharp Corner.", Transactions of the Institute of Naval Architects, Vol.55, pp. 219-230, (1913)

[35] Irwin, G.R.: Fracture, Handbuch der physic, S. Flugge(ed.), Springer-Verlag, Berlin, Vol.06, pp. 551-590 (1958)

[36] Isida , M. " On the tension of a strip with a central elliptical hole, " Transactions of Japanese society of mechanical engineering, Vol.21, pp. 507-518, (1955)

[37] J. Huynh, L. Molent , S. Barter, "Experimentally derived crack growth models for different stress concentration factors" International Journal of Fatigue Vol.30,pp.1766–1786(2008)

[38] J. SCHIJVE., "Fatigue of Structures and Materials". Kluwer Academic Publisher, (2001).

[39] J. Zapateroa, B. Morenoa, A. Gonza´lez-Herreraa, J. Domı´nguezb, "Numerical and experimental analysis of fatigue crack growth under random loading" International Journal of Fatigue Vol. 27, pp.878–890, (2005)

[40] J.E. LaRue, S.R. Daniewicz, "Predicting the effect of residual stress on fatigue crack growth." International Journal of Fatigue Vol. 29, pp. 508–515, (2007)

[41] J.M. Alegre, I.I. Cuesta, " Some aspects about the crack growth FEM simulations under mixed-mode loading" International Journal of Fatigue Vol. 32, pp. 1090–1095, (2010)

[42] Jankowiak, H. Jakubczak, G. Glinka, "Fatigue crack growth analysis using 2-D weight function." International Journal of Fatigue Vol. 31 pp.1921–1927, (2009)

[43] John A.R. Bomidi, Nick Weinzapfel, Chin-Pei Wang, Farshid Sadeghi, "Experimental and numerical investigation of fatigue of thin tensile specimen." International Journal of Fatigue Vol. 44, pp.116–130,(2012)

[44] Katcher, M., & Kaplan, M., "Effect of R-Factor & Crack Closure on Fatigue Crack Growth for Aluminium & Titanium Alloys", ASTM STP 559, pp 264-282, (1974)

[45] Kujawaski, D. & Ellyin, F., "A Fatigue Crack Propagation Model", Engg. Fracture Mechanics, Vol. 20, No.510, pp 695-704, (1984)

[46] Kumar, R., &Garg, S. B. L., "Effect of Stress Ratio on Effective Stress Ratio &Crack Growth in 6061-T6 Aluminium Alloy", Int. J., Pres. Ves. and piping, Vol. 6, pp.234-245(1988)

[47] L.C.H. Rechardo, "Determination of crack opening and closing stresses by Finite Element Method" University of Sao Pulao, Brazil.(1997)

[48] Lin XB, Smith RA. "Finite element modeling of fatigue crack growth of surface cracked plates." Part I: The numerical technique. Engineering Fracture Mechanics, Vol.63, pp.503-522,(1999)

[49] Lost, A., "Effort of Load Ratio on the m-logC Relationship", Int. J.Fatigue Vol.13 , pp 25-33, (1991).

[50] M. El-Zeghayar, T.H. Topper, K.A. Soudki , "A model of crack opening stresses in variable amplitude loading using smooth specimen fatigue test data for three steels." International Journal of Fatigue Vol.33,pp.1337–1350,(2011)

[51] M. El-Zeghayar, T.H. Topper, K.A. Soudki, "A model of crack opening stresses in variable amplitude loading using smooth specimen fatigue test data for three steels". International Journal of Fatigue Vol. 33,pp.1337–1350(2011)

[52] M. Sander, H.A. Richard, "Finite element analysis of fatigue crack growth with interspersed mode I and mixed mode overloads" ,International Journal of Fatigue Vol. 27,pp.905–913, (2005)

[53] Maddox, S.J., et al., "An investigation of the influence of applied stress ratio on fatigue crack propagation in structural steels" welding institute, research report 72/1978/E, (1978)

[54] Marco Antonio Meggiolaro, Jaime Tupiassu´ Pinho de Castro "On the dominant role of crack closure on fatigue crack growth Modeling" International Journal of Fatigue Vol.25 pp.843–854,(2003)

[55] Michel D. Sangid, Raginald H. Hamilton "High Resolution analysis of opening and sliding in fatigue crack growth".International Journal of Fatigue Vol. 37,pp.134–145,(2012)

[56] N. Ranganathan, H. Aldroe, F. Lacroix, F. Chalon, R. Leroy, A. Tougui, "Fatigue crack initiation at a notch" International Journal of Fatigue Vol.33 pp. 492–499,(2011)

[57] N. Sukumarz, N. Mooesx, B. Moran & T. Belytschko, "Extended finite element method for three-dimensional crack modeling". International Journal of Fatigue Vol. 21,pp.801–823,(2000)

[58] N.A. Fellows, J.F. Durodola, "Experimental measurement of crack opening and closure load for 6082 T6 subjected to periodic single and block overload and under load". International Journal of Fatigue Vol.5 pp.123–135,(1998)

[59] Nakagaki M, Atluri SN. "Fatigue crack closure and delay effects under mode I spectrum loading: an efficient elastic–plastic analysisprocedure". Fatigue Engg. Material Structure Vol. 5.pp 921–935.(2003)

[60] Neuber, H., "Theory of Stress Concentration for Shear-Strained Prismatical Bodies with Arbitrary Nonlinear Stress Strain Law." Journal of Applied Mechanics, Vol. 28,pp.544-556,(1961)

[61] Niccolls, E.H., "A Co-relation for Fatigue Crack Growth Rate", Scripta Metall Vol. 10, pp 295-298, (1976)

[62] Nicolas Mooesy, John Dolbowz & Ted Belytschko,"A finite element method for crack Growth without remeshing" International Journal For Numerical Methods In Engineering, Int. J. Numer. Meth. Engng. Vol.46, 131-150 (1999)

[63] Orowan, E. "Fracture and Strength of Solids." Reports on Progress in Physics, Vol. 12,pp.185-196,(1948)

[64] Osgood, C.C., "Fatigue Design "Cranbury, New Jersey, U.S.A., Pergamon Press, 1982.

[65] Pandey, A.K., "Effect of Load Parameters on Crack Growth Rate & Fatigue Life", M.E. thesis, Allahabad, 1988.

[66] Paris, P.C., & Erdogan, F., "A Critical Analysis of Crack Propagation Laws", Trans .ASME J. Basic Engg. Vol.55, pp528 – 534, (1963)

[67] Park S-J, Earmme Y-Y, Song J-H. "Determination of the most appropriate mesh size for a 2-D finite element analysis of fatigue crack closure behavior". Fatigue Fract. Engg. Material Structure, Vol 20(4), pp 533–45. (2007)

[68] Pearson, S., "Effect of Mean Stress in Aluminium Alloy in High & low Fracture Toughness", Engg. Fracture Mechanics, 4, pp 9-24, (1972).

[69] Pearson, S.: "Initiation of Fatigue Cracks in Commercial Aluminum Alloys and the Subsequent Propagation of Very Short Cracks", Engineering Fracture Mechanics, Vol.7, 235,(1975)

[70] Peterson, R. E., "Stress Concentration Design Factors", John Wiley, New York.(1953)

[71] Pommier S. "Cyclic plasticity and variable amplitude fatigue". IntJ. Fatigue, Vol. 25, pp 983–97(2003)

[72] R.Kumar, Effect Of Material Properties And Loading Parameters On Crack Closure In Fatigue". Ph.D Thesis, MNREC, (1986)

[73] Recommended Practice for Plane Strain Fracture Toughness Testing of High strength Metallic Materials Using a Fatigue Cracked Bend Specimen", TRP prepared by ASTM committee E-24, (1967)

[74] Rice, J.R. A path Independent Integral and Approximate Analysis of Strain Concentration by Notches and Cracks, Journal of Applied Mechanics, Vol. 35, pp.379-386(1969)

[75] Rice, J.R., "Mechanics of crack Tip Deformation & Extension by Fatigue, Fatigue Crack Propagation," ASTM STP 415, pp 247-309, (1967)

[76] Ritchie, R.O., "Influence of Microstructure on Near Threshold Fatigue Crack Propagation in Ultra High Strength Steel", Proceeding conference fatigue, Cambridge, pp 61-71, (1977)

[77] Rodes, D., Randon , J.C. & Culver, L.E., " Cyclic & Monotonic Crack Propagation in High Toughness Aluminium alloys", Inst. J. Fatigue, pp 61-67, (1980)

[78] S. Ismonov , S.R. Daniewicz. " Simulation and comparison of several crack closure assessment methodologies using three-dimensional finite element analysis" International Journal of Fatigue Vol. 32, pp. 1322–1329,(2010)

[79] S. Kalnaus, F. Fan, Y. Jiang, A.K. Vasudevan "An experimental investigation of fatigue crack growth of stainless steel 304L." International Journal of Fatigue Vol. 31, pp. 840–849,(2009)

[80] S. Machida, M. Toyosada, "Fatigue Crack propagation under various types of loading". International Journal of Fatigue Vol.55, pp.19–25,(2005)

[81] S. Mikheevskiy , G. Glinka, " Elastic–plastic fatigue crack growth analysis under variable amplitude loading spectra." International Journal of Fatigue Vol.31,pp. 1828–1836,(2009)

[82] S. Simandjuntak, H. Alizadeh, D.J. Smith, M.J. Pavier, "Three dimensional finite element prediction of crack closure and fatigue crack growth rate for a corner crack". International Journal of Fatigue Vol.28, pp. 335–345,(2006)

[83] Sander M, Richard HA. "Effects of block loading and mixed mode loading on the fatigue crack growth". Stockholm: EMAS vol. 5, p.p 2895–902.(2002)

[84] Sander M, Richard HA. "Influence of loading changes on the fatigue crack growth." Advances in fracture research. Proceedings of the 10th international conference on fracture(ICF 10). Fatigue and fracture, Honolulu, USA.(2010)

[85] Sarinova Simandjuntak, Hassan Alizadeh, Martyn J. Pavier, David J. Smith, "Fatigue crack closure of a corner crack: A comparison of experimental results with finite element predictions" International Journal of Fatigue Vol.27, pp. 914–919,(2005)

[86] Schijve, J. , "Some formulas for the crack opening stress level", Engineering Fracture Mechanics Vol.14, pp. 461-465, (1981)

[87] Shiozawa, K.; Matsushita, H. "Crack Initiation and Small Fatigue Crack Growth Behavior of Beta Ti-15V-3Cr- 3Al-3Sn Alloy", Proc. Fatigue '96, G. Lutjering, H. Nowack (Eds.), Berlin 301,(1996)

[88] Shrivastava, Y.P., "Fracture Toughness Determination of Boiler Quality Plate Material & its Application in Pressure Vessel Design" M.E. thesis, Allahabad, (1976)

[89] Skorupa M. Empirical trends and prediction models for fatigue crack growth under variable amplitude loading. ECN-R—96-007. Petten,Netherlands: Netherlands Energy Research Foundation; (1996)

[90] Standard Definition of terms Relating to Fatigue Testing& Statistical Analysis of Data, ASTM STP 595, pp 61-77, (1976)

[91] Stoyan Stoychev, Daniel Kujawski. "Analysis of crack propagation using ΔK and K_{max}" International Journal of Fatigue Vol. 27 pp.1425–1431,(2005)

[92] T. Chang, W. Guo, "Effects of strain hardening and stress state on fatigue crack closure." International Journal of Fatigue Vol.21,pp.881–888, (1999)

[93] T. H. Topper and K. Soudki, "Modeling of Crack-Opening Stress Levels under Different Service Loading Spectra and Stress Levels for a 1045 Annealed Steel" University of Waterloo, Waterloo (2000)

[94] Tada, H.; Paris, P.C.; Irwin, G.R.: The Stress Analysis Handbook, 3rd edition, ASME Press, New York (2000)

[95] Tanaka, K. & Matsuoka, S., "A Tentative Explanation for two Parameters C & m in Equation Fatigue Crack Growth Rate", Int. J. Fract. Vol.13, pp563-583, (1977)

[96] Tanaka, K., Matsuoka, C. & Nishijma, S., "The Generalized Relationship between Parameters C & m of the Paris Law for Fatigue Crack Growth", Scripta Metall15, 3 pp 259-264, (1981).

[97] Thomas-Peter Fries & Ted Belytschko. "The extended/generalized finite element method: An overview of the method and its applications",

International Journal For Numerical Methods In Engineering, Vol.6, pp.455-467, (2003)

[98] Tianwen Zhao, Jixi Zhang, Yanyao Jiang, " A study of fatigue crack growth of 7075-T651 aluminum alloy" International Journal of Fatigue Vol. 30, pp. 1169–1180, (2008)

[99] W.T. Reddile "Determining Fatigue Crack opening Loads from near Crack Tip displacement Measurement". ASTM STP 1343 (1999)

[100] Walker, K., "The Effect of Stress Ratio During Crack Propagation & Fatigue for 2024-T3 and 7075-T6 aluminum", ASTM STP 462, pp 1-14, (1970)

[101] Watwood Jr., V.B. "The finite element method for prediction of crack behavior", Nuclear Engineering and design, 11,pp.323-332, (1969)

[102] Wells, A.A. "Application of Fracture Mechanics at and beyond general yielding, "British Welding Journal,Vol. 10, pp. 563-570(1963)

[103] Y. Lei, "Finite element crack closure analysis of a compact tension specimen" International Journal of Fatigue Vol. 30, pp. 21–31,(2008)

[104] Y.P. Srivastava and S.B.L. Garg, "Influence on R on effective stress range ratio in crack growth. Engineering Fracture Mechanics." Vol. 22, 915-926, (1985)

[105] Zengliang Gao, Baoxiang Qiu, Xiaogui Wang, Y. Jiang b "An investigation of fatigue of a notched member" International Journal of Fatigue Vol.32 1960–1969,(2010)

[106] Zheng, X., 'Fatigue Crack Propagation in Steels ", Engg. Fracture Mechanics, Vol. 18, pp 965-973, (1983)

[107] McClung RC, Sehitoglu H. On the finite element analysis of fatigue crack closure—1. Basic modelling issues. Eng Fract Mech; Vol. 33, pp.237–52, (1989)

[108] Newman JC. A finite-element analysis of fatigue crack closure. In: Mechanics of crack growth, ASTM STP 590. Philadelphia: American Society for Testing and Materials, Vol. 20, pp. 281–301, (1976)